Modulation of cardiac titin stiffness in diabetic and exercised hearts

Inaugural-Dissertation

zur Erlangung des Doktorgrades der Mathematisch-Naturwissenschaftlichen Fakultät der Heinrich-Heine-Universität Düsseldorf

vorgelegt von
Anna-Eliane Müller
aus Bonn

Düsseldorf, November 2014

Aus dem Institut für kardiovaskuläre Physiologie der Heinrich-Heine Universität Düsseldorf

Gedruckt mit der Genehmigung der Mathematisch-Naturwissenschaftlichen Fakultät der Heinrich-Heine-Universität Düsseldorf

Referent: Prof. Dr. Martina Krüger
Koreferent: Prof. Dr. Hermann Aberle

Tag der mündlichen Prüfung:

Contents

List of Figures

List of Tables

Acknowledgements

Herewith, I would like to take the opportunity to express my special appreciation to my advisor Prof. Dr. Martina Krüger. I got the chance to learn a massive amount of insights into my fascinating, very much beloved project and beyond, thank you for encouraging my research. I am thankful for all the great conferences I was privileged to visit and constructive meetings we had, many of them one to one. Her door was always open, thank you! I am also very grateful to my supervisor Prof. Dr. Hermann Aberle and the committee members at the Mathematisch-Naturwissenschaftlichen Fakultät for appraising my thesis. My sincere gratitude and appreciation go the great team I (Robin) worked with, they are the best one can think of. Sepp aka Batman, thank you for your company, brilliant comments and suggestions on my work and your support on the metformin stimulation in ERC and the immunostainings. Sabine aka Catwoman, thank you for the excellent practical support and the great company every day of the last three years. Thanks also go to Christian aka Capitan America, for his professional input and for providing the data on insulin and metformin stimulated ERC. Philipp, for his enriching company especially at the European Muscle Conference 2013 and work on the PLB-phosphorylation and his football coaching; and Matthias for his company in the lab and work on the PKC activity in tissue of exercised rats and surely his cinnamon rolls. In addition, a great thank you goes to the physiology-teams of Prof. Dr. Gödecke and Prof. Dr. Schrader, especially Dr. Katharina Bottermann, Lucia Leitner and Dr. Nadine Borg for their support and friendship. Furthermore, many thanks go to Prof. Dr. Linke and his team in the physiology department at the Ruhr-University Bochum, especially to Marion for introducing me to a lot of the practical work, and all other former and present lab members for being

such awesome colleagues. Additional thanks go to Dr. Frank Suhr from the Sporthochschule Cologne as well as Prof. Dr. Röhl from the University Clinic in Bonn for their kind support and for providing the tissue samples needed for my studies. Many thanks also go to the participants of this study in Bonn. A special appreciaction goes to my family. Words cannot express how particularly grateful I am to Nita, Eliane, Seeb, Norbert with Heidi, Tante Heidi, Hans, Hallo with Gerd and Hein. I would also like to thank all of my friends who supported me in writing, and incented me to strive towards my goal. Special thanks go to Luisa, Jesko, Andreas Christina and Tim for their professional support as well as Anna and Linda with Jan and Vangelis and Afra, Tobi, Steffi, Stefan, Debo, Anphisa, Janneke and Nadja- your friendship is unmeasurable to me. At the end I would like to express the utmost appreciation to Fiete who was, is and will always be my best support.

Abstract

Titin is the largest protein known to date and one of the main molecular components contributing to the passive stiffness of striated muscle tissue. In the mammalian heart, titin-based myofilament stiffness is an important determinant of myocardial distensibility, and diastolic and systolic function. The passive mechanical properties of cardiac titin largely depend on the expression ratio of the isoforms N2BA ($\sim$ 3.2 to 3.7 MDa, more compliant) and N2B ($\sim$3.0 MDa, stiffer). In contrast to cardiac muscle, skeletal muscle only expresses the N2A isoform (3.3-3.7 MDa). Titin-based passive tension can be dynamically modified by phosphorylation through the kinases PKA, PKG, PKCα, CaMKIIδ and ERK 1/2. Importantly, phosphorylation of titin's N2-Bus region by CaMKIIδ, PKA and PKG reduces titin-based myofilament stiffness, whereas phosphorylation of titin's PEVK region by PKCα increases it.

This study investigated the effect of altered insulin availability on titin isoform composition and phosphorylation in human heart tissue sample from diabetes mellitus patients and insulin-treated embryonic and adult rat cardiomyocytes. The study further investigated altered titin stiffness and phosphorylation in adult rat cardiomyocytes induced by the oral anti-diabetic drug metformin.

Results of the study at hand revealed the influence of altered insulin homeostasis on titin isoform ratio and titin phosphorylation by using samples from right atria of diabetic and non diabetic patients that underwent cardiac surgery due to coronary artery disease. Diabetic heart samples showed a significant increase in titin N2BA expression that was most pronounced in patients with high HbA1c levels (Glycated hemoglobin). Western blot analyses using phospho-specific antibodies showed a hypophosphorylation of titin at Ser4099 and Ser4010 within the N2-Bus and concomitantly a hyperphosphorylation of the PEVK element of titin at Ser11878. These phosphorylation changes are known to cause an increase in passive myocyte tension (PT). The PT of isolated cardiomyocytes from diabetic patients showed in fact a significant increase, suggesting a reduction in PKA and PKCα activity. Insulin-dependent changes in titin phosphorylation

were further characterized using cultured embryonic and adult cardiomyocytes. Here, insulin and the oral anti-diabetic drug metformin caused a major increase in the relative phosphorylation at Ser4099 of titin's N2-Bus within 15 minutes of treatment. Furthermore, insulin treatment induced phosphorylation of the PKCα-sensitive site Ser11878 in the PEVK region of titin. Interestingly, PT was significantly increased in adult rat cardiomyocytes stimulated *in vitro* with metformin and insulin.

Additionally, the effects of acute and chronic exercise (concentric and eccentric) on titin phosphorylation and myofilament stiffness in cardiac and skeletal tissue samples from physically trained rats were investigated. Therefore, adult rats were exercised acutely (15 minutes) and chronically (6 weeks) and non-exercised animals served as controls. PT from all exercised cardiac samples was significantly increased, compared to controls. In cardiac tissue titin N2-Bus phosphorylation was significantly decreased at Ser4099. However, no significant changes were observed at Ser4010. PEVK phosphorylation at Ser11878 was significantly increased, which is probably mediated by the observed exercise-induced increase in PKCα activity. Interestingly, relative phosphorylation of Ser12022 was substantially decreased in the exercised samples. Surprisingly, in skeletal samples from acutely exercised animals a significant decrease in PEVK phosphorylation at Ser11878 and an increase in Ser12022 phosphorylation was detected; however, PKCα activity remained unchanged. The evaluated phosphorylation status suggests a decrease in PT. However, the effect on skeletal muscle and PT still needs to be determined. In summary, the generated data show that insulin and metformin can be identified as potent modulators of cardiac titin and may therefore play an important role in modifying myocardial stiffness in human hearts. Furthermore, different kinds of exercise affect titin domain phosphorylation and titin-based cardiomyocyte stiffness with obviously divergent effects in cardiac and skeletal muscle tissues. The observed changes in titin stiffness caused by acute triggers may regulate adaptation processes of the passive and active properties of the myocardium.

Zusammenfassung

Titin ist das größte bekannte Protein in Säugetieren und primär mitverantwortlich für die Sarkomersteifigkeit. Veränderungen in der Titin-basierten passiven Steifigkeit von Muskelzellen können besonderen Einfluss auf die Stabilität des menschlichen Herzens und dessen diastolische und systolische Funktion haben. Die passiven Sarkomereigenschaften im Herzen werden insbesondere auch durch das Expressionsverhältnis der verschiedenen Titin-isoformen definiert. Im Skelettmuskel sind nur die N2A-Isoformen (3,3-3,7 MDa) exprimiert, wohingegen im humanen Herzmuskel zwei Hauptisoformen des Titins ko-exprimiert werden: Die kurze und steife N2B-Isoform (3,0 MDa) und die längeren und weniger steifen N2BA-Isoformen (3,2-3,7 MDa). Eine weitere Möglichkeit zur Beeinflussung der passiven Steifigkeit liegt in der Phosphorylierung elastischer Titindomänen. Die Proteinkinasen CaMKIIδ, PKG und PKA führen zu einer reduzierten Versteifung durch Phosphorylierung der N2-Bus im Titinfilament, wohingegen die PKCα zu einer erhöhten Versteifung durch Phosphorylierung der PEVK im Titinfilament führt.

Im Rahmen der vorliegenden Arbeit wurden die durch veränderte Insulinverfügbarkeit ausgelösten physiologischen und pathophysiologischen Modulationen der Titin-basierten passiven Kräfte durch Phosphorylierungen näher untersucht. Am Beispiel der Krankheit Diabetes Mellitus wurde der Einfluss von Insulin und dem oralen Antidiabetikum Metformin auf Titin im humanen Herzen (Biopsien aus dem rechten Herzohr von Diabetes Mellitus-Patienten mit koronarer Herzerkrankung) analysiert.

Das Titin N2BA:N2B Isoformen-Verhältnis war bei Diabetikern im Vergleich zu Nicht-Diabetikern, wenn sie nach ihrem HbA1c (Glykosyliertes Hämoglobin) separiert wurden, signifikant verändert (Erhöhung der N2BA-Isoform Anteile). Zusätzlich konnte eine Hypophosphorylierung im Titin-Segment N2-Bus am Ser4099 und Ser4010 sowie eine Hyperphosphorylierung im PEVK Element am Ser11878 von Titin in den Proben von Diabetikern festgestellt werden.

Vorangegangene Studien hatten gezeigt, dass derartige Änderungen in der Phosphorylierung dieser Serin-Reste zu einer erhöhten passiven Steifigkeit führen. Die gemessene Titin-basierte passive Steifigkeit war in den Kardiomyozyten von Diabetikern im Vergleich zu Patienten, die nicht an Diabetes erkrankt sind, tatsächlich drastisch erhöht, was die diastolische Funktion im Herzen beeinträchtigen kann. Um den direkten Einfluss von Antidiabetika auf Titin genauer zu untersuchen, wurden primäre Zellkultur-Modelle der Ratte verwendet. Die Behandlung von adulten Kardiomyozyten mit Metformin und Insulin zeigte einen überaschenden Anstieg der passiven Kräfte, denn die PEVK Phosphorylierung blieb unverändert und in embryonalen und adulten Zellkulturen zeigen sich schon nach kürzester Zeit (15 Minuten) signifikante Anstiege der relativen Titin-Phosphorylierung am Ser4099.

Zusätzlich wurden im Tierversuch (Ratten auf Laufbändern), die entstehenden akuten und chronischen Anpassungen des Herz- und Skelett-Muskels an ein festes Laufregime und die daraus resultierenden möglichen Veränderungen der Titin-Phosphorylierung nach konzentrischen und exzentrischen Belastungen untersucht. Durch 15-minütige Belastungen traten signifikant erhöhte Phosphorylierungen der Titin-PEVK-Region am Ser11878 und Ser12022 und signifikante Reduzierungen der Phosphorylierung am Ser4010 und Ser4099 in der N2-Bus auf, die eine entscheidende Wirkung auf die Darstellung einer definierten kardialen Muskelsteifigkeit nach akuter konzentrischer oder exzentrischer Arbeit erkennen lassen. Diese Tiere wiesen ähnliche Veränderungen nicht nur akut, sondern auch nach sechswöchiger Laufbelastung auf. Interessanterweise war außerdem die passive Steifigkeit in den Kardiomyozyten trainierter Tiere signifikant erhöht im Vergleich zu den Kontrolltieren.

Es ist festzuhalten, dass die Titin basierte Steifigkeit durch eine Vielzahl von Faktoren beeinflusst werden kann. Sowohl die medikamentöse Behandlung von Diabetikern mit Insulin oder Metformin, als auch Training unterschiedlicher Art (im Tierversuch) führt zu einer akuten Veränderung am Titinmolekül und etwaig zur Adaption der passiven und aktiven Eigenschaften des Myokardiums und des Skelettmuskels.

1. Introduction

1.1. Structure and function of the human cardiac muscle

The heart is a hollow organ with a variety of important, live-sustaining tasks including to maintain blood circulation over a life-time period without any rest. However, every detail of the underlying mechanisms of the complex cardiovascular system is still not yet fully understood. Of distinct interest is still how the heart adapts and heals or the impact of external stimuli on intercellular signal-cascades, especially since cardiovascular diseases are one of the leading and steadily increasing causes of mortality worldwide. The heart muscle is divided into a left and a right side by the septal wall consisting of four different chambers, two on each side which are the atrium and the ventricle, separated by an atrioventricular (AV) valve (Figure 1.1.). Oxygen-rich blood is delivered by the left side of the heart to the body (systemic circulation) passing through the aortic valve to the aorta, whereas the right side pumps blood through the pulmonary artery and valve for an oxygen refill in the lungs (pulmonary circulation). During this cardiac cycle basically all blood is pumped through the whole body within a single minute. The blood flow through the two chambers and the respective atrium is marked by contraction or filling of the ventricle with systolic pressure and relaxation or release of the ventricle with diastolic pressure [103]. The heart thereby supplies all organs of the body through blood vessels with gases, nutrients and hormones. Musculature including the heart, is build up of muscle cells, being able to shorten (contract) upon a stimulus. There are different types of muscle tissue present in the

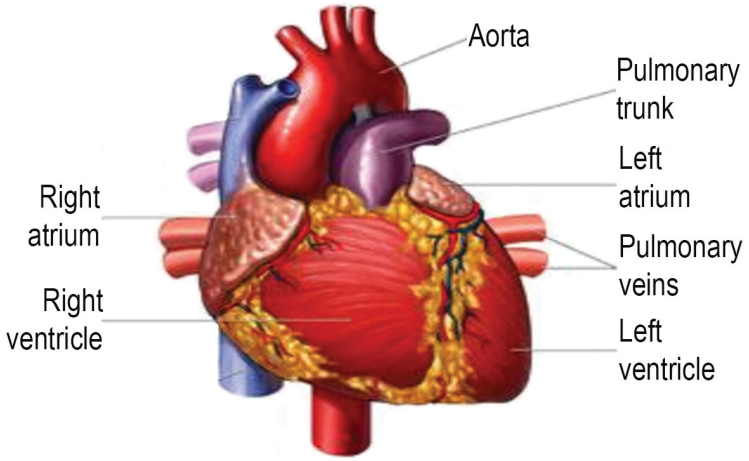

Figure 1.1.: Figure of the human heart. The walls of the heart are made up of three different layers, the cavity is divided into four different parts. There are two upper chambers, termed as the right and left atria, and two lower chambers, termed as the right and left ventricles. (Nucleus Medical Art, Inc. Getty Images), modified.

human body. Skeletal and cardiac muscles are known as striated muscle, since myofibrills are in order of regular appearing myosin and actin filaments, forming a pattern-like histological appearance [63]. The rhythmical contraction of the heart muscle is autonomously controlled. Specialized cells in the sino-atrial node generate an excitation signal that transmits an action potential to the active myocardium causing a concerted contraction of all myocytes. This process allows a stable resting heart rate in human adults of 60-80 beats per minute (bpm). Furthermore, additional mechanism are able to modify force and rate of contraction by adapting to variable conditions, for example physical stress. One of these mechanisms is the Frank-Starling mechanism of force, which represents the positive force-frequency relationship and the regulation by the autonomous nervous system.

1.2. The three-filament model of the sarcomere and muscle contraction

Each myofibril consists of several sarcomeres, which are the basic contractile elements in striated muscle cells and are constructed by a network of highly specialized proteins. The essential structural multi-protein complexes of the sarcomere (Figure 1.2.) are the Z-disc, the I-band (isotropic), the A-band (anisotropic) being the largest part of the sarcomere, and the M-band. The lateral border of one sarcomere is defined between Z-lines, connected by intermediate filament proteins [64]. The contractility is possible through myofibrillar components of the sarcomere that are interacting constantly. This functional interaction is highly regulated. Mutations of genes coding for different sarcomeric proteins, may lead to malfunction of the contractile apparatus and can therefore cause cardiomyopathies or muscle dystrophies [16]. The main components of the myofilament are the thin- (actin), thick- (myosin), titin-, and nebulin filaments. The actin filament system is integrated into the Z-disc and extends to the middle of the sarcomere, where it is positioned and functionally regulated by the actin binding protein nebulin. Polymerization and depolymerization of actin are regulated by the capping proteins tropomodulin and CapZ, which cover the barbed and pointed ends of the actin filament, respectively [58]. Connected to actin is the regulatory protein troponin through end-to-end linked tropomyosin molecules. Tropomyosin inhibits the attachment site for the myosin crossbridge, thus preventing contraction in a relaxed muscle. Contraction of a muscle cell is stimulated by an action potential, causing calcium channels to open in the sarcoplasmic membrane and release calcium into the sarcoplasm [23]. Large stores of calcium ions initiate in the sarcoplasmic reticulum where they are sequestered and then released upon excitation-contraction coupling when the muscle cell is stimulated [23]. Calcium-binding to troponin exposes binding sites for myosin on the actin filaments. The binding of myosin to actin causes crossbridge formation, resulting in muscle contraction [43]. Contractile forces are generated when the thin filaments and thick filaments interact in the A-band

region. The thick myosin filament is anchored in the H-Zone and extends from the A-band to the M-band and associates with the myosin binding protein-C. The third filament of the sarcomere is titin (also referred to as connectin), it spans a half-sarcomere, and represents with a thread-shaped appearance about 10 % of the overall muscle mass [64].

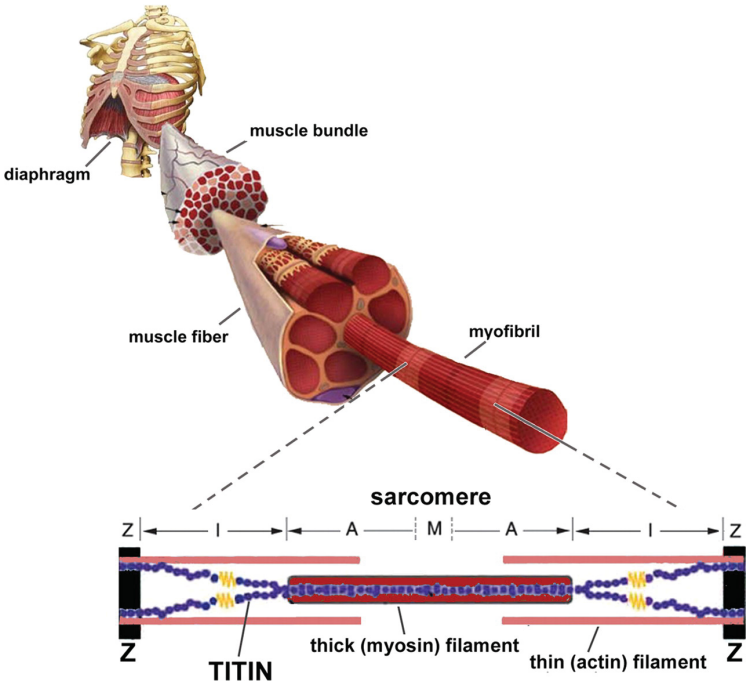

Figure 1.2.: Model of structural units of muscle tissue from the diaphragm, muscle bundles, muscle fibers and myofibrils to the sarcomere, the smallest contractile unit of striated muscle. The sarcomere comprises 3 major filaments: the thin (mostly actin) filaments, the thick (mostly myosin) filaments, and the giant filamentous molecule titin. The thin filaments are anchored in the Z-disk, where they are cross-linked by α-actinin. The thick filaments are centrally located in the sarcomere and constitute the sarcomeric A-band. The myosin heads, or cross-bridges, on the thick filament interact with actin during activation. Titin spans the half-sarcomeric distance from the Z-band to the M-band, thus forming a third sarcomeric filament. [17].

1.3. The molecular structure of titin

Titin is the largest protein found in the human body with a size of 1000 ηm and is encoded by a single gene [86]. The human titin gene is located on chromosome 2q3l with a size of 294 kb [34]. There are 363 exons in the human titin gene encoding 38.138 amino acids for a putative protein with a maximum size of 4.2 MDa [86]. It has been discovered by the scientific community in the 1980's [134] with the help of electron microscopy (Figure 1.3.) and specific antibodies. Titin, a molecular spring-like giant sarcomeric filament is known to be involved in functional, physiological and pathological processes, particularly in muscle tissue. The N-terminus of the molecule is anchored within the Z-disk and the C-terminus within the M-band. It additionally has an elastic part in the I-band region as well as a thick filament-binding area in the A-band. The A-band, M-band and Z-disk parts of titin are playing important roles in numerous signaling-dependent cellular processes regulating passive forces of the titin molecule. In the I-band region, titin is extensible and functions as a molecular spring that develops passive tension (PT) upon stretch, thus the passive forces also emerge during the diastole of the heart after sarcomere stretching.

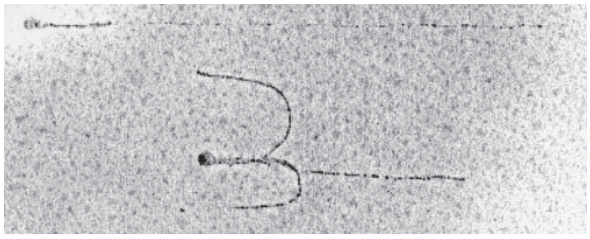

Figure 1.3.: Electron microscopy of the titin molecule with a molecular length of 0.9 μm to 1.5 μm, depending on sarcomere stretch (Prof. John Trinick, www.astbury.leeds.ac.uk).

The I-band contains a tandem Ig segment consisting of serially linked immunoglobulin (Ig)-like domains [27], the PEVK region predominantly rich in the following amino acids: proline (P), glutamic acid (E), valine (V) and lysine

(K) as well as the N2B segment including a heart specific N2B unique sequence (N2-Bus) and smaller N2-A unique sequences (Figure 1.4.). Longer isoforms additionally contain the so-called N2A region and were thus named N2BA isoforms. The I-band titin holds multiple binding sites for proteins associated with contraction, metabolism, and regulation of gene expression. Furthermore, titin overlaps with the thin filament system at the I-band region of the sarcomere, providing two binding sites for sarcomeric actin. One of these interaction sites is located at the Z-disc/I-band junction and suggested to anchor the I-band region of the titin molecule in the sarcomere [136]. At the other interaction site, actin filaments bind to titin's PEVK domain, possibly regulating passive forces, which is controlled by the calcium-binding protein S100A1 [105, 135]. The stiffness of the PEVK region can also be increased by direct binding of calcium to the PEVK domain [29]. Passive myocardial stiffness of the heart is based on the passive forces of titin and the extracellular matrix. The total protein has a size between 3 and 4 MDa made up of about 30.000 amino acids depending on the splice variant [115]. For instance a 625 kDa Novex-3-isoform and a 3.7 MDa huge form are found in human soleus, all deriving from the single titin gene [131]. Titin is known to be a scaffolding protein assembling the sarcomere and comprising it's mechanical characteristics [69, 33]. Within the I-band region, entropic spring-elements form an elastic part with different persistence lengths (PL) [133]. The PL is an indicator for the stiffness of a polymer chain, where a higher PL means less force is developed during elongation. The flexible parts of the titin molecule are the proximal and distal Ig-Domains with a PL of about 10 μm, the PEVK-region with a PL of approximately 1 μm and the cardiac specific N2-Bus with a PL of about 0.65 μm, extending sequentially during elongation of the sarcomere [134] [66] [31] [117]. The elastic forces of titin in combination with extracellular collagen form the passive stiffness of the muscles [71, 51]. Furthermore, titin interacts with a variety of proteins that are associated with signalling processes [79]. Such interactions have been identified within the Z-disc, the M-band, the N2-Bus and C-terminally located titin-kinase-domain. Examples are telethonin strongly binding the Z1/Z2 domain, as well as nebulin [65], filamin [115] and obscurin [98]. Other binding partners include the FHL1

and FHL2 or four-and-a-half LIM domain proteins binding the cardiac specific N2-Bus and the three homologous muscle ankyrin repeat proteins also known as MARPs, cardiac ankyrin repeat protein, diabetes-related ankyrin repeat protein, and Ankrd2 (ankyrin repeat domain protein-2), binding the N2-A region within titin's I-band [79]. Moreover, in the Z-disc and I-band junction, actin and titin filaments are associated [136]. Different isoforms of titin with a distinct spring composition are generated, due to variable alternative splicing of the titin gene. There are two major isoform types coexpressed in adult mammalian hearts [87], the stiffer and shorter isoform named N2B with a size of 3.0 MDa [86] and a group of more compliant and longer N2BA isoforms with a size of 3.2 to 3.7 MDa. In cardiac muscle an additional fetal form called fetal cardiac titin (FCT) is expressed [114]. However, there is only one characteristic isoform (3.3-3.7 MDa) present in skeletal muscle, with the largest form found in the soleus muscle [3, 71]. The N2B segment is a part of all isoforms in the heart. The N2A segment however, is exclusively present in the FCT as well as N2BA isoforms. Due to it's shorter I-band composition, the N2B isoform is much stiffer than the N2BA isoform and therefore stronger forces are required for extension of this isoform [66]. Therefore, passive forces of the sarcomere are very variable as they depend on expression level of titin isoforms [111]. The expression ratio of the isoforms in cardiac sarcomeres is one major determinant of titin based passive stiffness of the myocardium, due to the size of the I-band region determining those forces. In the left ventricle of a healthy human individual, this expression ratio is about 40:60 (N2BA:N2B)[22] but has been shown to vary both ways in individuals suffering from particular heart diseases [87]. The N2BA:N2B ratio is often increased in end-stage heart failure, resulting in an increase of titin elasticity. Titin isoform composition is differentially regulated in heart development and very often during progression to heart disease, e.g. in heart failure, where an isoform shift takes place leading to increased levels of the more compliant and longer N2BA isoform followed by a reduction of titin based stiffness [51]. The distribution of N2BA:N2B titin-expression ratios in mammalian heart varies massively, exemplary in rat hearts the short N2B isoform predominates with approximately 90% of total

titin. The molecular mechanisms that control titin isoform composition are not yet fully understood. However, previous studies suggest that titin isoform expression is largely modulated by hormone-dependent activation [76, 74] of the PI3K/AKT signaling pathway [75]. Furthermore, minimal isoform shifts have been detected in STZ-Rats (Streptozotocin-diabetic rat model), whereas patients with type II diabetes mellitus do not seem to develop significant titin isoform expression changes. The complex splicing events of titin mRNA are still to be investigated. However, the splicing factor RBM20 [130] has been recently identified as a key player in the regulatory processes that control titin isoform expression. Mutations of RBM20 not only drastically interfere with titin isoform expression, but also involve splicing processes of 30 other cardiac proteins [137]. Interestingly, decreased expression levels of RBM20 in heart disease are possibly leading to an upregulation of titin isoforms with increased compliance [130].

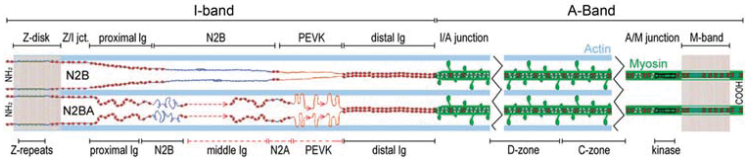

Figure 1.4.: Layout of the third filament titin in the cardiac sarcomere, showing the stiff N2B isoform coexpressed with compliant N2BA isoform. The C- and N-termini of titin are anchored in the M-line and Z-disc, respectively [132].

These changes in cardiac function due to titin isoform shifts can be considered as a long term or chronic process, since they depend on expression level of the respective isoforms. However, fast and therefore acute modifications can be observed, too. They are primarily seen as adjustments of cardiac function to external stimuli like for instance medication or exercise [18]. Titin can, as it has already been indicated, be phosphorylated. This process is reversible and means an additional phosphate-group is attached to the protein, possibly leading to changes in activity and function [72]. Different kinases phosphorylate titin [76, 19] within it's I-band domains. Titin based myofilament stiffness can

modulated by phosphorylation of it's elastic domains (N2-Bus and PEVK) by different kinases, such as PKG, PKA, PKCα (Figure 1.5.) and ERK1/2 and CaMKIIδ [76, 77, 19, 106, 92]. The human N2-Bus contains several conserved and not conserved serine residue (e.g. S497 and S469), phosphorylated by PKA and PKG. Both kinases are cAMP- and cGMP dependent and activated in response to β-adrenergic stimulation by catecholamines and nitric oxide (NO) or natriuretic peptides respectively [76, 77, 106, 4]. By increasing the PL, this phosphorylation leads to a decrease in titin based passive myocyte stiffness of approximately 20 % with no distinguishable differences between the protein kinases [76]. In contrast, the Ca^{2+}-dependent PKCα-mediated phosphorylation at serine residue 11878 and 12022 (conserved) of the PEVK-region increases passive fiber stiffness by approximately 15-20 % [18].

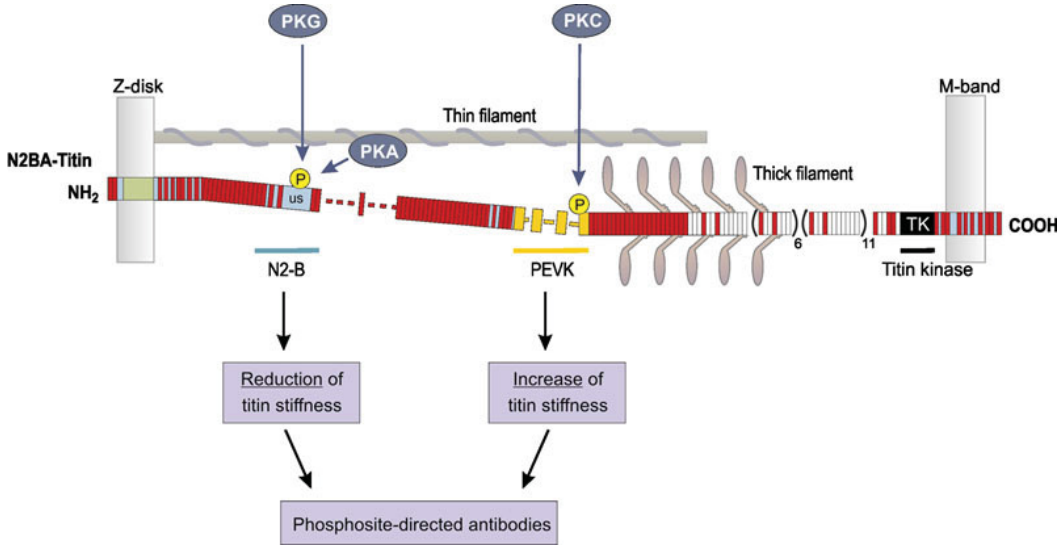

Figure 1.5.: Layout of the titin-domain architecture and how titin stiffness can be dynamically modified by antibody-detected phosphorylation of it's elastic I-band region through PKA, PKG and PKC, modified from [78].

Furthermore, PKG has been shown to phosphorylate the N2-A domain with no measurable effect on persistence length or Ig-domain stability of the N2A-domain [76] and therefore no measurable influences on titin stiffness [76]. In

the A-band, titin is inextensible due to its strong interaction with the thick filament [32]. The A-Band moreover comprises the major part of titin [86] with a size of 2.1 MDa. The A-band segment is critically involved in the binding of MuRF-1 (Muscle RING-finger protein-1 ligand) [119], which has been involved in the downstream signaling pathway of the adjacent protein kinase domain [116]. M-band titin interacts with myosin [120], obscurin (acting as a linker to the sarcoplasmic reticulum [7]) and the obscurin-like 1-Protein (Obsl-1) [4, 98]. The M-band segment of titin can only be tightened due to active forces, making it a potential indicator for contractile stress to the muscle [47, 49, 48].

1.4. Insulin, pharmacological treatment and the association with cardiovascular disease in diabetes mellitus

Muscle fibers belong to the tissue most important for insulin absorption. Here, insulin regulates the vital carbohydrate metabolism of the human body. The proteo-hormon insulin derives in the endocrine glands of the pancreas, where it is stored, biosynthesized and secreted [42]. Insulin is synthesized as a single precursor molecule called preproinsulin, which is posttranslationally modified to construct the mature hormone [42]. Since insulin is necessary for insulin-dependent tissue (besides muscle also brain and fat tissue) to uptake glucose via the glucose transporters [68], essential for cell and body metabolism, deficiencies lead to various severe symptoms [40]. Subsequently, the substrate-lack within the cells and the glucose increase in the blood cause diuresis, glucosuria and acidosis of the blood, which may result in a coma when untreated [40]. Therapeutically, only medication with artificial insulin is indicated in order to compensate for the deficiency [40]. Glucose is the the most important regulator of insulin gene expression, acting through a complex process that activates transcriptional and posttranscriptional mechanisms [42]. Since glucose uptake is increased in muscle tissue by insulin, glucose biosynthesis and glycolysis are

subsequently promoted [42]. Here, insulin inhibits the glucagon-stimulated glucogenesis. Furthermore, insulin decreases cyclic adenosine monophosphate (cAMP)-levels, by activating phosphodiesterases 5A (PDE5A) known to reduce cAMP and cyclic guanosine monophosphate (cGMP). A reduction of cAMP in turn inhibts glycogen degradation and therefore stimulated glycogensynthesis [42]. The previously described effect is initated acutely within seconds or minutes. On a long term basis, insulin initiates growth and proteinbioynthesis within hours and days. Recent studies also strengthen the importance of insulin in gene transcription responsible for specific enzymes, key factors in regulating carbohydrate and fat metabolism [42].

The intracellular effects of insulin are regulated by the binding of insulin to the cell membrane-associated insulin receptor (IR), promoting the association of insulin recpetor substrate (IRS) with the receptor. The IR can be a substrate for the cAMP- and cGMP-dependent kinases PKA and PKG, as well as for PKC [89]. PI3K binds the IRS substrate (IRS1) activating the catalytic subunit of PI3K. Hence, PDK and AKT are activated (Figure 1.6.), both representing signal proteins important for transduction of insulin signalling for glucose uptake of the cell [42]. Moreover, insulin is known to initiate signal cascades similar to thyroid hormones. Angiotensin II and the thyroid hormone triiodo-l-thyronine (T3) have been identified to contribute to titin modifications. There are indications of thyroid hormone signaling being essential for transcriptional regulation of titin-isoform composition [144, 75]. Hypothyroidism, when pharmacologically induced in adult rats leads to a large re-expression of the N2BA titin isoform, possibly due to a reduction in thyroid hormone levels and reactivation of a fetal gene program [144]. In addition, T3 plays a major role in cardiac development by regulating the expression of numerous cardiac-specific proteins, including myosin heavy chain isoforms, phospholamban, sarcoplasmic-reticulum, calcium ATPase, and collagen isoforms [112, 75]. T3 further has been identified to significantly stimulate the developmental titin-isoform transition from fetal N2BA to stiff N2B in ERC [99, 57, 6, 75]. The titin isoform composition alterations initiated by T3 are mediated via a non-genomic signalling pathway, namely the phosphatidylinositol-3-kinase

(PI3K)-dependent signaling-cascade [75]. Downstream mechanisms controlling splicing of titin mRNA and regulation of titin expression are thus far mainly unknown. However, insulin has been identified to initiate the PI3K pathway involving AKT and mTOR leading to a cardiac titin isoform switch with a pattern similar to T3 [57, 99, 6, 75]. Insulin potentially activates the so called 'survival'-pathway acting via, PI3K, eNOS, and PKG (Figure 1.6.), known to phosphorylate titin [75]. The NO-cGMP signaling has been identified to protect the heart against various stressors, including pro-hypertrophic cardiac stress [142, 6].

Cardiac contraction is among others regulated by beta-adrenergic signaling involving elevated levels of adenosine (cAMP) and guanosine (cGMP) cyclic nucleotides. Increased cAMP enhances contractility by activation of PKA, whereas simultaniuos stimulation of cGMP opposes this in part by activating 3',5'-cyclic monophosphate (cGMP)-dependent PKG [13], which attributes stimulation of the only known NO-receptor soluble guanylate cyclase (sGC) by NO and is able to modulate cardiac function and structure, particularly in hearts stimulated by mechanical stress or hormones [35]. Due to hormone binding, an activation of the sGC within the intracellular domains results in increased cGMP levels [96]. cGMP then activates downstream effectors (cGMP-dependent protein kinase, Ca^{2+} channels and phosphodiesterases) to ultimately cause muscle relaxation and vasodilation. Furthermore, sGC is the target of the earliest class of cardiovascular drugs known [96]. cGMP is also regulated by catabolic phosphodiesterases such as phosphodiesterase 5A (PDE5A), and PDE5A inhibition by the vasodilatation enhancing drug sildenafil and similar compounds increase cGMP levels in vascular tissue and has been associated with titin phosphorylation and improvement of diastolic distensibility *in vivo* [62]. However, the role for PDE5A in regulating cardiac function remains unclear. Thus, deeper knowledge about the basis of the underlying pathways has become increasingly important, since they are the target for chronic treatments of various diseases [35]. An additional downstream target of PKG is the enzyme VASP (Vasodilator-stimulated phosphoprotein) which is associated with filamentous actin formation and involved in cell adhesion,

whether VASP participates in the anti-inflammatory effects of vascular NO signaling remains unclear [13]. VASP is preferentially phosphorylated by PKG at Ser239, and in rodent models of diabetes, actin cytoskeleton rearrangements in vascular tissue have been correlated to reductions of both PKG and VASP signaling [13]. Several observations indicate that endothelial NO (eNOS) plays a physiological role to protect against vascular and cardiac disease [13]. Interestingly, restoration of normal NO levels through either pharmacological or genetic interventions reduces insulin resistance and vascular inflammation. On the contrary, experimental deficiency of eNOS has the opposite effect [13].

Furthermore, insulin is the mainstay of hyperglycemic control in diabetic patients. Diabetes mellitus (DM) is a common metabolic disease based on hyperglycemia, where glucose levels in the blood plasma are constantly increased [80]. Glucose is essential for cell metabolism in mammals and the substrate for glycolysis, used as an energy source and stored as glycogen (secondary short term energy source) in muscle and liver tissue. Moreover, glucose triggers cytoplasmic signaling including activation of phoshorylation cascades [110]. There are mainly two different types of DM. Type I DM is an autoimmune disease [5] also known as insulin dependent diabetes mellitus or juvenile diabetes. As a result of chronic inflammation, the patients' β -cells in the islets of Langerhans within the pancreas undergo apoptosis and are therefore not able to produce and secrete the anabolic hormone insulin [9, 42], leading to malfunctioning glycogen synthesis [67]. Type II diabetes mellitus is a dominant and increasingly expanding disease in western countries. Of all DM patients 90%-95% are suffering from the type II variant [80]. Type II DM can be induced through genetic predisposition and several various environmental factors including diet, obesity and lack of exercise [80]. In type II DM, patients are suffering from insulin resistance, where sufficient amounts of insulin are produced in the pancreas, but cell membranes supposed to transfer the glucose into the cells indirectly via insulin receptors (IR) are malfunctioning [67]. Mutations, low expression levels and insufficient insulin binding can also be a reason for disturbed insulin homeostasis. The pancreas is trying to compensate the lack of glucose in the cells by overproduction of insulin which may in turn also reduce IR expression levels [67]. In patients

suffering from type II DM, a co-morbidity like increased blood pressure is often the case. Furthermore, obesity is frequently found along with DM and is also named as a cause of the illness [126]. DM combined with obesity and arterial hypertension is regarded to as prediabetes or metabolic syndrome, known as a frequent precursor for cardiovascular disease [42]. In addition to a genetic predisposition of the patients, obesity may also cause a resistance of the insulin dependent tissue [101]. Here, the glucose-transporter type 4 (GLUT-4), localized in vesicles of mammals predominantly expressed in fat and muscle tissue is disturbed [36]. When insulin binds the IR embedded in the cell membrane (Figure 1.6.), GLUT-4 vesicles fuse with the membrane, stimulating the channeling of glucose, which can then be processed to pyruvates necessary for triglyceride production in fat cells or energy supply [36].

Type II DM patients are in fact associated with a 2-fold increase in cardiovascular death or hospitalization for heart failure (HF) [15]. Heart failure in particular is a predominant and the leading cause of death in patients with type II DM [141]. Those patients have a predisposition to suffer from diastolic dysfunction, often considered to be an early characteristic of diabetes-induced heart failure [129] and have increased risk factors for coronary heart disease (CHD), in which hyperglycemia and hypertension play a major role [123]. Different causes can trigger CHD, a dominant one is diastolic dysfunction [121], here cellular and molecular backgrounds are still to be investigated. In detail, combined with impaired left ventricular (LV) relaxation diastolic dysfunction forms the basis for a form of CHD called heart failure with preserved ejection fraction (HFpEF) [139]. HFpEF patients are additionally characterized by exercise intolerance. This form of heart disease can be caused by altered calcium signaling within the cardiomyocytes as well as by an increase in diastolic left ventricular (LV) stiffness [21] due to either collagen based stiffening of the extracellular matrix (higher fibrosis levels) or increased titin based passive stiffness [130]. HFpEF animal model are characterized by titin stiffening through altered isoform composition and phosphorylation, both are contributers to increased LV stiffness [93]. Whether the increase in titin based PT is a symptom of HFpEF or even a trigger remains to be elucidated.

HFpEF, also known as diastolic heart failure is increasing both in prevalence and incidence [38]. In a group of patients with objective evidence of HFpEF and reduced exercise capacity, the patients being additionally diagnosed with type II DM had a more severe disease phenotype characterized by more numerous comorbidities, increased left ventricular hypertrophy, and increased circulating markers of vasoconstriction, oxidative stress, inflammation as well as fibrosis [139]. These findings support the assumption that diabetic HFpEF patients are at particularly high risk given their comorbidity burden and somewhat distinctive pathophysiology [139]. However, how titin phosporylation is regulated in diastolic dysfunction is not fully understood, but a titin phosphorylation deficit in heart failure has been identified [139]. Increased titin phosphorylation in diastolic dysfunction may serve as an explanation for HFpEF. A decrease in titin phosphorylation might as well be due to oxidative stress, as suggests by recent studies [139].

Insulin treatment in cell culture of primary rat cells leads to increased total titin phosphorylation [75]. In line with this stands a hypo-phosphorylation of titin in functional insulin deficiency in context with type II DM going along with an increase in titin based myofilament stiffness [50]. Insulin induced changes within the titin molecule being titin-isoform composition, total titin phosphorylation, kinase activity and consequently altered titin based stiffness (on bioartificial cardiac tissue) have been shown in cell culture models [75]. How these affect patients, remains to be elucidated. To deepen the knowledge about physiological processes of titin changes like posttranslational modifications and isoform switching due to insulin and the commonly prescribed anti-diabetic metformin treatment, responsible pathways (e.g. PI3K/AKT/mTOR pathway) still need to be evaluated. Metformin is administered much more in type II DM than insulin, due to it's easier handling and effectiveness especially in order to regulate patients' HbA1c (Glycated hemoglobin). However, exact cellular and molecular mechanism action of the biguanide class oral antidiabetic drug metformin are far from being fully understood [125, 44]. Metformin was already clinically introduced in the 1950's, it suppresses glucose production in the liver and therefore increases peripheral tissue insulin sensitivity [25]. Metformin may

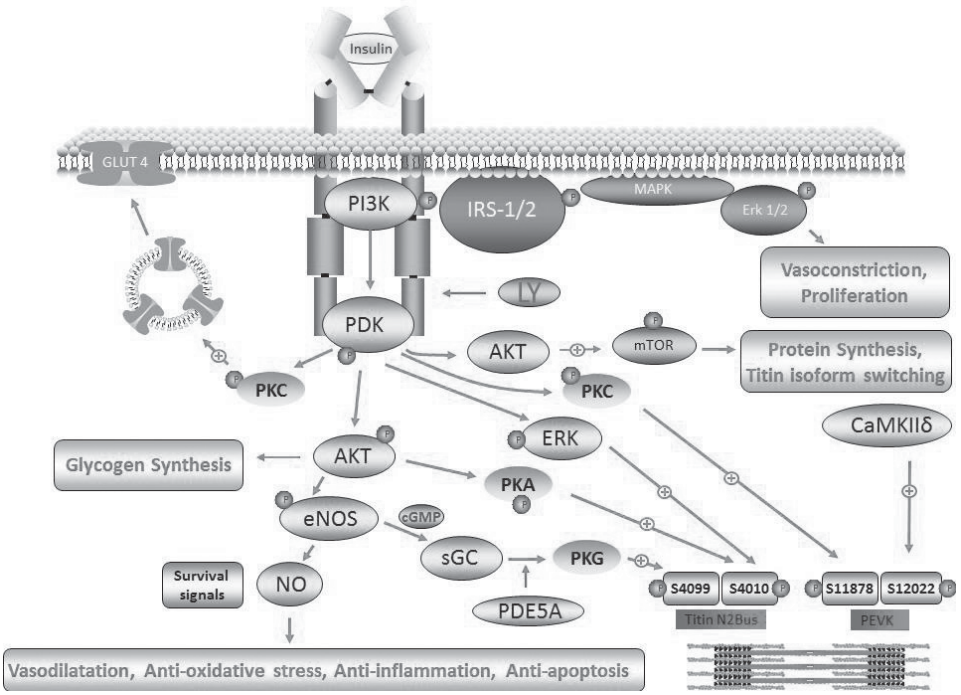

Figure 1.6.: Illustration of the insulin-initiated PI3K-Akt-eNOS-NO survival signaling and cardiovascular protection pathway. Insulin binds to cell membrane insulin receptor, leading to the activation of PI3K-Akt-eNOS, resulting in metabolic modulation and cardiovascular protection. Among the insulin-activated signaling cascades, PI3K-Akt-eNOS-NO represents a special link between insulin and the cardiovascular system with regard to health and pathology. Activation of this signaling cascade, together with other Akt-activated molecules can lead to vasodilatation, anti-apoptosis, anti-inflammation, and anti-oxidative/nitrative stress. Legend: CaMKII, Calcium/calmodulin dependent protein kinase II; cGMP, cyclic guanosine monophosphate; eNOS, Endothelial Nitric Oxide Synthase; ERK2, extracellular signal-regulated kinase-2; GLUT4, glucose transporter 4; IRS, Insulin receptor substrate; MAPK, mitogen-activated protein kinase; mTOR, mammalian target of rapamycin; NO, nitric oxide; PDE5A, cGMP-specific phosphodiesterase type 5; PDK, Phosphoinositide-dependent kinase; PI3K, phosphatidyl inositol-3-OH-kinase; PKA, protein kinase-A; PKB, protein kinase-B; PKC, protein kinase-C; PKG, protein kinase-G; sGC, soluble guanylyl cyclase.

additionally have therapeutic efficacy in other conditions, including different forms of cancer like leukemia [122], diabetic nephropathy or ameliorative property against tubular cell injury [45]. The cellular mechanisms including activated pathways that control phosphorylation of I-band titin are not yet fully retractable, also after either metformin or insulin stimulation. Modifications of titin properties (either by phosphorylation, isoform ratio changes or passive stiffness) are also found in diastolic dysfunction being a major condition going along with DM [50]. For this study, patients with the same medical treatment and cardiac surgery were sorted into two groups. The first group were formed by those with a low HbA1c (indicating no diabetes or good compliance) and served as the control group (named "Control" in all figures). The second group was formed by those with a high HbA1c (rather depicting diabetes and bad compliance), and was therefore named "Diabetic" in all figures. HbA1c levels are dictated by both basal and postprandial glucose levels forming an indicator for well medicated patients [85], either with insulin or the more often clinically applied, orally given substitute metformin. In the study at hand, all patients were medicated with metformin. Those pharmacological treatments may serve as a possible explanation for high variability in titin phosphorylation shown in former studies. Samples from both patient groups were measured for their titin based passive myocyte stiffness, domain specific (N2-Bus and PEVK) analysis of titin phosphorylation as well as isoform ratios were investigated. For further pharmacological analysis, embryonic rat cardiomyocytes (ERC) as well as adult rat cardiomyocytes (CM) were stimulated with insulin and metformin. In ERC members of the mTOR (mechanistic target of rapamycin) pathway were examined, as metformin influences the mTOR pathway and AKT and mTOR are essential for the insulin pathway. Within the N2BA phosphorylation seems to be of particular importance for myofilament stiffness [50]. Consequently, insulin- and metformin- dependent signal-cascades leading to titin phosphorylation were investigated in cell culture models of primary cells from adult and embryonic cardiac tissue.

1.5. Physical exercise-related modifications in the heart

Exercise is known to have a beneficial effect on the cardiovascular system. Not only in healthy humans, but particularly in the setting of cardiovascular diseases, such as heart failure (HF), regular exercise training has been shown to improve cardiac outcome, including a stronger circulation and lower blood pressure [30]. Hypertension in aging subjects is often associated with cardiac β-adrenergic receptor (β-AR) dysfunction and over-activity of the sympathetic nervous system (SNS) [88]. According to the current hypotheses regular exercise at least partly restores the normal SNS activity and thereby improves cardiac function [30]. In aged subjects this exercise-induced improvement has been shown to be mediated by an enhanced left ventricular inotropic response to Ca^{2+} [2, 109]. Furthermore, exercise and insulin concentration are connected, since glucose levels are dropping during exercise and are increasing during food uptake [101]. Exercise is also found to improve insulin sensitivity by providing a simplified glucose transfer into muscle cells [101].

1.6. Acute and chronic exercise as modulators of skeletal and cardiac titin

Studies suggest that changes in the passive titin based myofilament stiffness may also contribute to the beneficial effects of physical activity such as running on a treadmill [20]. There is a connection between titin stiffness and ventricular function and it has been shown that increased titin compliance improves diastolic function (reviewed in Linke and Hamdani 2014 [94]). On the other hand, titin stiffening may also support the length-dependent activation involved in the Frank Starling mechanism of the heart, which is responsible for the elevated cardiac output in response to increased preload [82]. In recent experiments, adult mice were exercised for 3 weeks and biopsies of their cardiac tissue were analyzed. Significant phosphorylation changes in the posttranslational

modification of the two titin domains N2-Bus and PEVK were detected [20]. The investigated changes imply an exercise-induced decrease in cardiac titin stiffness, which may help diastolic filling and thereby improve cardiac output in the trained animals. In contrast, the changes in titin modification detected in trained skeletal muscles suggest an increase in titin stiffness, which may help to maintain the structural integrity of the exercised muscle tissue [20].

1.7. Aim

Insulin has been identified to be involved in the regulation of isoform switching and signal transduction leading to phosphorylation of the essential scaffolding muscle protein titin. Since insulin signaling is altered in heart disease such as diabetic cardiomyopathy, titin-dependent changes in a specific disease setting where insulin homeostasis is disturbed are to be identified, resulting in the basic hypothesis of the work at hand. Therefore, the aim of this study was to firstly investigate how phosphorylation of the molecular spring titin and associated cardiac proteins are controlled and influenced in heart muscle tissue of diabetes mellitus type II patients that underwent cardiac surgery. Moreover, how the anti-diabetic drug medication and already modified insulin signaling in DM might subsequently have an impact on titin based myofilament stiffness in the myocradium, possibly explaining diastolic dysfunction frequently associated with DM. In order to investigate the direct influence of anti-diabetic medication on cardiac titin and on the basis of previous findings, treatment with insulin and metformin in cell culture models with primary isolated cardiomyocytes from adult and embryonic rats were performed.

In the second part, the effect of different types of exercise regimes with adult rats were conducted in order to investigate physiological effects on heart and skeletal muscle titin. Specifically, the modification of titin based passive stiffness, the phosphorylation status and pathway interactions of cardiac and skeletal titin upon physical exercise were investigated.

2. Materials and Methods

2.1. Materials

All kits, reagents and stains were if not noted otherwise applied as recommended in the manufacturer instructions.

i. Laboratory equipment

Device	**Type**	**Manufacturer**
Centrifuge	Biofuge 13	Heraeus
Centrifuge	Megafuge 1.0	Heraeus
Centrifuge	Rotofix 32	Heraeus
Chemiluminescence imager	FUSION SOLO	Vilbert
CO2 Incubator	Heracell 150i	Thermo scientific
Electro - blotting	Trans Blot Turbo	Biorad
Electro - blotting	Fastblot B44	Biometra
Electrophoresis - board	Mini-Twin	Biometra
Freezer	Typ 311104	Liebherr
Infrared imaging system	Oyssey	Licor
Magnetic mixer	IKA RTC Classic	IKA
Micro centrifuge	mini CX73.1	Roth
Microscope	ID03	Zeiss
Microwave	Micromat 135	AEG
Mixer	KL2	Bohler
Monitor screen	Flatron E22 10T	LG
Myocyte force measuring device	Force Transducer System 403A	Aurora Scientific
Orbital shaker	Shaker DOS 10L	Neo Lab
Perialstic pump	Miniplus 3	Gilson
Personal computer	Paola FX	Chieftec
pH meter	MP220	Mettler Toledo
Phospho-Chemiluminescent Imager	LAS-4000	Fuji
Power supplies	Power Pack P25	Biometra
Reagent shaker (Vortex)	444-1372	VWR

Refrigerator	KT1730	Liebherr
Rotating and swaying mixer	RMS-30V	CAT
Rotation mixer	SB2	IKA
Scale	Kern 572	Kern
Special accuracy weighing machine	Ae163	Mettler
Stereo mikroscope	S8APO	Leica
Thermo mixer	Compact 5350	Eppendorf
Thermostat	Thermo C10	Haake
Ultra-Turrax	VOS 14	VWR
Vacuum pump	NO 2522-02	Welch
Water quench	Julabo 20B	Julabo
Water treatment	Milli Q	Millipore
Work bench	Safe 220	Thermo scientific

Table 2.1.: Inventory of the laboratory equipment used for experiments

ii. Buffers and solutions

Buffer	**Composition**
Anode buffer	300 mM Tris(hydroxymethyl)amino methan 100 mM Tricine/ HCL, pH 8.8
Blocking solution	3% BSA in 1x TBST
Collagenase solution	Collagenase B 1 mg/mL Low Ca2+-solution 10 mL, 0.03 mM Calcium chloride
Coomassie stain	40 % Methanol 10 % Acetic acid 50 % aq. dest. 0.1 % Serva blue G
Coomassie destain 1	50 % Ethanol 7 % Acetic acid
Coomassie destain 2	5 % Ethanol 7 % Acetic acid
Gelatine solution	1% Gelatine in PBS
Cathode buffer	300 mM Aminocaproic acid 30 mM Tris / HCL , pH 8.7
LB Medium	10 g Bacto Tryptone 10 g Sodium chloride 5 g Bacto Yeast Extract
LB Medium with agar	10 g Bacto Tryptone 10 g Sodium chloride 5 g Bacto Yeast Extract 15 g Agar
10 x Running buffer	250 mM Tris (hydroxymethyl) amino methan 1.92 M Glycine 1% Sodium dodecyl sulfate
Low Ca^{2+} solution	120 mM sodium chloride 5.4 mM Potassium chloride 5 mM Magnesium sulfate 5 mM Sodium pyruvat 20 mm Taurin 10 mM HEPES 20 mM Glucose 6.9 mM Sodium hydroxide, pH 6.9
Medium	79.9% Iscoves Modified Dulbecco's Medium (IMDM) 20% (v/v) Foetales calf serum (FKS) 1 % (v/v) Penicillin-Streptomycin Aoution (10.000 U/mL) 1 % (v/v) Non-Essential Amino Acids (MEM, 100x) 0.1 % (v/v)β-Mercaptoethanol 5 ng/mL bFGF (Fibrocytegrowfactor)
Phosphat buffered saline	150 mM Sodium chloride 2.5 mM Potassium chloride 1.5 mM Potassium diehydrogen phosphate 3 mM Disodium hydrogen phosphat
ProQ Fixations buffer	50 % Methanol 10 % Acetic acid
ProQ Washing solution	10 % Methanol 7 % Acetic acid
ProQ Destain solution (1L)	50 mM Sodium acetate, pH 4.0 20 % Acetonitrile
Phosphatase Inhibitor Cocktail	500 M Sodium Fluoride, 10 mM Sodium Orthovanadate, 100 mM Sodium Pyrophosphate, Decahydrate, 100 mM beta-Glycerophosphate
PVDF stain	0.075 % Serva Blue in Methanol
PVDF destain	10 % Acetic acid 40 % Ethanol 50% Aqua bidest
Relaxation solution	10 mM Imidazole 3 mM Ethylene glycol tetraacetic acid 10 mM Adenosine 5'triphosphate disodium salt 3 mM Magnesium chloride 47.7 mM Creatinphosphate 2 mM Dithiothreitol
SDS collection gel buffer	500 mM Tris / HCL pH 6.8 0,4% (v/v) Sodium dodecyl sulfate
SDS departing gel buffer	1,5M Tris / HCL pH 8.8 0.4% (v/v) Sodium dodecyl sulfate

SDS sample buffer	8 M Urea 2 M Thiourea 3% (v/v) Sodium dodecyl sulfate 0.035 Serva Blue 10% Glycerol
Stripping buffer	6M Guanidin hydrochloride 20 mM Tris 0.2% Nonident P40 0.1 M β-Mercaptoethanol
50 x TAE	50 mM Ethylendiaminetetraacetic acid 2 M Tris /HCL pH 8 17.5% Acetic acid
10 x TBST	0.5 M Tris/ HCL, pH 8.0 1.5 M Sodium chloride 0.5% Tween - 20

Table 2.2.: List of the buffers and solutions used for experiments

iii. Chemicals

Chemical	**Company**
Albumin fraction V	Roth
2,3 Butanedione monoxime	Sigma
Acetic acid	Appli Chem
Acetone	Sigma
Acetonitrile	Merck
Acrylamide	Roth
Active charcoal	VWR
Adenosine 5‘triphosphate disodium salt	Sigma
Agarose	Biozym
Aminocaproic acid	Appli Chem
Ammonium persulfate	Appli Chem
Angiotensin II human	Sigma
Blebbistatin	Sigma
Boric acid	Sigma
Bovine Serum Albumine	Sigma
Bromphenolblue	Sigma
Calcium chloride	Sigma
Carnitine	Sigma
Collagenase B	Roche
Collagenase Typ 2	Worthington
Creatine	Sigma
Creatinphosphate Na2CrP	Appli Chem
Cytocholasin D	Sigma
Dithiothreitol	Appli Chem
ECL (Western blotting detection reagent)	GE Healthcare
Ethanol	Sigma
Ethylene glycol tetraacetic acid	Sigma
Ethylene diamine tetraacetic acid	Sigma
Fetal Calf Serum	PAA
Glucose	Sigma
Glutathione	Sigma
Glycerol	Sigma
Glycine	MP
Guanidine hydrochlorid	Appli Chem
Heparin	Calbiochem
Hepes	Sigma
Hydrochlorid acid 37%	Appli Chem
Igepal	Sigma
Imidazol	Sigma
Imperial protein stain	Pierce
Insulin	Sigma
Isofluran	Baxter AG
Isopropyl fl-D-1-thiogalactopyranoside	Sigma

Laminin	Roche
L-Name (n-Nitro-L-Arginine Methyl Esther Hydrochl)	Sigma
Lysozym	Sigma
LY294002	Cell Signalling
Magnesium acetate	Sigma
Magnesium chloride	Sigma
Magnesium chloride hexahydrat	Sigma
Magnesium sulfate	Sigma
Medium 199	PAA
Metformin	Sigma
Methanol	Sigma
Mowiol 4-88	Roth
Non Essential Amino Acids	Biochrom
Nonfat dried milk powder	Appli Chem
Nonident P40	Sigma
P-Aminobenzamidine Agarose	Sigma
Penicillin Streptomycin	PAA
Phenol Red	Sigma
Glycoprotein Staining Kit	Pierce
ProLong Gold Antifade Mountant	Life Technology
Potassium chloride	Sigma
Potassium dihydrogen phosphate	Sigma
Potassium hydroxide	Sigma
Pro Q diamond	Invitrogen
Protease Inhibitor Cocktail	Sigma
Protease XIV	Sigma
Pyruvate	Sigma
Rubidium chloride	Merck
Saponin	Sigma
Serva Blue R	Serva Electrophoresis
Skimmed milk powder	Appli Chem
Sodium acetate	Sigma
Sodium chloride	Sigma
Sodium dihydrogen phosphate	Sigma
Sodium dodecyl sulfate	Appli Chem
Sodium hydroxide	Roth
Sodium pyruvate	Sigma
β-Mercaptoethanol	Sigma
Sypro Ruby	Invitrogen
Taurine	Sigma
Temed	Appli Chem
Tergitol	Sigma
Thiourea	Appli Chem
Tricin	Sigma
Tris (hydroxymethyl) amino methan	Appli Chem

Triton X	Appli Chem
Trizol	Invitrogen
Tween 20	Appli Chem
Urea	Appli Chem
Xylenxyanol	Sigma
Ladder page ruler 26616	Thermo scientific

Table 2.3.: Overview of the chemicals used for experiments

iv. Antibodies

Antibody	Dilution	Company
α Actinin	1:1000	Cell Signaling
anti α Actinin	1:1000	Sigma
anti α Actinin	1:1000	Sigma
PKA C phospho (Thr 197)	1:1000	Cell signaling
PKA C α	1:1000	Cell signaling
anti PKC α Phospho	1:1000	Abcam
PKC α	1:1000	Cell Signaling
Phospho-VASP (Ser239)	1:1000	Cell Signaling
Phospho-VASP (Ser157)	1:500	Cell Signaling
VASP	1:500	Cell Signaling
anti PDE5A	1:500	Abcam
anti sGC	1:100	Abcam
anti Insulin Receptor (phospho Y972)	1:1000	Abcam
Phospho Insulin Rezeptor β	1:1000	Cell Signaling
anti GAPDH	1:1000	Sigma
anti Guanylyl Cyclase beta 1 (SGC)	1:100	Abcam
Insulin Rezeptor β (4B8)	1:1000	Cell Signaling
Phosphalamban A1	1:1000	Badrilla
Phosphalamban phospho	1:1000	Badrilla
anti mouse IgG HRP	1:3000	Cell Signaling
anti mouse IgG HRP	1:3000	Cell Signaling
Anti rabbit IGG HRP	1:5000	Acris
Anti mouse IGG HRP	1:3000	Cell Signaling
phospho-PEVK rat	1:100	Eurogentec DE11216
PEVK-control rat	1:1000	Eurogentec
phospho-N2Bus rat (S28)	1:200	Eueogentec DE11215
N2B- control rat	1:1000	Eueogentec
Phosho N2-Bus human 4010	1:500	Eueogentec DE12041
N2B- control human 4010	1:500	Eueogentec
phospho-N2Bus 4099	1:500	Eueogentec ED12002
N2B- control 4099	1:500	Eueogentec
p- N2-Bus S469	1:500	Eueogentec
N2-Bus S469	1:500	Eueogentec
p- N2-Bus S267	1:500	Eueogentec
N2-Bus S267	1:1000	Eueogentec
p - N2Bus S383	1:500	Eueogentec
N2Bus S383	1:1000	Eueogentec
phospho eNOS	1:1000	Cell Signaling
RBM20	1:1000	Eueogentec

Table 2.4.: Table of antibodies used for Western blotting and immofluorescent stainings

Primary and secondary antibodies

Polyclonal titin total as well as phopsho-specific antibodies were generated in rabbits immunized with peptides containing phospho -Ser4010 (VRIEEGK-SLRFPC), -Ser4099 (QANLFSEWLRNID), N2-Bus of full-length human titin, here the peptide nomenclature refers to human cardiac titin; UniProtKB: Q8WZ42), or phospho-Ser11878 (CEVVLKSVLRKR) from the PEVK-region. All antibodies were made and affinity-purified by Eurogentech, Belgium. The primary antibodies were diluted 1:1000. The incubation was done overnight at 4°C for primary antibodies.

Secondary antibodies were diluted 1:500 in 0.5% BSA in TBST. Incubation was performed for 2 hours at room temperature.

v. Human heart samples

For this study 42 patients undergoing cardiac bypass surgery for a period from June 2010 until May 2013 were selected. The group was separated in diabetic (n=23) and non diabetic (n=19) patients. Biopsies were taken from the right artrial auricle and directly deep-frozen in liquid nitrogen and stored at $-80\,^{\circ}\mathrm{C}$ for further analysis. The study has been approved by the ethics committee of the university of Bonn, conforming with the principles determined by the declaration of Helsinki. As all patient underwent similar surgery procedures involving comparable medication, those patients not being additionally associated with type II diabetes mellitus served as a control group. For comparability and classification purposes, the clinical data of patients obtained by their attending physician were anonymized and evaluated. Hemodynamic data, including BP (blood pressure), LVPSP (left ventricular (LV) peak-systolic pressure), LVEDP (LV end-diastolic pressure), CI (cardiac index), LVESV (LV end-systolic volume), LVEDV (LV end-diastolic volume), LVEDVI (LV end-diastolic volume index), LVEF (LV ejection fraction), LVPWT (LV posterior wall thickness), IVST (interventricular-septum thickness), AVAI (aortic valve area index) and LVMI (LV mass index) remain to be compared for both groups.

vi. Rat cardiac and skeletal muscle samples

Female Sprague Dawley rats were trained for the exercise study. They were 13 weeks old and had a weight of approximately 200 grams. Samples from hearts and Latissimus Dorsi muscle (located posterior to the frontal extremities) were obtained. For single cell measurements, Langendorff heart perfusion was performed on hearts of 8-13 week old male Sprague Dawley rats, kept under species-appropriate standard conditions. For ERC, pregnant female Wistar rats were used, also being kept under species-appropriate standard conditions.

vii. Animals and exercise regime

The animals were exercised according to the ethics committee of the university of Cologne and in accordance with the institutional and national guidelines and regulations [90] [91]. All following experimental procedures were approved by the local animal health and care unit as well. In particular, adult female Sprague Dawley rats were exercised for acute exercise, using a treadmill (20 meters per minute) for a single 15 minutes level running bout of either level running (concentric) or with a 20 degrees angle for downhill running (eccentric). For chronic exercise, the animals had two training bouts per day at five days a week over a period of six weeks, again either level or downhill with a 20 degrees angle of the treadmill and with a velocity of 20 meters per minute. The chronic group performed a total of sixty training bouts compared to the acute group with only one bout. All animals were euthanized directly after finishing the last training bout. The control groups were not exercised at all but directly euthanized. Muscle samples were dissected from the left ventricle of the heart and the Latissimus Dorsi muscle (LAT). Samples were deep-frozen in liquid nitrogen immediately after preparation and stored then at $-80\,^{\circ}\mathrm{C}$ until use. Cardiac tissue samples from 6 control animals and 3 level running animals of the acutely and the chronically exercised group were tested. For the skeletal muscle samples, 10 control and 6 level running LAT tissue samples were obtained from both groups.

2.2. Methods

i. Cell culture

All procedures regarding rat-tissue or cells, were conducted in accordance to the guideline of the local animal care and use committee at the university of Düsseldorf.

Preparation of adult rat cardiomyocytes

Adult rat cardiomyocytes (CM) were isolated using a Langendorff perfusion system. Therefore, adult male Sprague Dawley rats with an age of 8 to 12 weeks were terminally anesthetized with isofluran (2% in an exsiccator) followed by an additional cervically dislocated. The thorax was then opened to disrupt the diaphragm. The heart was removed surgically from the rat by dissecting the aorta at a maximal cranial point behind the aortic arch. Cotton was used to soak up following blood. The heart was then put into a prepared petri dish filled with heparin solution to avoid the remaining blood inside from coagulating, as it might impair the perfusion later. The aorta was then canulated and connected to a perfusion apparatus (see figure 2.1.) filled with perfusion buffer. The perfusion buffer was gassed with 100% oxygen and left to perfuse with 5 mL/min for as long as the eluate contained blood. After about 7 minutes, the heart was perfused with an enzymatic buffer containing collagenase and protease for about 25-35 minutes depending on the weight of the heart. Afterwards, the heart had a light reddish coloration and a very soft consistency. The heart was then carefully removed from the perfusion apparatus and transferred into a dish with another enzymatic solution containing calcium. Here, the heart was smoothly torn apart with forceps, then pipetted into a 50 mL falcon and then left in a gently shaking waterbath with 37 °C. The suspension was pipetted up and down every 5 minutes during this incubation. Thereafter, the solution was put through a 200 μm filter to remove excess tissue that could not be dissolved. The cells were spun in a falcon for 2 minutes at 300 rpm. The supernatant was pipetted off the top carefully to remove the enzyme but no cells. The cells were

then transfered into a low concentrated calcium solution, spun again like before and the supernatant was again discarded. This step was repeated another time with a high concentrated calcium solution. The cells were then transferred into prewarmed M199 Hanks cell culture medium containing Pen/Strep and resuspended. Cells were counted and plated ($10000/cm^2$) on dishes previously coated with laminin, to be then left to settle. The medium was augmented with the calcium desensitizer Blebbistatin (12.5 nM) to prevent contraction of the cells. Depending on later experiments the following stimuli were added to the medium: Insulin with a concentration of 175 nM, metformin with 20 mM, the inhibitor LY294002, PLB, PKCα, PKG and PKA.

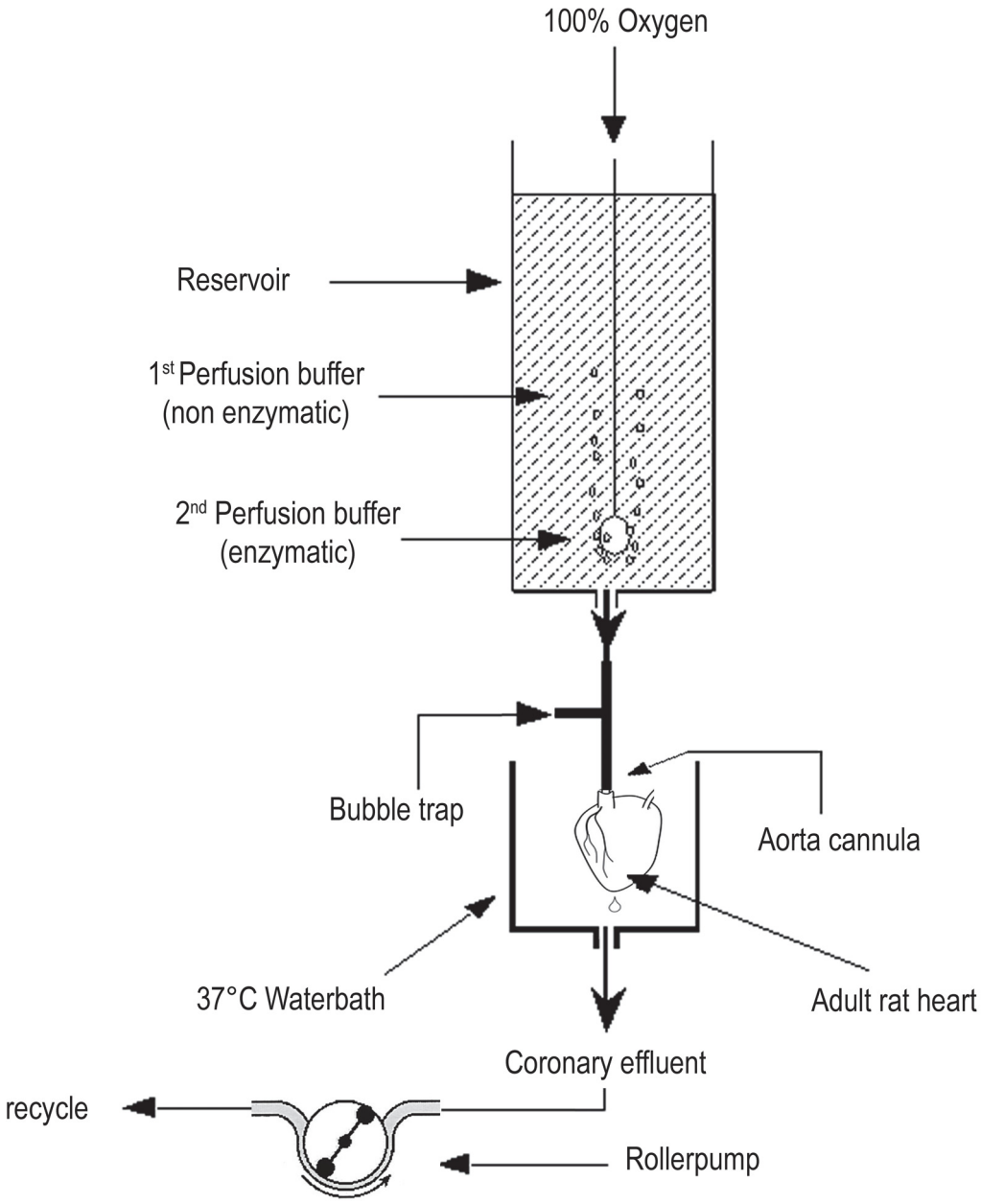

Figure 2.1.: Graphic of the isolated perfused heart, modified from [56].

Preparation of embryonic rat cardiomyocytes

For the isolation and primary cultures of embryonic rat cardiomyocytes (ERC), pregnant rats (gestanial day 18) were anesthetized with isofluran (2%) and killed by cervical dislocation. The 7- 14 embryos were removed from the womb and then decapitated. Their torso was opened with a scissor and the hearts carefully pulled out with forceps and then collected on ice in a petri dish containing PBS. The hearts were first mechanically dissociated with scalpels following enzymatic digestion for 15 to 20 minutes in 30 mg/mL Trypsin and 1 mg/mL collagenase TypII in digestion-puffer at 37 °C. The solution was occasionally pipetted up and down. After 45 minutes 250 μL of prewarmed 1x Trypsin-EDTA-solution was added. 15 minutes later the cell suspension was strained with a 40 μm cell strainer, spun, the supernatant removed and after sedimentation suspended in 15% FBS DMEM. The ERC were plated on gelatine-pre-coated six-well plates (0.5 million/well) and cultured at 37 °C and 5% CO_2. After one night, the medium was changed carefully in order to remove dead cells. On day 2 the cells were serum-starved (1% FBS-starved) for 24 hours. For insulin (10 $\mu g/mL$) or metformin (20 mM) stimulation, the control cells were supplemented with LY294002 (LY) (50 μM) one hour before stimulation. The stimulations were performed for 15, 30 and 45 minutes and 96 hours (only metformin was added on day 8 of cultivation) following lysis in titin sample puffer.

Isolation of rat cardiomyocytes and passive force measurements

For isolation of single rat cardiomyocytes, small samples (3-6 mg) were obtained from left ventricular muscle strips and transferred into relaxing solution (7.8 mM ATP, 20 mM creatine phosphate, 20 mM imidazole, 4 mM EGTA, 12 mM Mg-propionate, 97.6 mM K-propionate, pH 7.0), freshly supplemented with 30 mM 2,3-butanedione monoxime (BDM), 1 mM dithiothreitol (DTT), 1:100 Protease Inhibitor Cocktail (PrIC), and 1:200 Phosphatase Inhibitor Cocktail (PIC). Samples were then repeatedly homogenized with an ultrathurrax at 750 rpm. The myocyte suspension was then centrifuged with 1000 rpm for 3

minutes, resuspended and permeabilized for 3 minutes in the relaxing solution additionally supplemented with 3% Triton-X-100. Myocytes were washed in three to five centrifugation steps at 4 °C and 2000 *rpm* using relaxing solution. After each centrifugation step the supernatant was discarded and the myocyte pellet was resuspended in fresh relaxing solution without Triton-X-100 . The final cardiomyocyte suspension was kept on ice until further experimental use.

ii. Biochemical methods

Protein isolation

The adherent cells were carefully washed with PBS, afterwards 500 μL titin sample buffer (for recipe see table 2.5.) were added to the 2 cm cell culture dish and then cells were harvested with a cell scraper to be transferred into an Eppendorf tube afterwards. The solution was kept on ice or at $-20\,^{\circ}\mathrm{C}$ for further use. Tissue samples were removed from the $-80\,^{\circ}\mathrm{C}$ freezer, put on a watch-glass on ice together with 80-500 μL of titin sample buffer (depending on tissue size) and then mechanically sheared with scalpels. The thick and sticky dilution was transfered into a tube and kept on ice before use. Before applying the sample solution to either SDS-gels or titin-gels, samples were vortexed, spun with a table centrifuge for up to 3 minutes and then heated to $96\,^{\circ}\mathrm{C}$ to be then centrifuged again for another 1-3 minutes.

Solution	**Concentration**
Urea	8 M
Thiourea	2 M
Tris/HCL, pH 6.8	0.05 M
Glycerol (v/v)	10%
TEMED	3%
SDS (v/v)	150 μL
DTT	0.075 M
Serva Blue	0.035 g

Table 2.5.: Titin sample buffer (modified Lämmli-Buffer) recipe

Protein concentration measurement

In order to obtain specific protein concentration a colorimetric protein assay was applied, which is based on an absorbance (in nanometer) shift of the dye. Bradford-reagent was used as instructed in the manual, protein concentration within a solution (in aq. dest.) was measured in a 96-well plate with a

Luminometer. An amount of 20 microgramm dry weight per lane was applied for titin analysis.

Gel electrophoresis

To separate the proteins smaller than titin such as PDE5A (105 kDa), sGC (77 kDa), VASP (46.5 kDa), IR (156 kDa), AKT (56 kDa) and GAPDH (37 kDa), samples with the same protein concentration were loaded onto a 12.5 % denaturating Sodiumdodecylsulphate-Polyacrylamide (SDS)-gel. Firstly a separation gel was poured between two clean glass plates and after polymerization a collection gel was poured on top. The recipe for these gels is shown in table 2.6..

Solution	**Separation gel**	**Collection Gel**
30%Acrylamide-/ Bisacrylamide	6.25 mL	0.667 mL
H_2O, deionised	5 mL	3.65 mL
H_2O/Glycerin	0.75 mL	-
Lower Tris Buffer	3.75 mL	-
Collection Buffer	-	0.625 mL
TEMED	7.5 μL	15 μL
10% APS	75 μL	50 μL

Table 2.6.: SDS gel recipe

To separate the titin molecule, a different recipe for SDS gels was applied. Due to the enormous size of the protein, a much lower acrylamide concentration was used to increase the pore size within the gel to allow all smaller proteins to pass whereas titin can be trapped (Table 2.7.). For titin gels, all ingredients but APS and agarose must be mixed in a beaker and heated to approximately 48 °C. Afterwards, freshly made APS solution and in the microwave shortly melted and cooled down agarose-solution (60 °C, monitored with a thermometer) were added. The mixture was directly pipetted between clean glass plates. Gels

were kept at 4 °C for 3-5 hours to polymerize and then loaded with cells or tissue diluted in titin sample buffer to be run over night in 1 x running buffer for at least 12 hours at 2 mA with a mini-twin electrophoresis system.

Solution	**2.1%**
H_2O	6.5 mL
Lower Tris Buffer	5 mL
30 % Acrylamide- / Bisacrylamide	1.45 mL
20 % SDS	100 μL
TEMED	11.5 μL
APS	150 μL
1.5 % Agarose	6.78 mL

Table 2.7.: Titin gel recipe

Isoform detection with Coomassie Brilliant Blue R-250 SDS gel staining

To detect the separated titin isoforms and estimate their size and ratio, the organic stain Coomassie Brilliant Blue R-250 or Imperial Stain was used as instructed in the manual to stain the protein bands within the SDS gel. After Coomassie staining, two separate destains were necessary to remove surplus staining solution.

Total protein phosphorylation

Total titin phosphorylation was evaluated using the phosphoprotein stain ProQ Diamond. Titin gels (as described above) were incubated in fixation solution for 2 x 40 minutes after running. Afterwards, they were washed carefully in H_2O for 3 x 10 minutes. Then, 35 mL of the ProQ Diamond staining solution were added to stain all phosphorylated proteins present and the gels were kept in a dark room to incubate for 1 hour. After destaining of 40 minutes, the gels were scanned with a Fuji LAS-4000 with an excitation of 530-550 nm and an emission of 580-600 nm. To normalize the phospho-signal to the overall protein

amount, the gels were then incubated with Sypro Ruby staining solution (35 mL) over night. On the next morning, gels were destained to be then scanned again with excitation peaks at about 280 nm and 450 nm as well as emission maxima near 610 nm. The same protein band was stained and scanned twice to evaluate the amount of phosphorylated protein and the total amount of protein within the sample to detect the total phosphorylation status of titin.

Total protein glycosilation

Glycosilation of titin was detected by running SDS gels specifically modified for the size of the molecule (see above) to be then stained with a magenta based stain, detecting all proteins glycosilated in the gel. Afterwards a destain was applied. Both solutions were taken from the Pierce Glycoprotein Staining Kit and used as recommended in the instructions given. SDS gels were photographed with the FUSION SOLO Chemiluminescent Imager for densitometric analysis.

Western Blotting

Separated protein bands on SDS gels were transferred with the turbo blot system to a PVDF membrane to evaluate expression or phosphorylation level through immunodetection. To transfer the protein bands, four 3 MM Whatman-papers were cut to the size of the gel and then soaked in anode buffer and put onto the blotting apparatus. A same-sized PVDF-membrane was firstly activated in methanol, then equilibrated in anode buffer and then positioned on top. The SDS gel followed, as well as another four 3 MM Whatman-papers generously soaked in cathode buffer. Protein transfer of all proteins but titin took 30-50 minutes at about 230 mA, whereas titin was blotted for up to 5 hours at 500 mA with the Biometra system and about 20 minutes at 1.5 mA with the Trans-Blot Turbo Transfer System from Bio Rad. After the blotting procedure, membranes were stained with a PVDF-stain to check for successful protein transfer, then destained with the respective destain (see solution list ii. above) to be then washed with 1 x TBST solution to remove left destain residues. Subsequently, the membrane was incubated with 5%

BSA in TBST for blockage of possible unspecific binding-sites of the antibody. Primary antibodies were added after 1 hour with their respective concentration diluted in 1 x TBST and left to incubate over night at 4 °C on a shaker. On the next morning, the membrane was washed three times thoroughly with 1 x TBST to be then incubated for 1 hour at room temperature with the respective secondary antibody diluted in 1 x TBST as well. Afterwards, the membrane was washed again to be then scanned after adding the ECL- detection reagent for detection of horseradish peroxidase (HRP) enzyme activity with either the Fuji LAS-4000 or the FUSION SOLO Chemiluminescent Imager with exposures depending on antibody properties.

Fluorescence immunostaining

Cells were fixated on a laminin-coated cover slip previously placed in a 24-well-cell culture plate with PFA. In order to permeabilize the cell membrane 0.5% Triton X-100 or Saponin was pipetted on top and left to incubate for 10 minutes. Afterwards, the cells were washed with PBS twice for 5 minutes at a time. Then the first antibody (in 2% BSA) was left on the cells for an hour and was then washed of again three times with PBS. A control group was incubated with PBS in 2% BSA instead of the first antibody, to avoid unspecific binding. The secondary antibody (in 2% BSA) was applied in the dark (FITC, DAPI or Cy3-linked) for another hour, to avoid light reactions. Three washing steps with PBS later, the cover slips were mounted onto a microscope slide with a drop of Mowiol or ProLong Gold, already containing DAPI. They were left to dry at RT over night. Some cells were stimulated in advance, namely with insulin (175 nM), metformin (20 mM) and a control (Aq. dest.), adult rat CMs were only stimulated for 15 minutes due to their fragility and shorter life span after isolation.

Fluorescence immunostaining of stretched adult rat cardiomyocytes

After isolation of the adult rat cardiomyocytes with a Langendorff perfusion, cells were transferred into an Eppendorf tube containing perfusion buffer and

a medium calcium concentration. Cells were skinned with 0.5% Triton. The first antibody (see above) was added directly to the tube. It was then gently inverted and left on a slow shaker to incubate. The second antibody was pippetted into the cell-suspension containing tube, after covering it with tin foil to keep it from light. All washing steps were performed particularly careful to avoid damaging of the fragile cells. A small drop of already stained cell suspension was then pipetted onto a slide and then cells were sorted under the microscope and fixated between a force transducer and a length controler (Figure 2.2.) to take pictures under slack and stretched conditions.

iii. Biophysical methods

Force measurements on isolated cardiomyocytes

PT measurements were performed on adult rat CMs isolated by Langendorff perfusion as described above, and on human cardiomyocytes isolated from tissue biopsies as previously described [1]. Therefore, biopsies (3-6 mg) from diabetic and control patients were therefore transferred into relaxing solution and then repeatedly homogenized with an ultrathurrax to disrupt the small tissue samples at 750 rpm for 3 seconds. These mechanically isolated human cardiomyocytes and with the help of Langendorff perfusion isolated adult rat cardiomyocytes were at all times kept in relaxing solution supplemented with BDM-30 mM 2.3-butanedione monoxime, PrIC-Protease Inhibitor Cocktail (P8340), DTT- Dithiothreitol and PIC-Phosphatase Inhibitor Cocktail (PP1). Afterwards, they were permeabilized in this respective solution continuing 3% Triton X-100 for three minutes. Several centrifugation steps were performed in order to wash the pellet and remove the detergent containing supernatant. Therefore the cells were spun at 4 °C and 2000 rpm and then kept on ice until use. The CM-suspension was then transferred on a cover slip mounted on an inverse phase contrast microscope (Nikon eclipse Ti) were one single cell was fixated between a piezoelectric motor and a force transducer 403A (aurora scientific) both tipped in silicone glue (Dow Corning) (Figure 2.2.). Passive tension (PT) of each cell was determined in correlation with the sarcomere

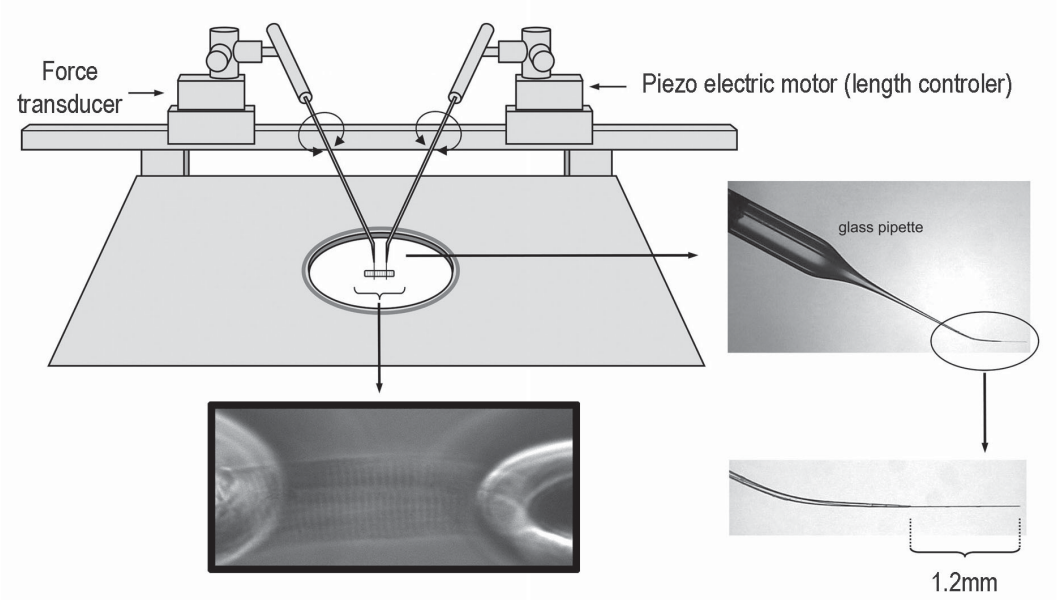

Figure 2.2.: Overview of the stretching device used for isolated cardiomyocytes. Sledges, mounted to an optical railing system, allow for coarse manual positioning and support precise alignment of piezo translators that are used for fine control during force-length manipulations. Passive tension (mN over mm^2) of single cardiomyocyte fixed between a force transducer and a piezo-controlled length driver are measurable, modified from [41].

length in a range of 1.9 μm to 2.4 μm with an IMPERX camera. Stretching of one cell was performed with a step-wise protocol until 150% maximum slack length was reached.

Cells were stretched from slack SL (average, 1.8 μm) in five steps to a maximum sarcomere length (SL) of 2.6 μm. In between the stretches a short hold period of 5 seconds was performed to wait for stress relaxation. Following the last stretch-hold, cardiomyocytes were released back to slack SL to test for possible shifts of baseline force. During the stretch protocol, sarcomere length was recorded with the camera. From the recordings the force at the end of each hold period (near steady-state force) was analyzed. Passive force was related to cross-sectional area (passive tension) determined from the diameter of the cardiomyocytes (assuming a rectangular shape).

iv. Data analysis

For statistical evaluation, bands stained with Imperial, Coomassie stain, ProQ-Sypro Ruby or from Western Blot analysis were measured densitometrically with Multi Gauge V4.2 (Phoretix). The values shown represent the mean and the corresponding standard error of the mean (SEM). Each experiment was replicated three to seven times independently for statistical relevance. Statistical analysis was performed using unpaired student t-test and the Mann-Whitney U test. p-Values under 0.05 were taken as statistically significant.

v. Software

Apart from being mentioned in context, primarily used software included TeXworks, Microsoft Excel, Microsoft Powerpoint, Multi Gauge V3.2., sigma plot 10, OriginLab 9.1, Correl Draw, Photoshop, texmaker and science slides.

3. Results

3.1. Clinical characteristics and titin isoform expression of patients with aortic stenosis and aortic stenosis with diabetes mellitus

Clinical data of a group of aortic stenosis patients all undergoing cardiac surgery were medically examined and registered at the heart and thorax surgery ward of the university clinic of Bonn, according to medical standard procedures (see table 3.1.). These included physical characteristics, sex, age and their medication. In particular anti-diabetic drugs for the aortic stenosis patients concomitantly suffering from type II diabetes mellitus. Therefore, the data were used to classify patients clinically into a type II DM and a non-type II DM group, due to their insulin and metformin administration and check for their comparability. However, classification of samples regarding clinical data and pharmacological treatment lead to the result, that no significant changes in titin isoform composition were detectable in patients with type II DM (DM) compared to the patients with no type II DM (Control). In non diabetic heart samples, the average titin isoform composition was 50.5 ± 1.1% N2B and 49.5 ± 1.1% N2BA and 45.5 ± 0.88% N2B and 54.5 ± 0.88% N2BA (Figure 3.1.). Interestingly, some DM-patients were associated with low or near to normal HbA1c levels, indicating high compliance and optimal medication. In contrast to the previous classification, the patient pool was therefore separated into two groups of those with an HbA1c (see table 3.1.) of less than 6.5% and those showing HbA1c values over 7.5% resulting in significant titin composition

changes measurable. The patients' HbA1c has been correlated with their N2BA composition, being significantly increased in those with elevated HbA1c values. Figure 3.1. shows the N2BA expression increase to 64 ± 0.91% N2BA and for the N2B subsequent reduction to 36 ± 0.91%. The two groups of patient-biopsies compared in this study, remained separated by their HbA1c for all following results, but were marked as diabetics, since the group with a high HbA1c (above 7.5%) exclusively contained type II diabetics, whereas the control also includes well medicated and compliant type II diabetics, with low HbA1c values below 6.5%.

Criteria	**Control Group (Aortic stenosis) (n=19)**	**Diabetic Group (Aortic stenosis - Diabetes mellitus) (n=23)**
Age, y	68.8 ± 7.4	68.2 ± 8.6
Male, n	16	17
Body mass index, kg/m^2	28.9 ± 6.1	29.7 ± 4.8
Obesity, n	6/19	10/23
Hypertension, n	19/19	23/23
Insulin	0/19	0/23
Metformin	0/19	12/23
β-blocker	17/19	17/23
HbA1c	5.6 ± 0.25	7.1 ± 0.71

Table 3.1.: Clinical characteristics of aortic stenosis and aortic stenosis-diabetes mellitus patients

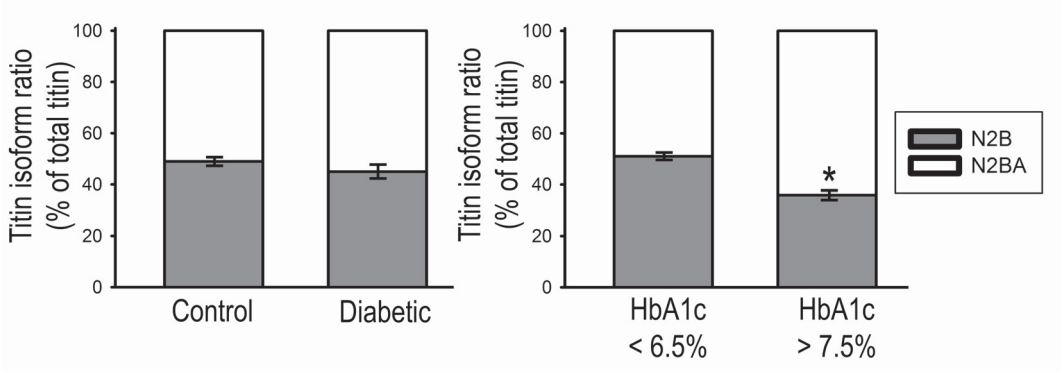

Figure 3.1.: Titin isoform composition from control and diabetes mellitus patients (N2BA+N2B=100%) on the left determined from coomassie-stained SDS gels and N2BA titin isoform in correlation to HbA1c on the right. Samples were taken from right atria of diabetic (n=12) and non diabetic (n=9) patients that underwent cardiac surgery due to coronary artery disease. Statistical significance is marked by asterisks ($p < 0.05$ in Student's t-test).

3.2. Passive tension of cardiomyocytes from type II diabetics with elevated HbA1c levels

Skinned and relaxed cells of the patients diagnosed with diabetes in comparison to the control were measured for their passive tension by obtaining the correlation between the passive length-tension and the sarcomere-length (see figure 3.2.). Although significant changes were detectable by grouping patients by their diagnosis and not their blood test results, like already applied for isoform analysis (see figure 3.1.) the patient pool was firstly again differentiated by their status of being diabetic and not their increased HbA1c levels. Those patients diagnosed with diabetes showed significantly higher PT values at SL from 1.9 μ to 2.2 μ compared to the control group (see figure 3.2. left graph).

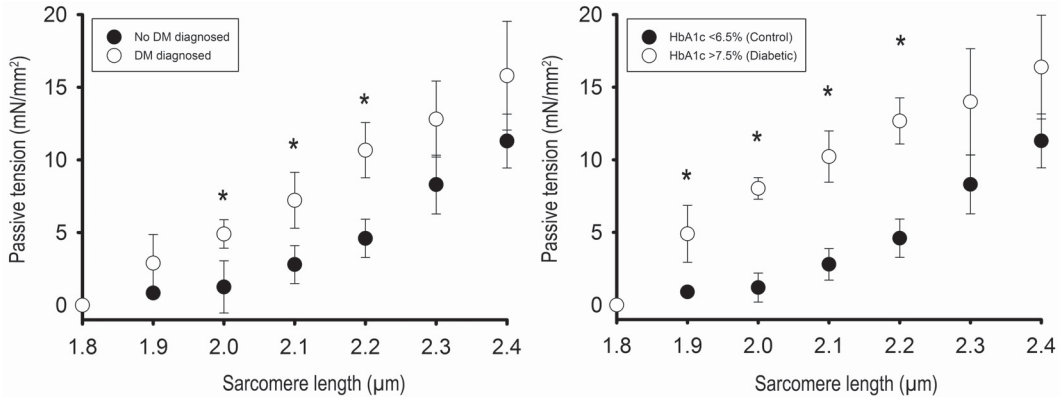

Figure 3.2.: Force extension curve (left) showing passive tension of patients with a diagnosed diabetes compared to passive forces of cardiomyocytes from a pool of patients with no diabetes serving as a control group (DM diagnosed: n=6, No DM diagnosed: n=8, at least three different cells per individual for both groups) and force extension curve (right) showing passive tension of cardiomyocytes from diabetic and non diabetic patients when classified according to their HbA1c. Statistical significance is marked by asterisks ($p < 0.05$ in Student's t-test).

When grouping the patient pool according to their HbA1c (also serving as an indicator for the degree of the illness) (high HbA1c, n=6 and low HbA1c, n=5) differences in PT were even more pronounced (see figure 3.2. right graph). Between 1.9 μm and 2.2 μm passive tension of the group with an HbA1c >7.5% was significantly higher (At SL 1.9 μm by over 500%, at SL 2.0 μm by over 600%, at SL 2.1 μm by over 300%, and at SL 2.2 μm by close to 300%) than in the group with a HbA1c <6.5% and differences in passive forces were even more dominant than in comparison to the graph on the left in figure 3.2.. Statistical significance of passive forces at different sarcomere lengths for the diabetic and control patient pool is highlighted in a bar graph in figure 3.3.. The patient pool marked as control had a HbA1c lower than 6.5% and only contained patients never diagnosed as diabetic or particularly well medicated and compliant type II DM patients. The patient pool marked as diabetic only contained patients with a HbA1c higher than 7.5% and a type II diabetes diagnosis.

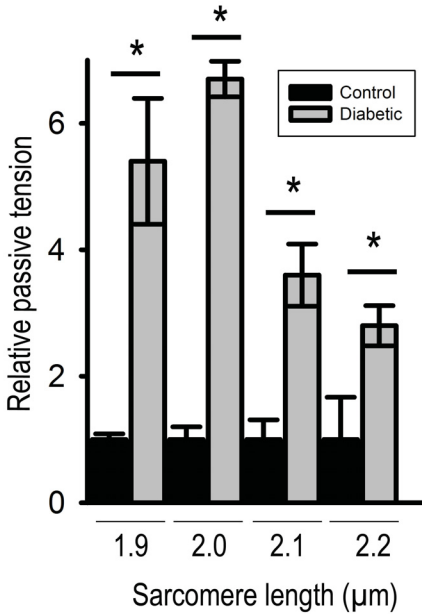

Figure 3.3.: Bar graphs highlight the statistically significant differences in passive tension of cardiomyocytes from diabetic patients with a high HbA1c of >7.5% and non diabetic patients with a low HbA1c of <6.5% (Control) when classified according to their HbA1c at sarcomere length (SL) 1.9, 2.0, 2.1 and 2.2 μm (high HbA1c: n=5, low HbA1c: n=6, at least three different cells per individual for both groups). Statistical significance is marked by asterisks (p <0.05 in Student's t-test).

3.3. Cardiac titin phosphorylation in type II diabetic mellitus patients with elevated HbA1c levels

The biopsies from type II DM patients with a high HbA1c (Diabetic) and the control group were further analyzed in order to identify differences in titin phosphorylation which may result in altered passive stiffness of the patients' cardiomyocytes. Phosphorylation at specific sites within the titin molecule was determined with the help of immonublotting and custom-made phosphospecific antibodies to N2-Bus Ser4010 (targeted by PKA and ERK) and Ser4099 (targeted by PKG) of full-length human titin and the PEVK region Ser11878 (targeted by the PKCα).

The average phosphorylation of titin N2-Bus at Ser4099 and for the N2BA isoform at Ser4010 was significantly lower in the DM group versus the control. For Serine residue 4010, type II diabetics showed 16% to 0.84± 0.05 less phosphorylation of the N2BA isoform and for the N2B isoform 10% to 0.9± 0.08 less phosphorylation (without significance compared to the control for the N2B). The second Serine residue analyzed was 4099, where diabetics showed 21% (0.79± 0.015) less phosphorylation of the N2BA isoform and over 30% less phosphorylation to 0.65± 0.027 of the N2B isoform (Figure 3.4.). In contrast, the average PEVK phosphorylation at Ser11878 showed a significant increase to 1.27± 0.024 of the N2BA and to 1.49± 0.048 of the N2B isoform in the diabetic group compared to the control (Figure 3.5.).

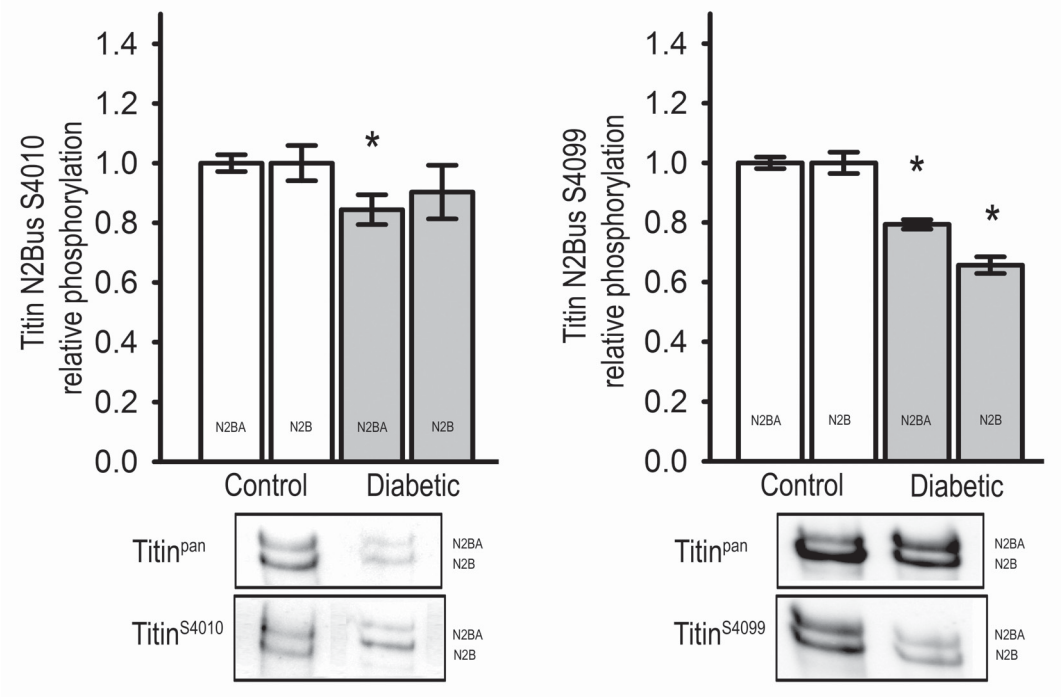

Figure 3.4.: Western blot analysis of membranes probed with antibodies recognizing either pSer4010 (left) and pSer4099 (right) in the titin N2-Bus region (n=9 control and n=12 diabetics). Statistical significance is marked by asterisks ($p < 0.05$ in Student's t-test).
Bottom: Representative Western blots show titin bands visualized by antibodies to total N2-Bus and the respective phosphosite (pN2-Bus).

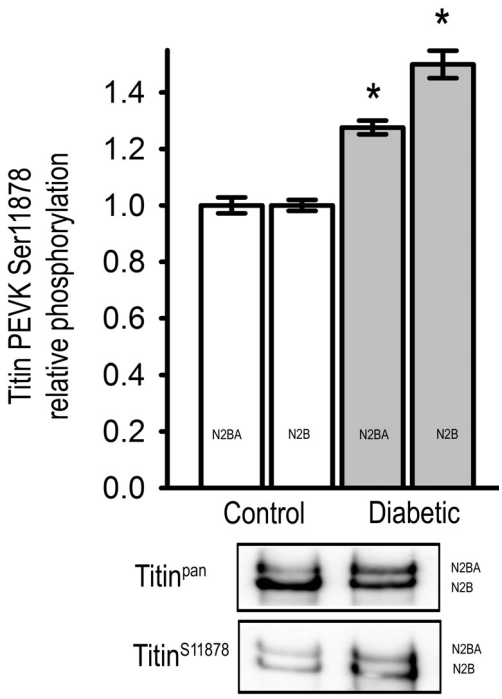

Figure 3.5.: Western blot analysis of membranes probed with antibodies against the pSer11878 in the PEVK region of titin (n=9 control and n=12 diabetics). Statistical significance is marked by asterisks ($p < 0.05$ in Student's t-test).
Bottom: Representative Western blots show titin bands visualized by antibodies to total PEVK and the respective phosphosite (pPEVK).

3.4. Phosphorylation and expression levels of myocardial proteins involved in titin phosphorylation

The increased phosphorylation of titin's PEVK region at Serine residue 11878 suggested elevated activity of PKCα. Phosphorylation at T497 indicated activation of the PKCα and was determined by Western blot analysis using phospho-specific antibodies. Indeed PKCα T497 levels were higher in diabetic samples, but results were not statistically significant. The next aim was to find possible reasons for reduced titin phosphorylation levels at Serine 4099 of diabetic patients. The PKG signal cascade was examined, as PKG phosphorylates the titin molecule at this specific site. Factors limiting the cofactor cGMP of PKG are sGC, stimulated by PKG and PDE5A (that selectively degrades cGMP), inhibited by PKG.

Antibodies targeting the phosphodiesterade 5A (PDE5A), soluble guanyl cyclase (sGC), Vasodilator-stimulated phosphoprotein (VASP), Insulin Receptor (IR) and GAPDH (Glyceraldehyde 3-phosphate dehydrogenase) were applied to Western blot membranes in order to identify the expression level of the respective protein in biopsies of diabetic and control patients (see figure 3.7.). Expression levels of IR, PDE5A and sGC were normalized to the expression levels of GAPDH, which serves as a loading control. PDE5A catalyzes cAMP and cGMP hydrolysis, expression level can therefore be correlated to PKG activity. sGC in turn promotes cGMP production, which in turn can be inhibited by PDE5A. It can therfore additonally be correlated to expression levels of the PKG which in turn phosphorylates the giant protein titin on many different phosphosites, causing substantial changes in titin-based passive tension of cardiomyocytes in the myocardium. VASP is a PKG substrate and therefore also serves as an indirect activity indicator. The Insulin Receptor Y972 being a tyrosine kinase receptor is present in cell membranes of insulin sensitive tissue and expressed upon insulin production in the pancreas. Expression levels of PDE5A showed an increase to 2.19 ± 0.13, whereas sGC levels were

significantly decreased by nearly 50% to 0.52 ± 0.11. VASP, showed increased level of activity since phosphorylation was over 20% higher at 1.23± 0.04 in diabetic patients (Figure 3.8.). The Insulin Receptor Y972 showed a 20% significant elevation to 1.22 ± 0.05, when normalized to GAPDH expression level (see figure 3.8.).

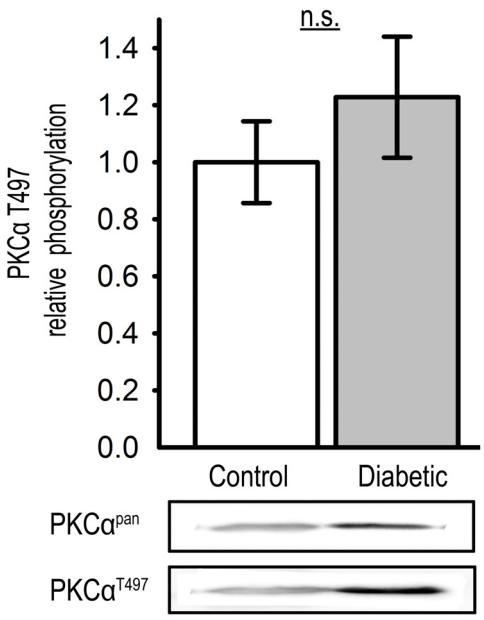

Figure 3.6.: Detection of total and phospho (T497) PKCα in diabetics with high HbA1c levels (>7.5%) compared to the control (Control and Diabetic (n=3, respectively). Statistical significance is marked by asterisks (p <0.05 in Student's t-test).
Bottom: Representative Western blots show PKCα bands visualized by antibodies to total PKCα-pan and the respective phosphosite (PKCα T497).

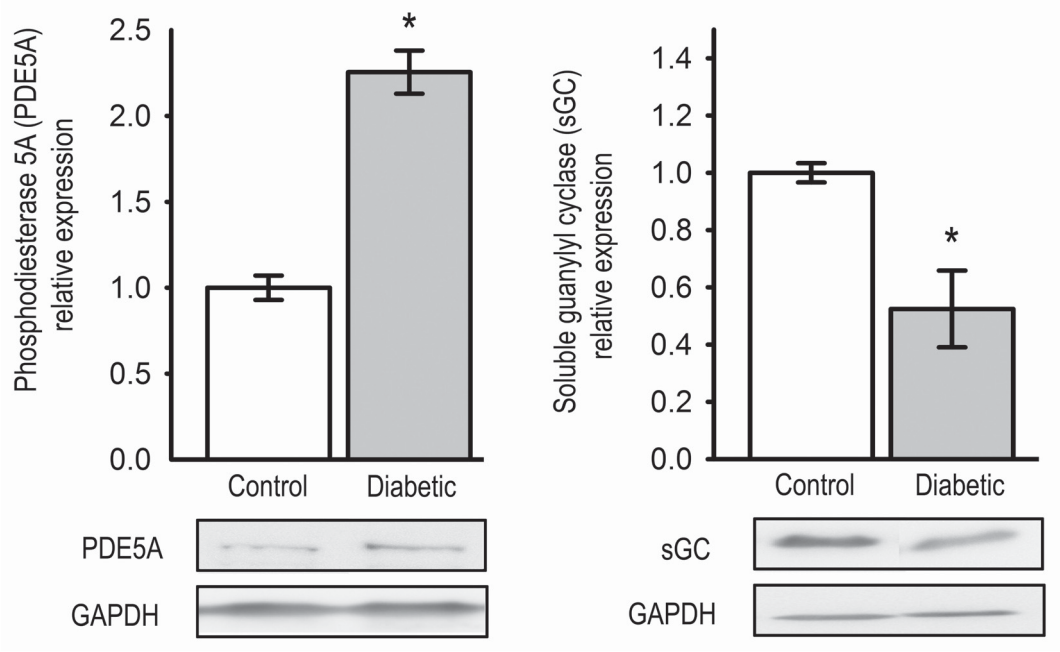

Figure 3.7.: Analysis of PDE5A (n=5) expression levels (left) normalized to GAPDH and expression of myocardial sGC (n=4) (right) in diabetics with high HbA1c levels (>7.5%) compared to the control, analyzed with Western blot methodes. Statistical significance is marked by asterisks.
Bottom: Representative Western blots show PDE5A and sGC bands visualized by antibodies to both cardiac proteins and GAPDH.

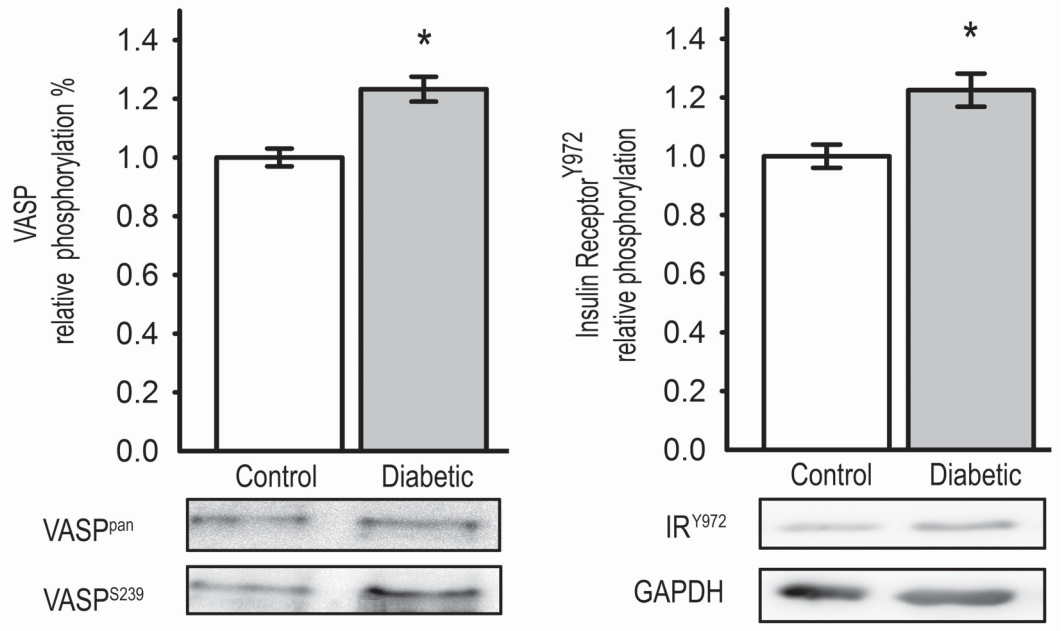

Figure 3.8.: Western blot analysis of VASP (n=3) level applying anti phospho VASP and anti total VASP antibodies (left) and relative phosphorylation of IR Y972 (right) in diabetic patients with increased HbA1c levels (>7.5%) compared to the control group, normalized to GAPDH (n=4). Statistical significance is marked by asterisks ($p < 0.05$ in Student's t-test).
Bottom: Representative Western blots show VASP and IR bands visualized by antibodies to total VASP (PAN) and the respective phosphosite (VASP S329) as well as total IR (Y972) and GAPDH.

3.5. Titin N2-Bus phosphorylation in insulin and metformin treated adult rat cardiomyocytes

In order to specifically analyze insulin-dependent signaling in cardiomyocytes, cell culture models were applied. Thus, the phosphorylation status at Ser4099 of titin's N2-Bus after stimulating adult rat cardiomyocytes isolated via Langendorff perfusion with insulin and metformin *in vitro* was determined. The culture medium was supplemented with insulin (175 nM) or metformin (20 mM) with or without addition of the PI3K-inhibitor LY294002 (LY) (50 μM). Cells were stimulated with insulin for 15 min in order to check for immediate effects and for 24 hours to evaluate longer lasting effects regarding titin phosphorylation. After 15 minutes of insulin stimulation (n=17), a significant increase of 40% to 1.4± 0.05 in N2-Bus phosphorylation at Ser4099 was detectable (Figure 3.9.). Insulin-induced titin phosphorylation was successfully and significantly inhibited by LY294002 (n=9) to 0.75± 0.11 with insulin and to 1.09± 0.14 without stimuli. After 24 hours (n=13) a over 30% increase to 1.32± 0.08 of Ser4099 phosphorylation was still detectable, compared to the control. Inhibition indicated less phosphorylation than in stimulated cells. Metformin stimulation for 15 minutes (n=6) showed comparable results titin N2-Bus Ser4099 phosphorylation. After 15 minutes of stimulation to 1.38± 0.09 as well as for 24 hours (n=3) of metformin stimulation to 1.25± 0.12 and inhibition (n=3) with LY and metformin to 0.95± 0.18 and without stimuli to 1.09± 0.14.

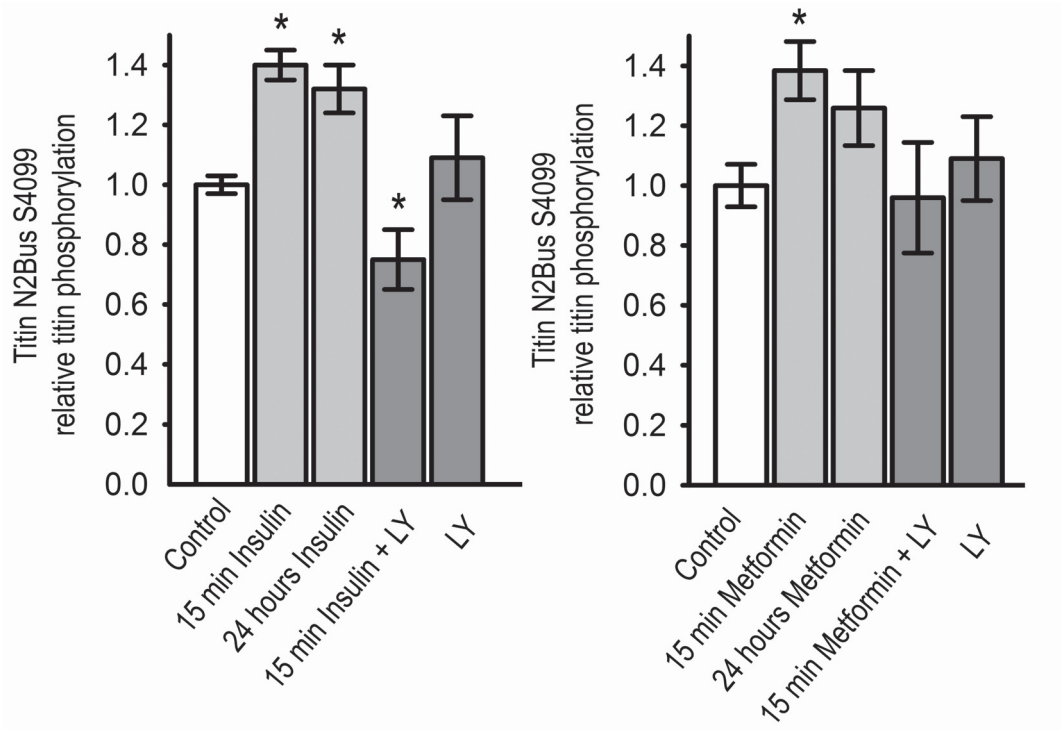

Figure 3.9.: Phosphorylation status of titin's N2-Bus at Ser4099 in isolated adult rat cardiomyocytes after treatment with insulin (175 nM) for 15 minutes and 24 hours respectively, and after treatment with the PI3K inhibitor LY294002 (left), (Insulin, 15 min n=17; 24h n=13; LY + Insulin, 15 min n=9; LY, 15 min n=4). Phosphorylation status of titin's N2-Bus at Ser4099 in isolated adult rat cardiomyocytes after treatment with metformin (20 mM) for 15 minutes and 24 hours respectively, and after treatment with the PI3K inhibitor LY294002 (right), (Metformin, 15 min n=6, 24h n=3; LY, 15 min n=4; LY + Metformin, 15 min n=3; LY, 15 min n=4). Statistical significance is marked by asterisks (p <0.05 in Student's t-test).

3.6. Titin PEVK phosphorylation in insulin and metformin treated adult rat cardiomyocytes

The phosphorylation status of titin's PEVK after stimulating adult rat cardiomyocytes isolated via Langendorff perfusion with insulin and metformin *in vitro* was determined. The culture medium was supplemented with insulin (175 nM) or metformin (20 mM) with or without addition of the PI3K-inhibitor LY294002 (LY) (50 μM). Cells were stimulated with insulin or metformin for 15 min in order to check for immediate effects and for 24 hours to evaluate longer lasting effects regarding titin phosphorylation. After 15 minutes of insulin (1.02± 0.38 and with LY: 1.09± 0.36) and metformin (1.11± 0.11 and with LY: 0.99± 0.21) stimulation as well as after 24 hours (insulin: 1.12± 0.26 and metformin: 1.02± 0.31) and exclusively with LY (left bar graph: 1.19± 0.24 and right bar graph: 1.11± 0.31), no significant changes in PEVK phosphorylation at Ser11878 were detectable, compared to the control (Figure 3.10.).

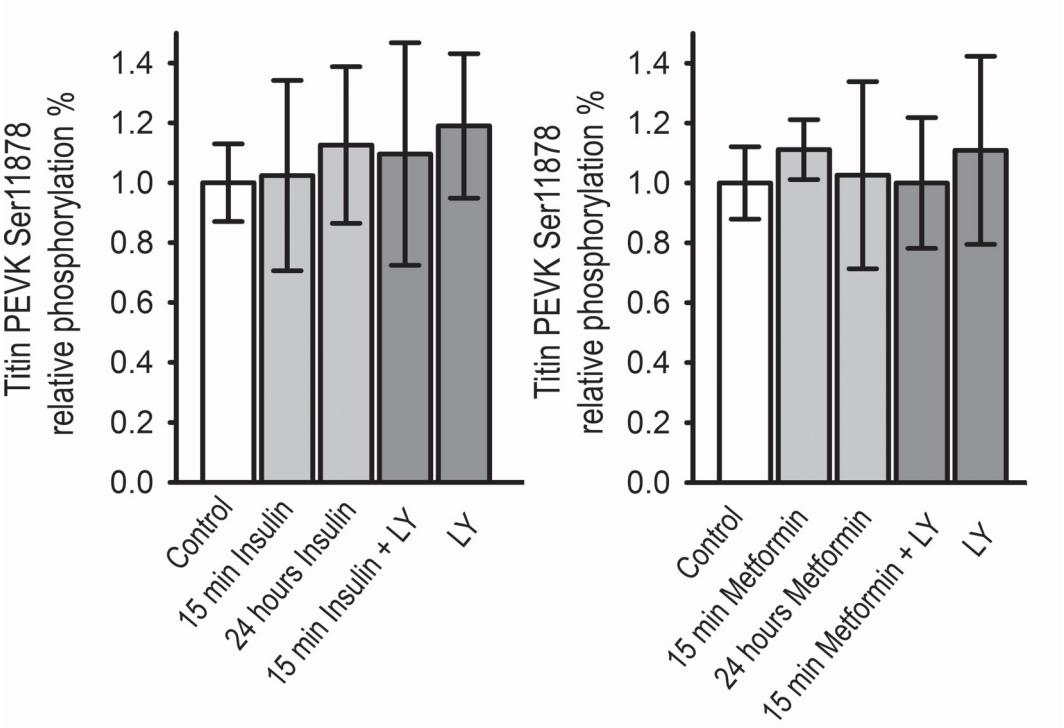

Figure 3.10.: Phosphorylation status of titin's PEVK at Ser11878 in isolated adult rat cardiomyocytes after treatment with insulin (175 nM) for 15 minutes and 24 hours respectively, and after treatment with the PI3K inhibitor LY294002 (left), (Insulin, 15 min n=3; 24h n=3; LY + Insulin, 15 min n=3; LY, 15 min n=3). Phosphorylation status of titin's PEVK at Ser11878 in isolated adult rat cardiomyocytes after treatment with metformin (20 mM) for 15 minutes and 24 hours respectively, and after treatment with the PI3K inhibitor LY294002 (right), (Metformin, 15 min n=3, 24h n=3; LY, 15 min n=3; LY + Metformin, 15 min n=3; LY, 15 min n=3) ($p < 0.05$ in Student's t-test).

3.7. Relative titin glycosilation

In order to investigate, whether altered insulin signaling associated high glucose levels insulin treated(like in type II DM-patients) increase titin glycosilation, the post-translational modification glycosilation (direct binding of glycans) on titin upon stimulation for 15 minutes with insulin (175 nM) and metformin (20 mM) *in vitro* in primary cells from adult rats was evaluated (Figure 3.11.). Titin gels were analyzed with a specific glycosilation stain, showing significantly increased levels of titin glycosilation of over 40% to 1.46± 0.08 after insulin- and over 30% to 1.32± 0.13 after metformin-treatment.

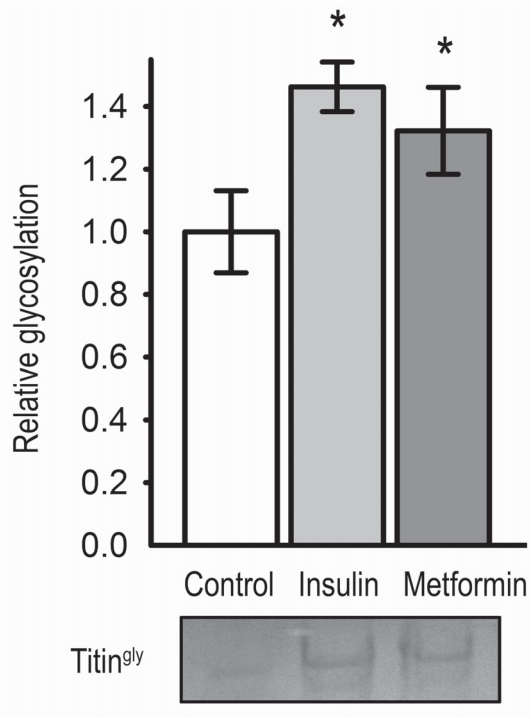

Figure 3.11.: Sensitive and specific staining of glycosylated titin in adult rat cardiomyocytes treated with insulin and metformin, compared to a control group with no treatment (n=3). Statistical significance is marked by asterisks ($p < 0.05$ in Student's t-test).
Bottom: Representative SDS gels show titin bands visualized glycosilation stain, targeting glycosilated proteins.

3.8. AKT phosphorylation in insulin treated adult rat cardiomyocytes

To confirm activation of the insulin signaling cascade relative AKT phosphorylation was determined in isolated adult rat CMs treated with insulin (175 nM) *in vitro* for 15 minutes. Similar results for both phosphosites at Ser473 and at Thr308 can be observed. For Ser473 a 100% to 1.99± 0.36 increase was measurable and for Thr308 it was over 70% to 1.78± 0.19 (Figure 3.12.). For detection purposes phospho-specific antibodies were applied to WB membranes.

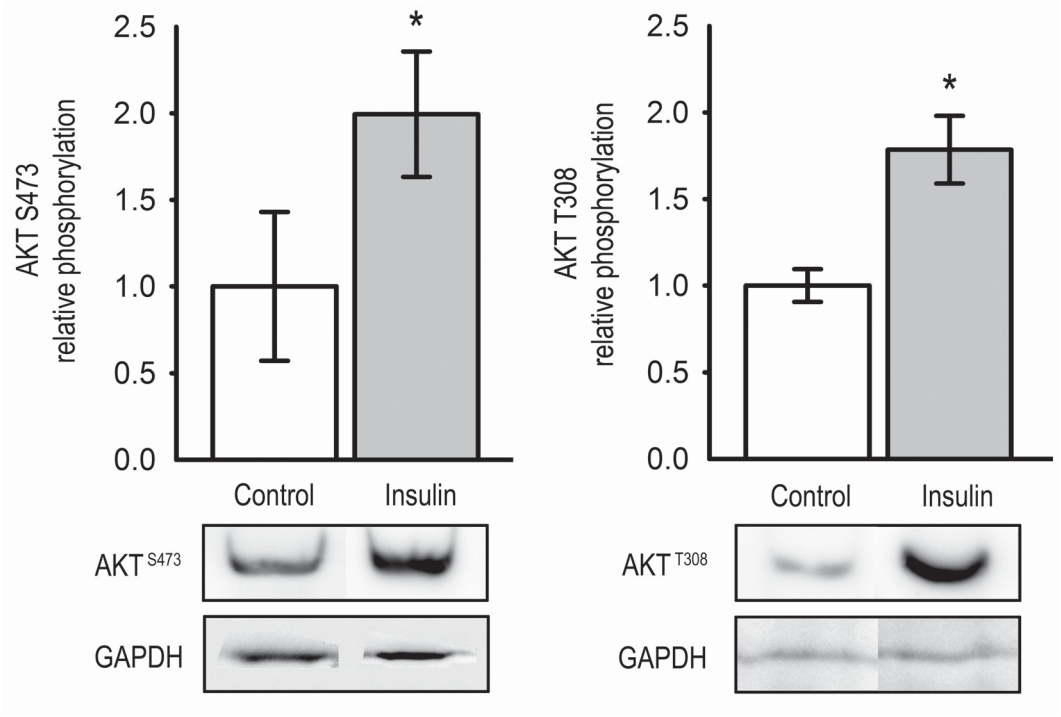

Figure 3.12.: AKT phosphorylation at Ser473 (left) and T308 (right) in adult rat CMs (treated with insulin and untreated, n=3, respectively). Statistical significance is marked by asterisks ($p < 0.05$ in Student's t-test).
Bottom: Representative Western blots show bands for Ser473 and Thr308 visualized by binding of phospho-specific antibodies for both AKT-phosphosites and GAPDH for normalization.

3.9. eNOS phosphorylation in adult rat cardiomyocytes upon insulin stimulation

The endothelial nitric oxide synthase (eNOS) generates NO primarily blood vessels and is activated by AKT via the PI3K-pathway. Hence, NO synthesis is reduced in insulin resistant tissue. To investigate the direct effect of insulin treatment in isolated adult rat cardiomyocytes, eNOS activity was analyzed, since it is additionally known to have cardio-protective properties (Figure 3.13.). In primary CM, eNOS activity was increased by about 30% to 1.33± 0.14 when stimulated with insulin and seems to be inhibited (though not significantly compared to the control), when treated with LY (LY 0.72± 0.51 and insulin with LY to 0.7± 0.39). All stimulations were applied for 15 minutes *in vitro*.

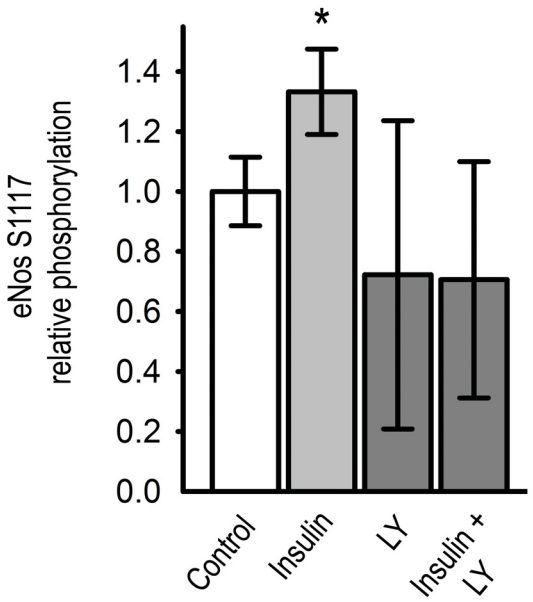

Figure 3.13.: Activation of eNOS by relative phosphorylation in adult rat cardiomyocytes treated with insulin, LY and both (for 15 minutes) compared to the control (n=4). Statistical significance is marked by asterisks ($p < 0.05$ in Student's t-test).

3.10. Mechanical measurements of adult rat cardiomyocytes

Adult rat cardiomyocytes isolated by Langendorff perfusion were additionally stimulated. Therefore the culture medium was supplemented with insulin (n=12) with 175 nM, metformin (n=4) with 20 mM, PKCα (n=3) with 125 units, or left untreated as a control (n=17) (Figure 3.14.-3.16). Furthermore, cells were treated with PKG and PKA (125 units each), which showed no evaluable alterations in passive stiffness of the cardiomyocytes (Data not shown). In order to determine the stimulation effect on the passive force properties of the CM, cells were attached with silicone adhesive between a force transducer and a piezoelectric motor and measured for their PT. Between a SL of 2.0 μm and 2.4 μm, treated cells were significantly stiffer compared to the control. For insulin treatment at SL 2.0 μm by over 200%, at SL 2.1 μm by nearly 250%, at SL 2.2 μm by close to 240%, at SL 2.3 μm by nearly 200% and at SL 2.4 μm by close to 250%) treated cells were up to 300% increased in passive stiffness as well as those treated with metformin at SL 2.0 μm by over 150%, at SL 2.1 μm by nearly 60%, and at SL 2.2 μm by close to 170%) and with PKCα at SL 1.9 μm by over 350%, at SL 2.1 μm by nearly 60%, and at SL 2.2 μm by close to 30%.

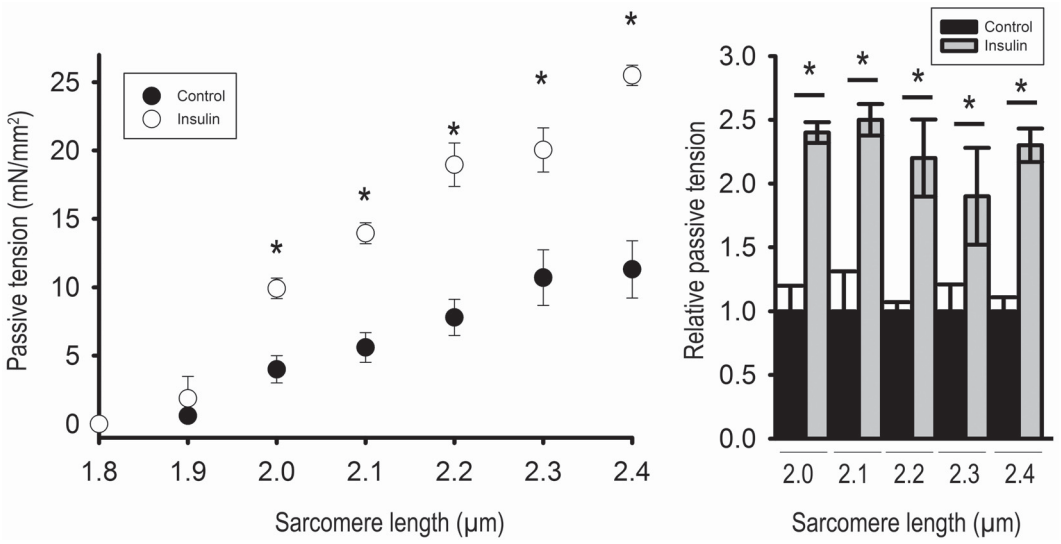

Figure 3.14.: Passive tension of adult rat CMs stimulated with insulin for 15 minutes (n=12) in comparison to untreated cells (n=17). Statistical significance is marked by asterisks ($p < 0.05$ in Student's t-test).

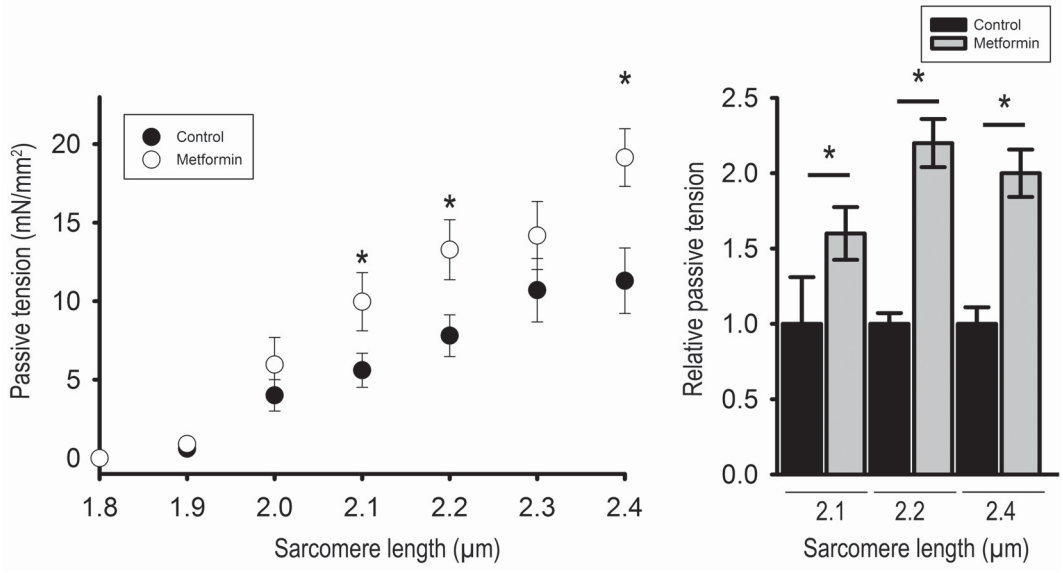

Figure 3.15.: Passive tension of adult rat CMs stimulated with metformin for 15 minutes (n=4) in comparison to untreated cells (n=17). Statistical significance is marked by asterisks ($p < 0.05$ in Student's t-test).

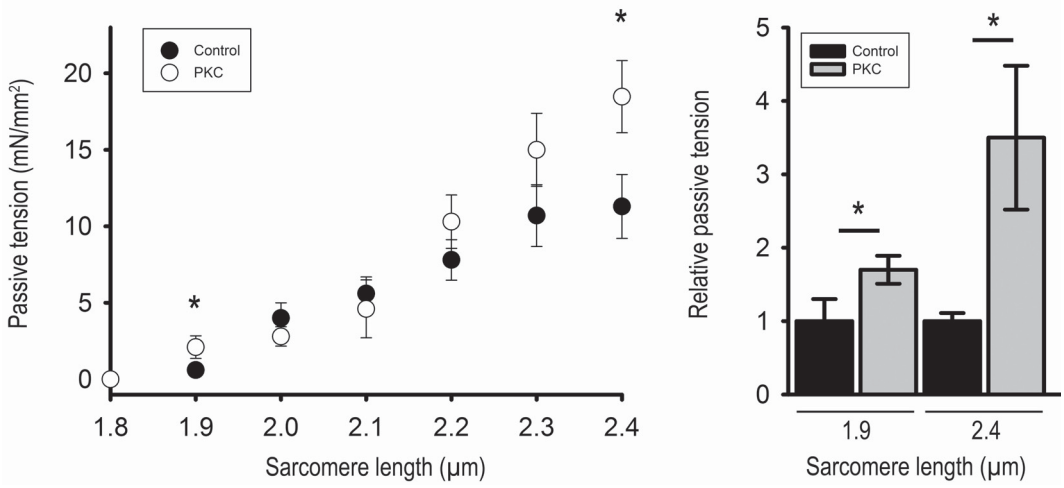

Figure 3.16.: Passive tension of adult rat CMs stimulated with PKCα for 15 minutes (n=3) in comparison to untreated cells (n=17). Statistical significance is marked by asterisks ($p < 0.05$ in Student's t-test).

3.11. Isoform shift in ERC induced by metformin treatment

ERC serve as a very stable *in vitro*-model, depicting adult cardiac tissue reliably. To investigate whether metformin directly affects titin isoform composition, ERC were cultured for 8 days under control conditions and then treated with the anti diabetic drug *in vitro* until day 12 (Figure 3.17.). The relative N2B content of the cells was determined by evaluating Imperial-stained titin gels densitometrically. After 96 hours of stimulation, relative N2B content was significantly lowered by 20% to 0.79± 0.02 compared to the untreated control.

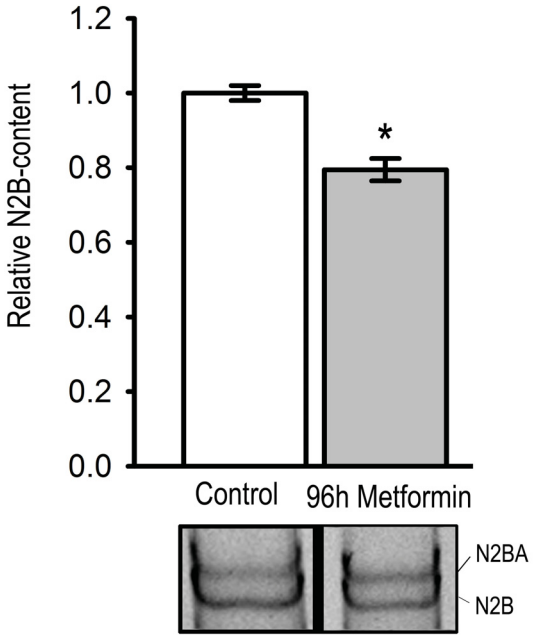

Figure 3.17.: Metformin (20 mM; 96h) negatively affects titin isoform composition in ERC after 12 days in culture (n=5). Statistical significance is marked by asterisks ($p < 0.05$ in Student's t-test).
Bottom: Representative SDS gels show titin bands visualized with Imperial-stain for protein detection.

3.12. RBM20 expression levels in ERC are reduced by metformin treatment

To investigate whether metformin directly affects titin splicing factor expression levels, ERC were cultured for 8 days under control conditions and then treated with the anti diabetic drug *in vitro* on day 12 (Figure 3.18.). Antibodies targeting the gene encoding RNA binding motif protein 20 were applied to WB membranes in order to identify the relative expression levels. After 96 hours of stimulation, relative RBM20 expression levels were significantly lowered by 40% to 0.6± 0.04, when compared to the untreated cells.

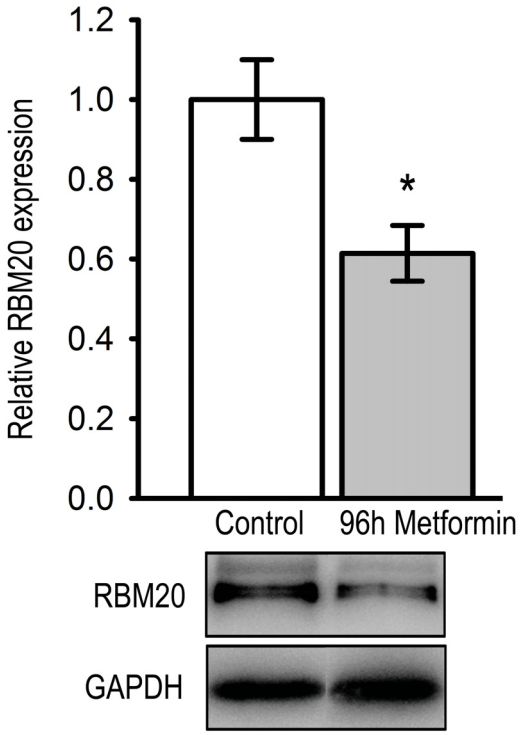

Figure 3.18.: Metformin (20 mM; for 96h) significantly decreased expression levels of the titin splicing factor RBM20 in ERC after 12 days in culture (n=5). Statistical significance is marked by asterisks (p <0.05 in Student's t-test).
Bottom: Representative Western Blots show RBM20 bands visualized by antibodies to the titin splicing factor and GAPDH.

3.13. Insulin and metformin induce phosphorylation of titin N2-Bus, PEVK and PKCα in ERC

In order to investigate whether insulin and metformin directly affect titin phosphorylation, ERC were isolated and cultured under control conditions and then treated with the anti diabetic drugs *in vitro*. Cells were harvested after different time points of insulin stimulation (175 nM) and metformin stimulation (50 nM) in order to compare them to unstimulated cells serving as a control. To correlate the treatment effects on titin to insulin signaling the insulin pathway was activated for 0 minutes, 15 minutes, 30 minutes and 45 minutes and inhibited at the time point with 15 minutes of stimulation with the PI3 kinase inhibitor LY294002 (LY) (50 nM). Phospho-specific antibodies targeting the Serine residues 4010 and 4099 within titin's N2-Bus, were applied to Western blots. Insulin and metformin increased the PKG (Ser4099) and PKA (Ser4010) dependent titin phosphorylation significantly, whereas the inhibition by LY blocked the increase (Figure 3.19. and Figure 3.20.). For insulin treatment a maximum of over 250% to 254.33 ± 36.33 increase was measurable after 45 minutes of stimulation at Serine residue 4010. At Serine residue 4099 an increase to 162.44 ± 18.32 was detected already after 30 minutes. For metformin treatment a significant maximum of 170.54 ± 32.12 was detected after 45 minutes of stimulation at Serine residue 4010, for Serine residue 4099 the maximum was after 30 minutes of metformin treatment increased to 169.78 ± 21.45.

Insulin and metformin induced changes in PKCα dependent PEVK phosphorylation were detected with a phospho-specific titin antibody for Serine residue 11878. This phosphosite showed increased phosphorylation levels after insulin and metformin treatment and furthermore a successful inhibition with the PI3K inhibitor LY (Figure 3.21.). A maximum of over 500% increase to 548.31 ± 41.32 was detected after only 30 minutes of insulin stimulation and to 182.22 ± 23.21 after 30 minutes of metformin treatment at pSer11878. Accord-

ingly, PKCα activity was detected with an antibody specifically binding the phosphorylated Threonine residue 497. After 30 minutes of insulin treatment a significant increase to 261.58 $\pm$ 47.76 was detectable. In metformin treated cells, PKCα activity was drastically elevated to 1340.90 $\pm$ 372.59. For both treatments, PKCα activation was again effectively inhibited with the PI3K inhibitor LY (Figure 3.22.).

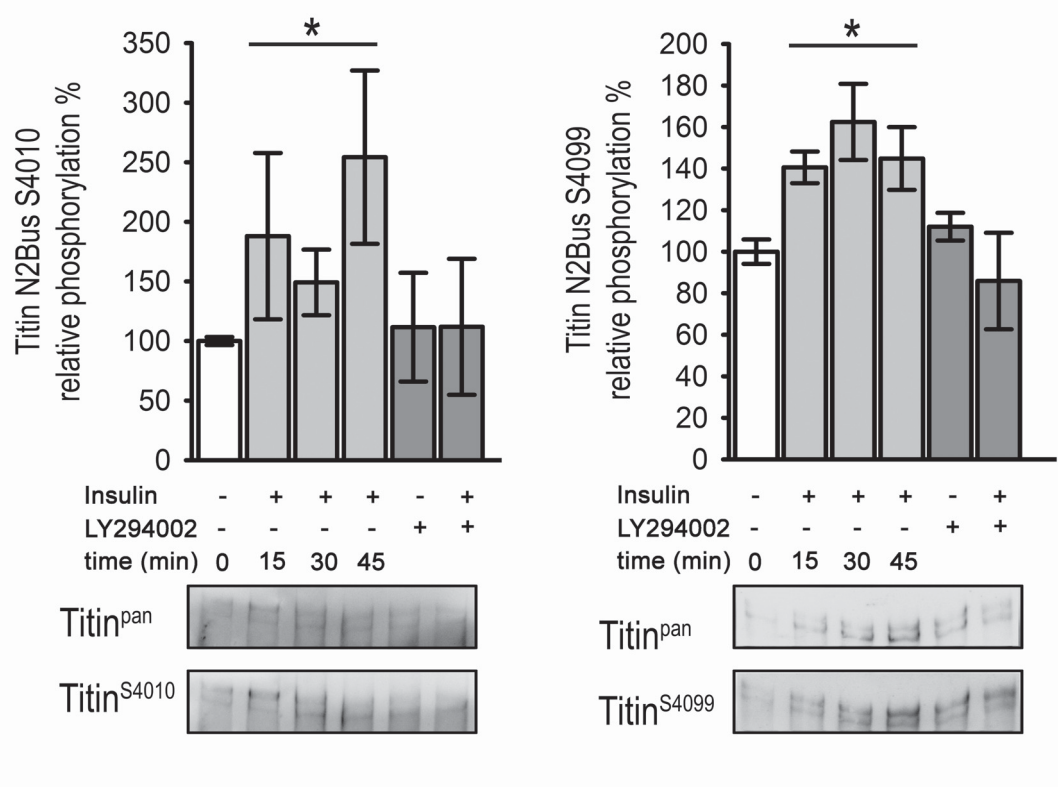

Figure 3.19.: Insulin-induced changes in titin N2-Bus Ser4010 (PKA- and ERK-specific) and Ser4099 (PKG-specific) phosphorylation in ERC. Bar graphs show N2-Bus phosphorylation changes under different stimulation conditions (n=3). Statistical significance is marked by asterisks ($p < 0.05$ in Student's t-test).
Bottom: Representative Western blots show titin bands visualized by antibodies to total N2-Bus and the respective phosphosite (pN2-Bus).

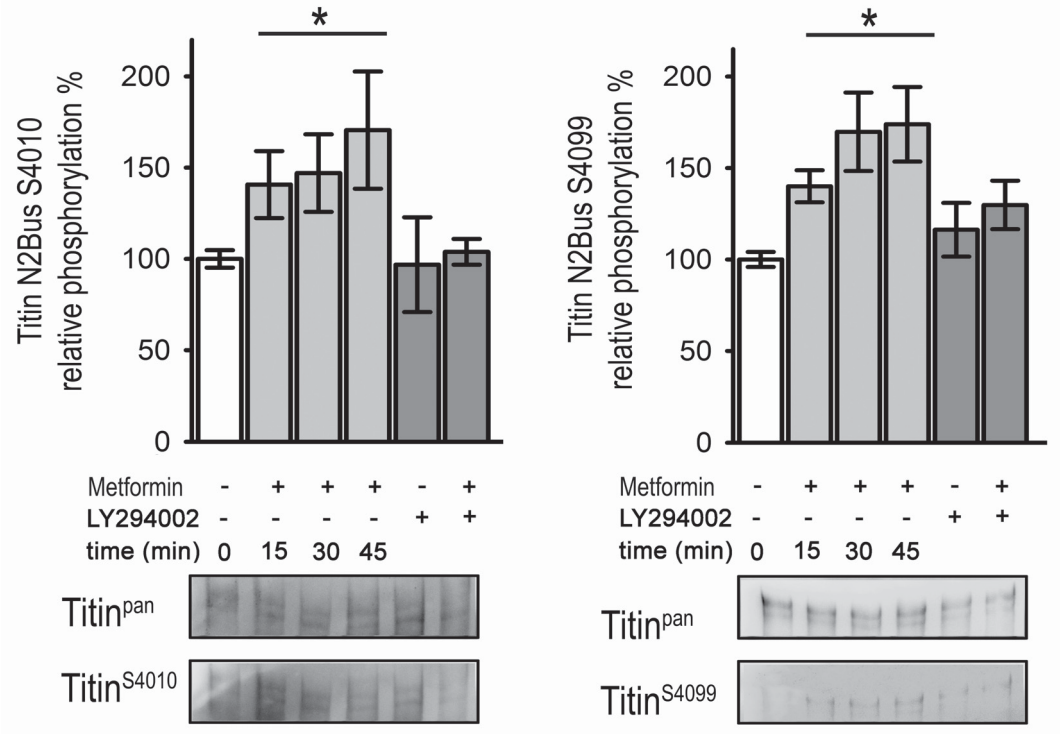

Figure 3.20.: Metformin-induced changes in titin N2-Bus Ser4010 (PKA- and ERK-specific) and Ser4099 (PKG-specific) phosphorylation in ERC. Bar graphs show N2-Bus phosphorylation changes under different stimulation conditions (n=3). Statistical significance is marked by asterisks ($p < 0.05$ in Student's t-test).
Bottom: Representative Western blots show titin bands visualized by antibodies to total N2-Bus and the respective phosphosite (pN2-Bus).

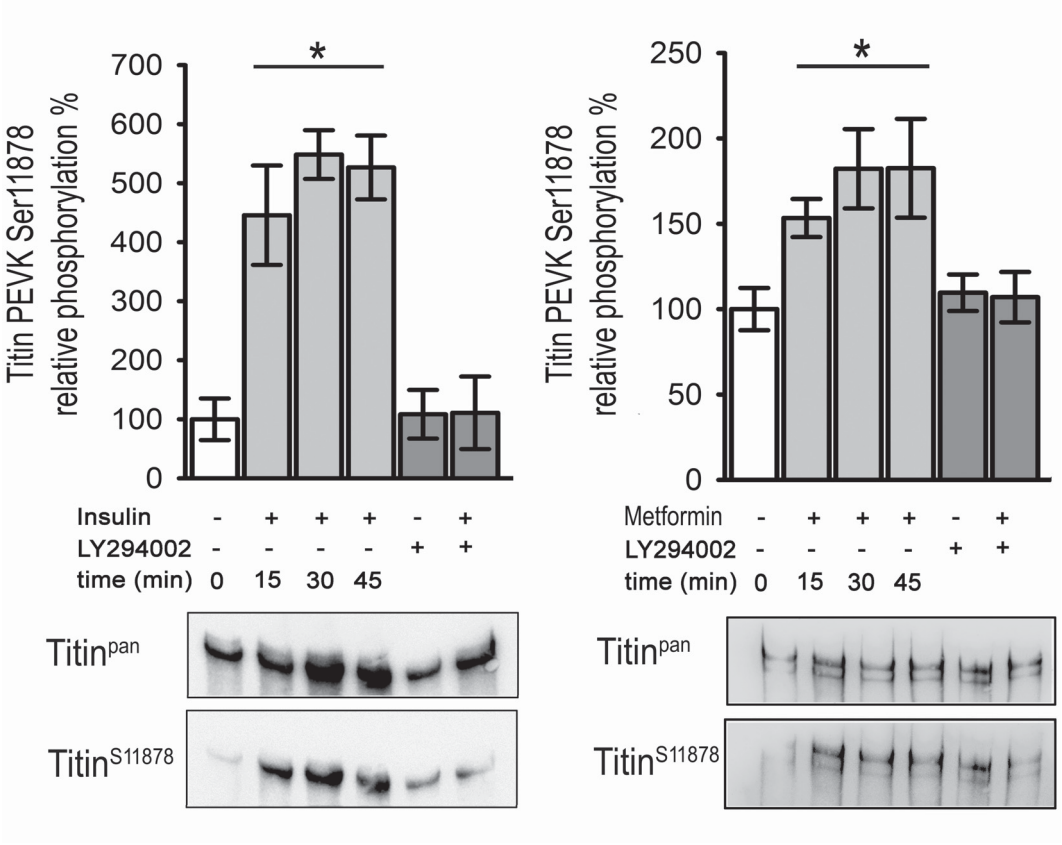

Figure 3.21.: Antibody-based detection of titin and phospho-titin (Ser11878, PKCα specific). Embryonic rat cardiomyocytes were treated with or without insulin and metformin including the negative control and the inhibitor LY294002 (n=4). Statistical significance is marked by asterisks ($p < 0.05$ in Student's t-test).
Bottom: Representative Western blots show titin bands visualized by antibodies to total PEVK (pan) and the respective phosphosite (pPEVK S11878).

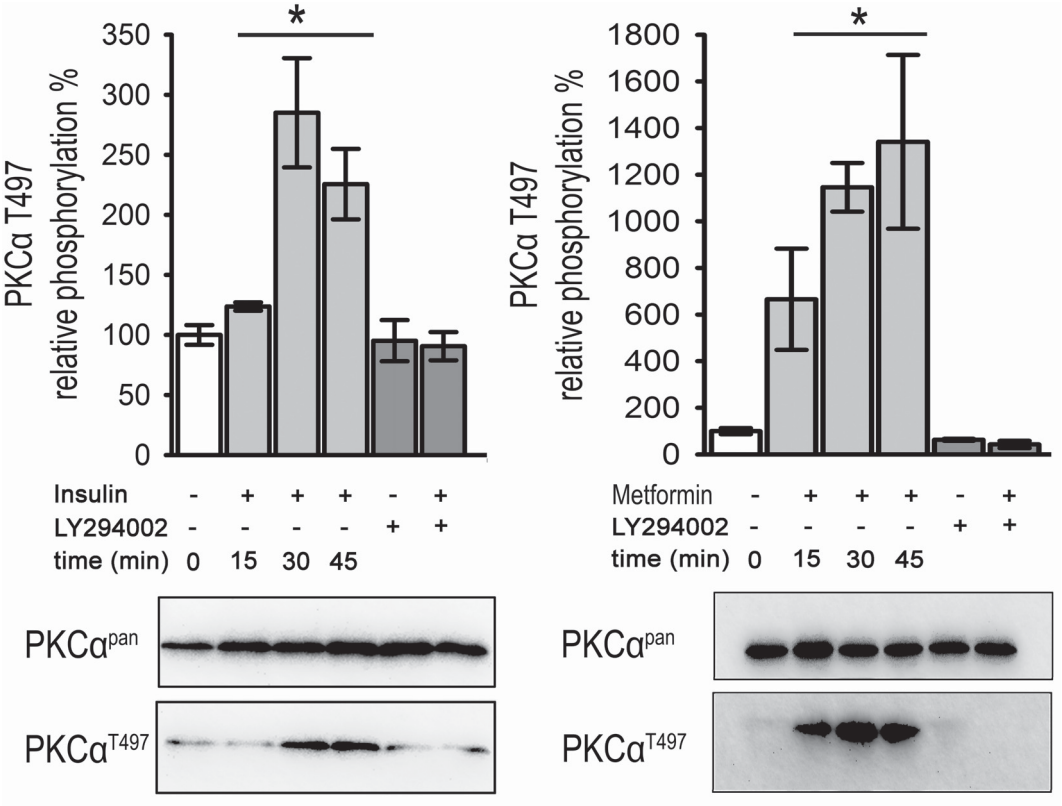

Figure 3.22.: Antibody-based detection of total and phospho (T497) PKCα. Embryonic rat cardiomyocytes were treated with or without insulin and metformin including the negative control and the inhibitor LY294002 (n=4). Statistical significance is marked by asterisks ($p < 0.05$ in Student's t-test).
Bottom: Representative Western blots show PKCα bands visualized by antibodies to total PKCalpha (pan) and the respective phosphosite (T497).

3.14. PKCα-phospho localization in slack and stretched adult cardiomyocytes

In order to locate phosphorylated PKCα in adult rat cardiomyocytes being slacked and stretched (mimicking diastolic and systolic conditions) and as a proof of concept, cells were isolated (Langendorff perfusion) and cultivated under standard conditions. To determine the sarcomere and to serve as a positive control, cells were additionally stained with α-actinin antibodies (specific for α-skeletal and α-cardiac muscle actinins) targeting the Z-disc. In order to investigate a potential binding of PKCα to the sarcomere during slacking or stretching, pictures were taken of the same cell under both circumstances (Figure 3.23.). Results may qualitatively indicate less PKCα phosphorylation when the SL is increased and the cells are stretched.

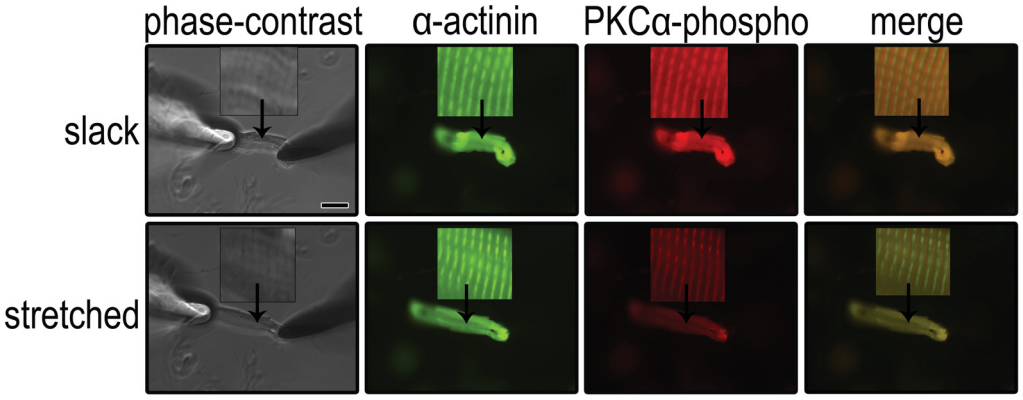

Figure 3.23.: Localization of T497 phosphorylated PKCα in primary adult rat cardiomyocytes. Co-stained with the α-actinin (specific for α-skeletal and α-cardiac muscle actinins) and PKCα phospho and total antibodies as well as fluorescent-linked secondary antibodies. The cardiomyocyte was photographed when in slack and in stretched position (scale bar: 25 μm).

3.15. PKCα-phospho localization in ERC and adult cardiomyocytes at different time points

To locate and identify interaction between PKCα (total and phosphorylated) and the titin filament under physiological and medicated (metformin and insulin) conditions, embryonic and adult rat cardiomyocytes were analyzed. The cells were cultivated with different stimuli and harvested at different time points after stimulation in order to differentiate PKCα localization amounts on a time scale and in an earlier (ERC) and an advanced (adult CM) stage of cardiac development. In adult CMs without stimulation, stained directly after isolation, less phosphorylated PKCα (T497) appeared to be visible than of the total PKCα (Figure 3.24.). Similar pictures were taken, when scanning embryonic rat cardiomyocytes stained with a PKCα-phospho and -total antibody directly after preparation (Figure 3.25.). When stimulating adult CMs for 15 minutes with insulin, metformin and as a control with aq. dest., the phosphorylated PKCα was found to be more dominantly present in those cells being stimulated than the ones with no insulin or metformin treatment (Figure 3.26.). ERC were stimulated for different time periods. After 15 minutes no particular increase in phosyphorylated PKCα was visible in those cells being stimulated compared to the control (Figure 3.27.). After 30 minutes of stimulation (Figure 3.28.) pPKCα appeared more dominant in cells being stimulated with insulin. This might be even better differentiated after 45 minutes of treatment with insulin, see in figure 3.29.. A direct interaction of PKCα and titin can not be concluded. However, a localisation of PKCα at the sarcomere was visible in the pictures obtained, indicating a link previously assumed by Western blot analysis of PKCα and PEVK phosphorylation levels of titin.

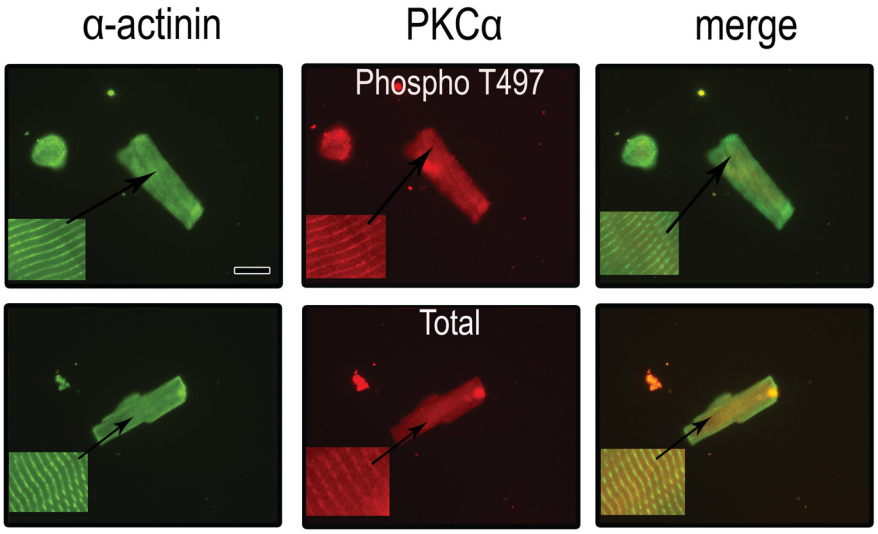

Figure 3.24.: Localization of T497 phosphorylated PKCα in primary adult rat CM. Co-stained with the α-actinin and PKCα antibodies as well as fluorescent-linked secondary antibodies (scale bar: 20 μm).

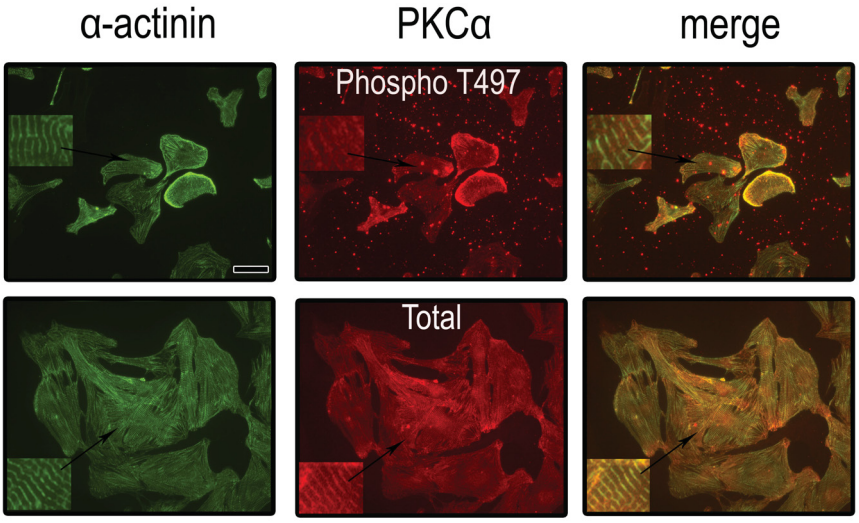

Figure 3.25.: Localization of PKCα (T497) phosphorylation in primary ERC, cultured, fixated and then co-stained with the α-actinin and PKCα phospho and total antibodies as well as fluorescent-linked secondary antibodies (scale bar: 15 μm).

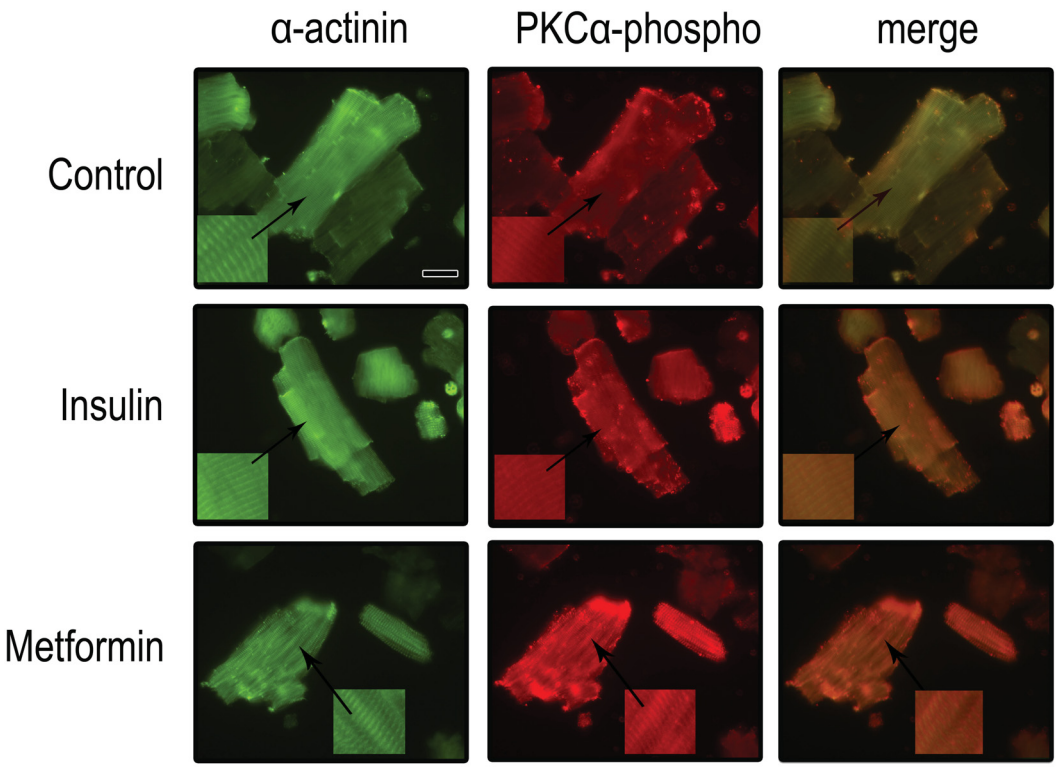

Figure 3.26.: Localization of PKCα (T497) phosphorylation in primary adult rat cardiomyocytes, cultured and stimulated for 15 minutes with either insulin, metformin or aq.dest. as a control, fixated and then stained with the primary α-actinin (specific for α-skeletal and α-cardiac muscle actinins), PKCα phospho antibodies and fluorescent-linked secondary antibodies (scale bar: 10 μm).

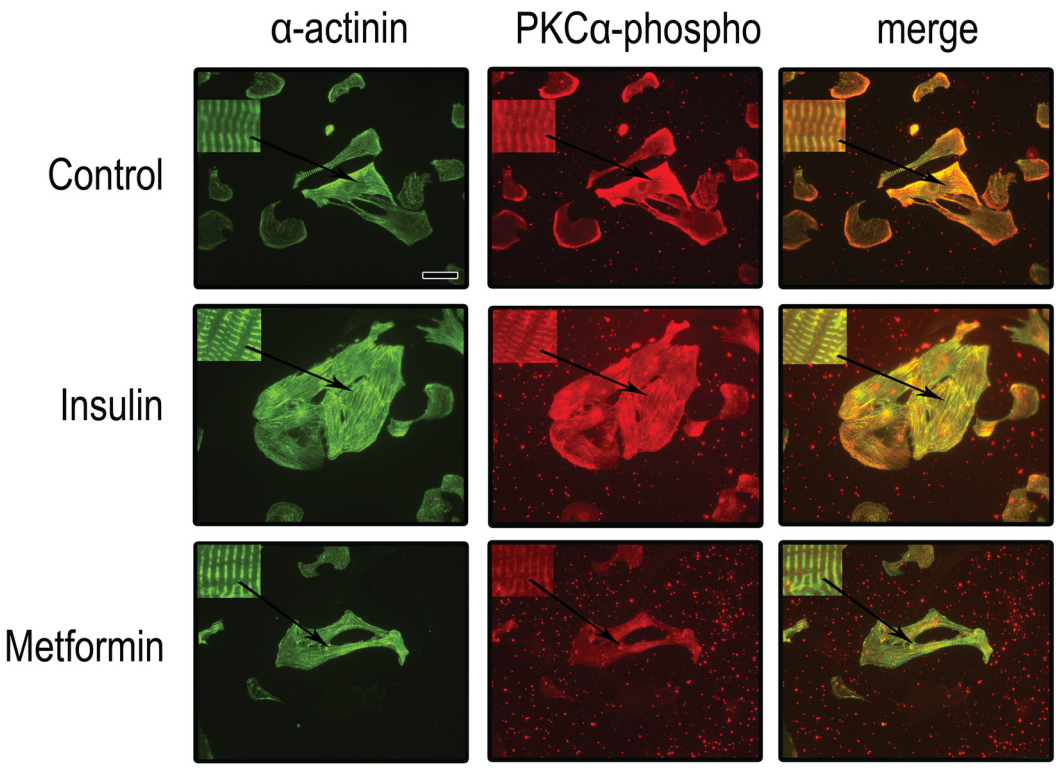

Figure 3.27.: Localization of PKCα (T497) phosphorylation in primary embryonic rat cardiomyocytes, cultured and stimulated with either insulin, metformin or aq.dest. as a control for 15 minutes, fixated and then co-stained with the α-actinin (specific for α-skeletal and α-cardiac muscle actinins), PKCα phospho antibodies and fluorescent-linked secondary antibodies (scale bar: 15 μm).

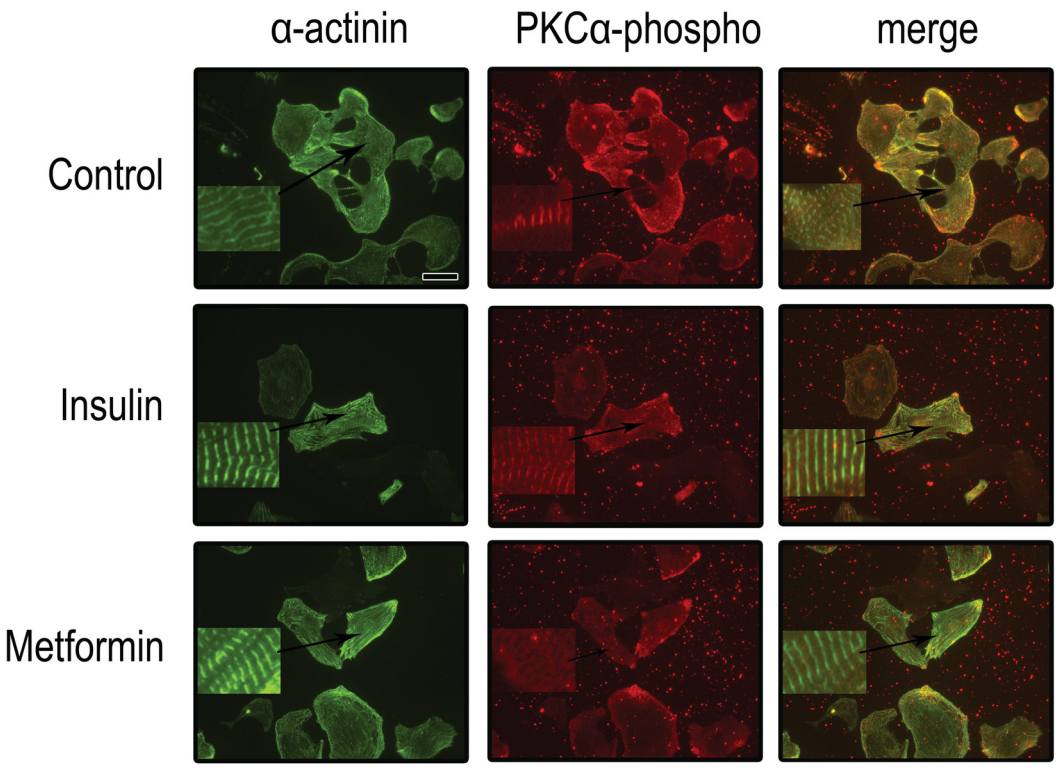

Figure 3.28.: Localization of PKCα (T497) phosphorylation in primary embryonic rat cardiomyocytes, cultured and stimulated with either insulin, metformin or aq.dest. as a control for 30 minutes, fixated and then co-stained with the α-actinin (specific for α-skeletal and α-cardiac muscle actinins), PKCα phospho antibodies and fluorescent-linked secondary antibodies (scale bar: 15 μm).

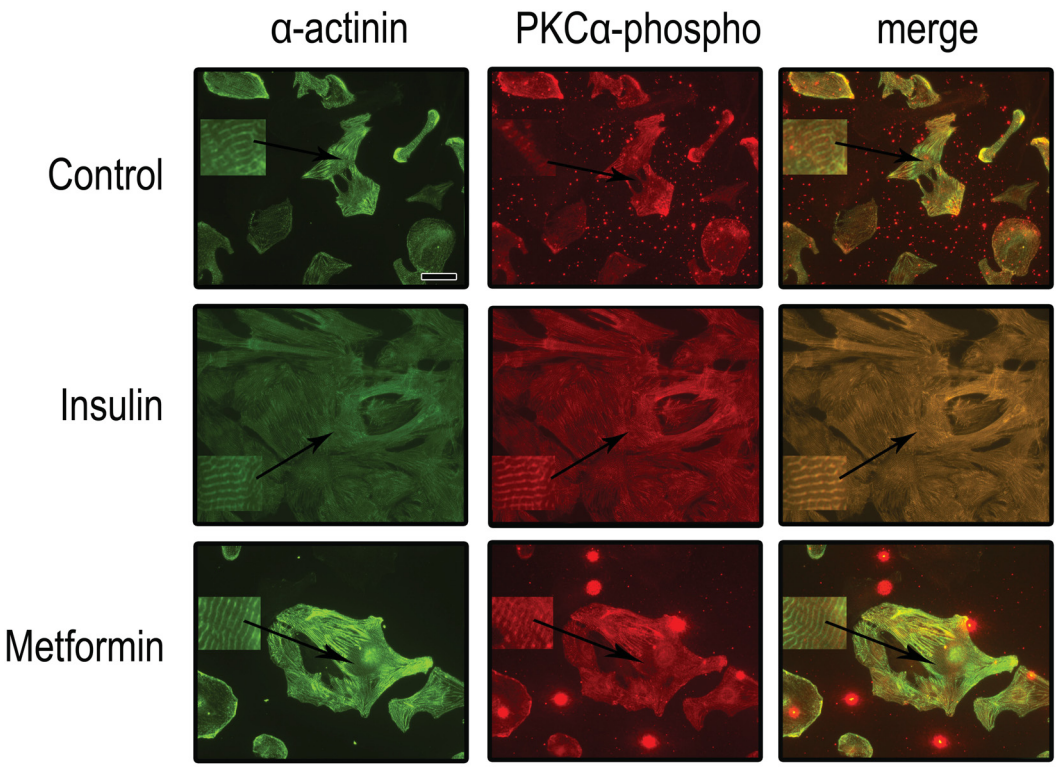

Figure 3.29.: Localization of PKCα (T497) phosphorylation in primary embryonic rat cardiomyocytes, cultured and stimulated with either insulin, metformin or aq.dest. as a control for 45 minutes, fixated and then co-stained with the α-actinin (specific for α-skeletal and α-cardiac muscle actinins), PKCα phospho antibodies and fluorescent-linked secondary antibodies (scale bar: 15 μm).

3.16. Exercise acutely changes cardiac titin phosphorylation in adult rats

The effects of acute and chronic physical exercise under different conditions (downhill and level running) on titin I-band phosphorylation determining cardiac passive myofilament stiffness were analyzed by using phosphosite-directed antibodies to Ser4010 (PKA- and ERK2-targeted) and Ser4099 (PKG-targeted) in the cardiac-specific N2-Bus region, and to Ser11878 and Ser12022 (PKCα and CaMKIIδ-targeted) in the ubiquitously expressed part of the PEVK region. Relative phosphorylation was determined by normalizing the phospho:total ratio of the control group to that of the exercised group.

i. Cardiac titin phosphorylation changes in acutely level running adult rats

Phosphorylation of residue Ser4010 in the N2-Bus differed largely among the analyzed exercise samples, due to the large standard errors. With an increased relative phosphorylation of over 25% to 1.26 ± 0.97 compared to the control group the observed changes were not statistically significant (Figure 3.30.). In contrast, relative phosphorylation of Ser4099 in the N2-Bus was significantly reduced in the cardiac tissue of acutely level exercised animals by nearly 40% to 5.91 ± 0.12 compared to the control level (Figure 3.30.). Additionally, changes in phosphorylation at Ser11878 and Ser12022 in the PEVK region of titin were analyzed. Applied Western blot analyses detected that the relative phosphorylation of Ser11878 was significantly increased in the acute level exercised samples by over 200% to 2.15 ± 0.26 compared to control samples; whereas relative phosphorylation of the Serine residue 12022 was significantly decreased by 40% to 0.62 ± 0.14 (Figure 3.31.).

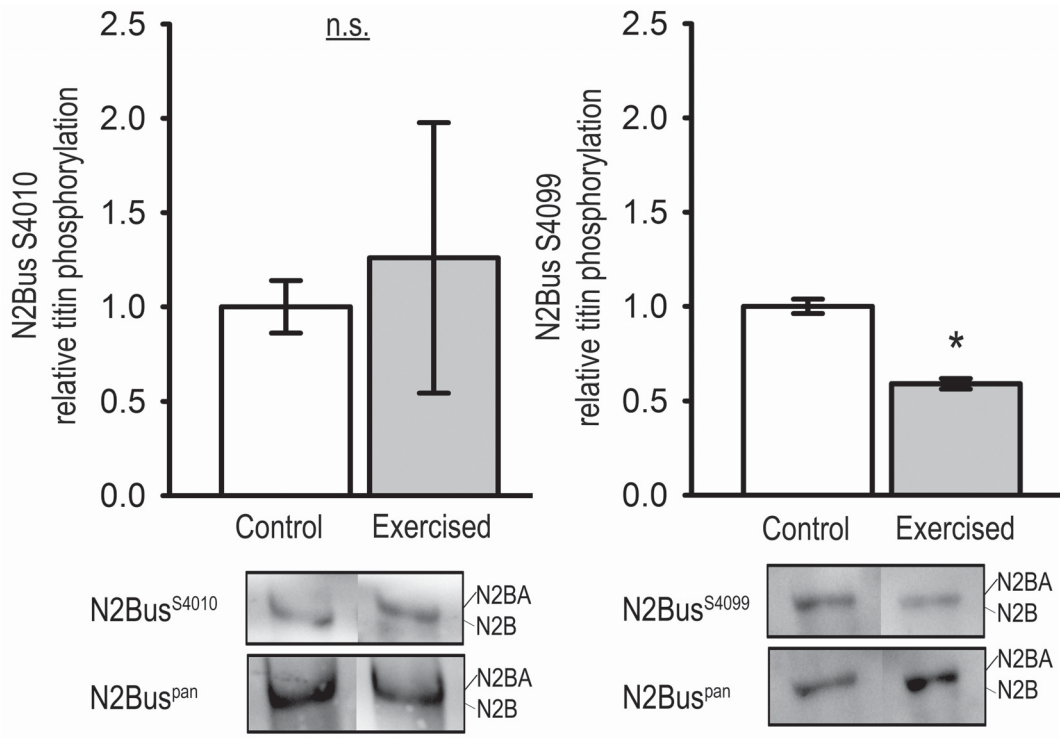

Figure 3.30.: Titin phosphorylation in cardiac tissue from acute-level-exercised (Exercised, n=7) and sedentary (Control, n=7) animals. Bar graphs show statistical data from Western blot analysis using antibodies recognizing pSer4010 (left) and pSer4099 (right). Statistical significance is marked by asterisks ($p < 0.05$ in Student's t-test).
Bottom: Representative Western blots show titin bands visualized by antibodies to total N2-Bus and the respective phosphosite (pN2-Bus).

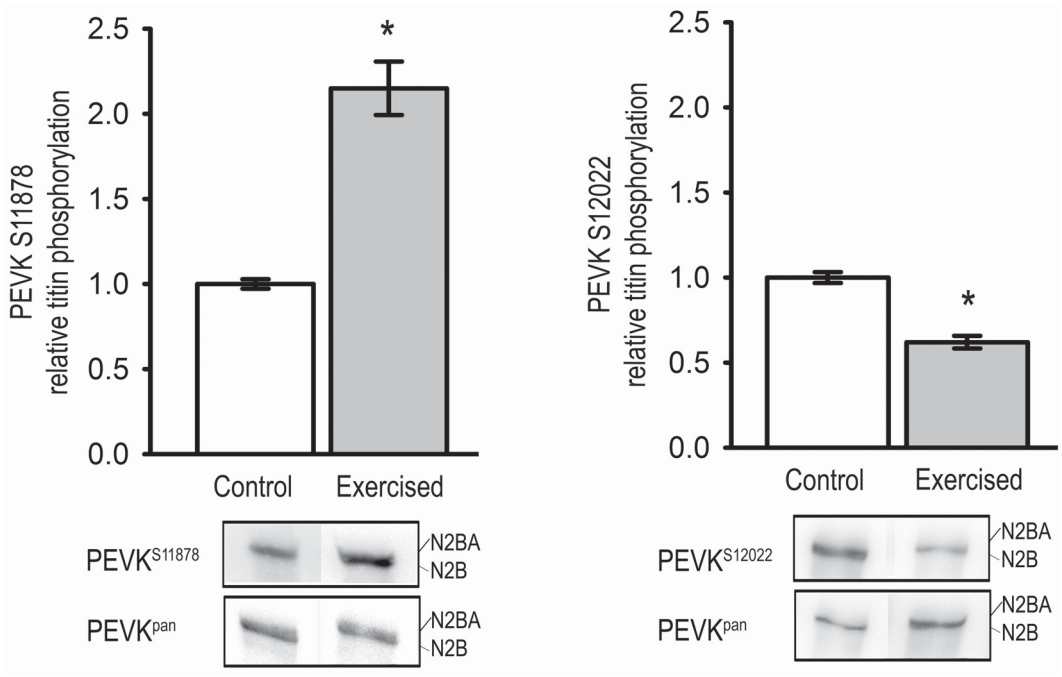

Figure 3.31.: Titin phosphorylation in cardiac tissue from acute-level-exercised (Exercised, n=7) and sedentary (Control, n=7) animals. Bar graphs show statistical data from Western blot analysis using antibodies recognizing pSer11878 (left) and pSer12022 (right). Statistical significance is marked by asterisks ($p < 0.05$ in Student's t-test).
Bottom: Representative Western blots show titin bands visualized by antibodies to total PEVK and the respective phosphosite (pPEVK).

ii. Cardiac titin phosphorylation changes in acutely and chronically downhill running adult rats

In acutely exercised rats running downhill on a treadmill, relative phosphorylation of Ser4099 in the N2-Bus remained unchanged (1.04 ± 0.12) in cardiac tissue, whereas relative phosphorylation of the PEVK (Ser11878) was significantly decreased by over 50% to 0.47 ± 0.19 (Figure 3.32.).

In chronically exercised rats running downhill on a treadmill, relative phosphorylation of Ser4099 in the N2-Bus was significantly reduced in the cardiac tissue by about 90% to 0.13 ± 0.01, whereas relative phosphorylation of the Serine residue 11878 in the PEVK was significantly increased by nearly 700% to 6.64 ± 0.44 (Figure 3.33.).

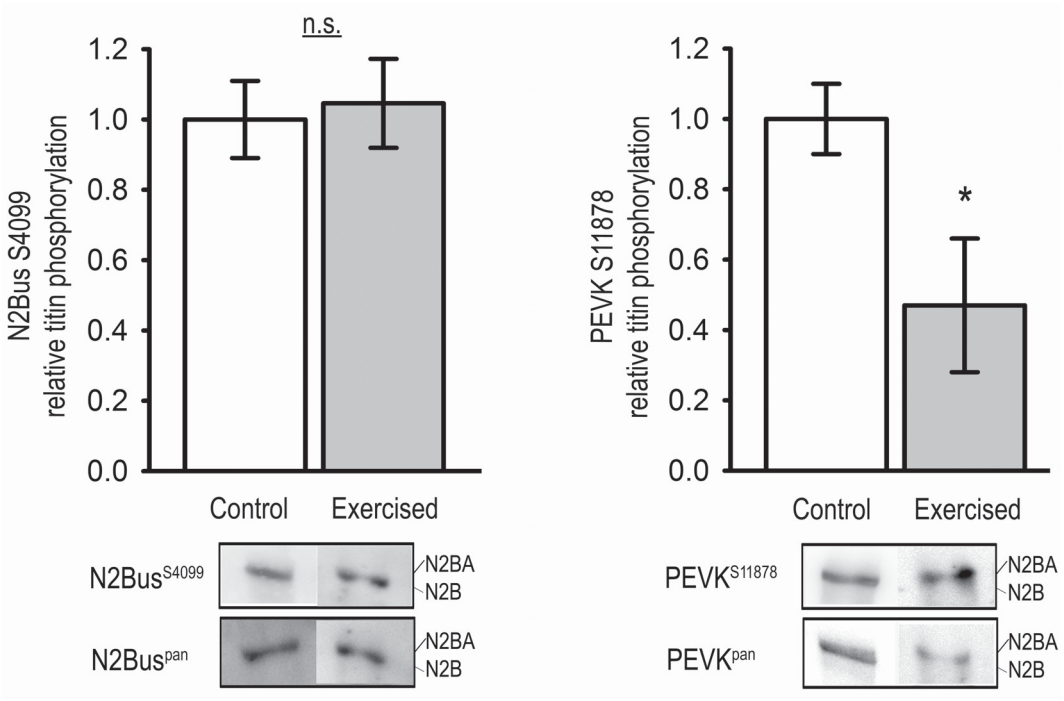

Figure 3.32.: Titin phosphorylation in cardiac tissue from acutely downhill exercised (Exercised, n=7) and sedentary (Control, n=7) rats. Bar graphs show statistical data from Western blot analysis using antibodies recognizing pSer4099 (left) and pSer11878 (right). Statistical significance is marked by asterisks ($p < 0.05$ in Student's t-test).
Bottom: Representative Western blots show titin bands visualized by antibodies to total N2-Bus/PEVK and the respective phosphosite (pN2-Bus/pPEVK).

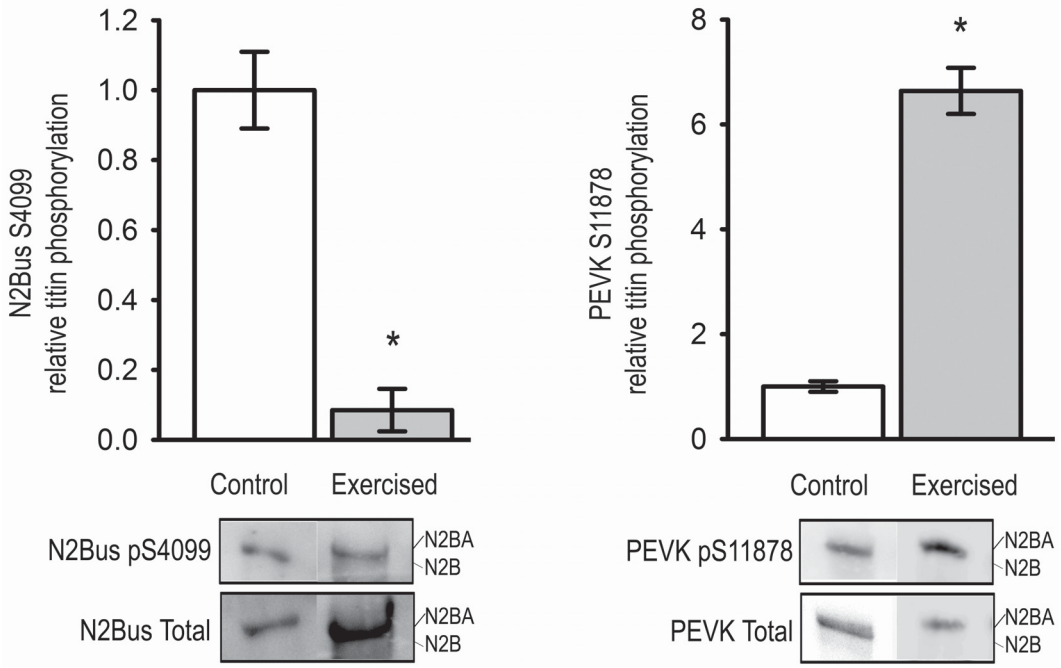

Figure 3.33.: Titin phosphorylation in cardiac tissue from chronically downhill exercised (Exercised, n=7) and sedentary (Control, n=7) animals. Bar graphs show statistical data from Western blot analysis using antibodies recognizing pSer4099 (left) and pSer11878 (right). Statistical significance is marked by asterisks ($p < 0.05$ in Student's t-test). Bottom: Representative Western blots show titin bands visualized by antibodies to total N2-Bus/PEVK and the respective phosphosite (pN2-Bus/pPEVK).

3.17. Exercise increases passive cardiac myofilament stiffness

To determine the effects of exercise on the passive properties of the myocardium, mechanically isolated single cardiomyocytes were measured to determine the passive tension in relation to the sarcomere length. For this purpose, cardiomyocytes were stretched in five steps to sarcomere lengths ranging from 1.9 to 2.4 μm and passive forces were recorded for each step. Passive tension (PT) was significantly higher in cardiomyocytes isolated from exercised animals, compared to controls (Figure 3.34-3.37). In acute level running adult rats (Figure 3.34.), passive tension was increased at SL 2.0 μm by nearly 300%, 2.2 μm by close to 200%, and at SL 2.4 μm by over 150%. In those rats running acutely downhill (Figure 3.35.) passive stiffness of single CMs was increased at SL 2.0 μm by more than 150%, at SL 2.1 μm by nearly 350%, and at SL 2.2 μm by close to 50%. The group of rats running chronically level (Figure 3.36.) meaning concentric muscle straining, only showed increased passive stiffness at SL 1.9 μm with nearly 200%. In contrast, in chronically downhill running rats (Figure 3.37.) passive stiffness of single CMs was increased at SL 1.9 μm with nearly 250%, at SL 2.0 μm by more than 250%, at SL 2.1 μm by nearly 500%, at SL 2.2 μm by nearly 250%, at SL 2.3 μm by nearly 50% and at SL 2.4 μm by close to 200%.

Acute-Level-Exercise

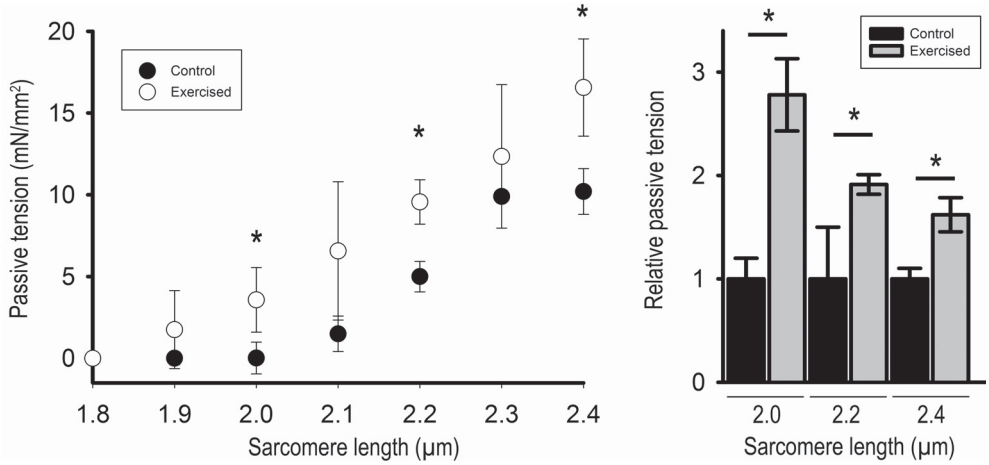

Figure 3.34.: Force extension curve showing PT (mN/mm^2) of acute level exercised compared to control CM. Bar graphs highlight the statistically significant differences in PT at SL 2.0, 2.2 and 2.4 μm. Statistical significance is marked by asterisks (p <0.05 in Student's t-test).

Acute-Downhill-Exercise

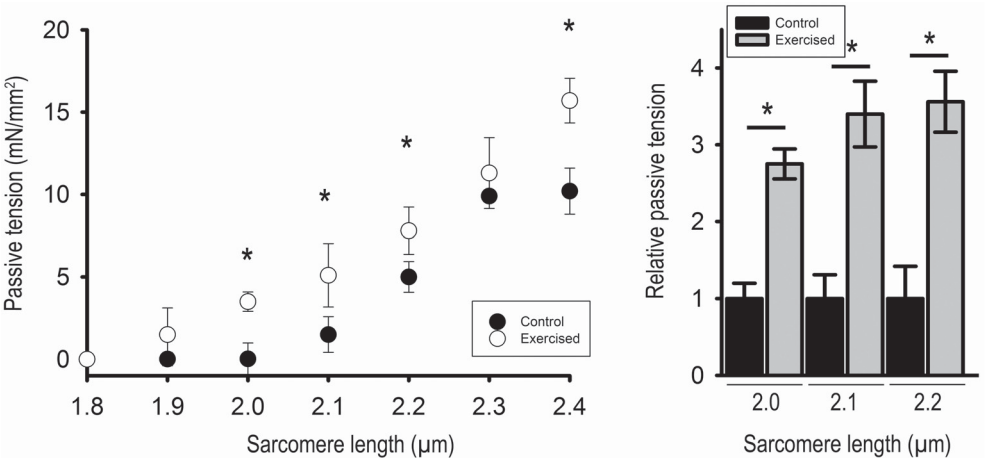

Figure 3.35.: Force extension curve showing PT (mN/mm^2) of acute downhill exercised compared to control CM. Bar graphs highlight the statistically significant differences in PT at SL 2.0, 2.1 and 2.2 μm. Statistical significance is marked by asterisks (p <0.05 in Student's t-test).

Chronic-Level-Exercise

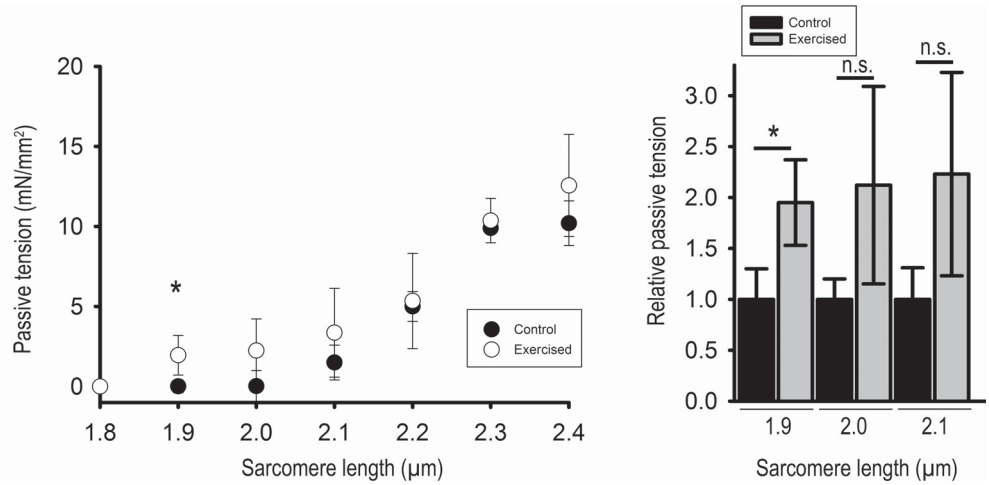

Figure 3.36.: Force extension curve showing PT (mN/mm^2) of chronic level exercised compared to control CM. Bar graphs highlight the statistically significant differences in PT at SL 1.9, 2.0 and 2.1 μm. Statistical significance is marked by asterisks (p <0.05 in Student's t-test).

Chronic-Downhill-Exercise

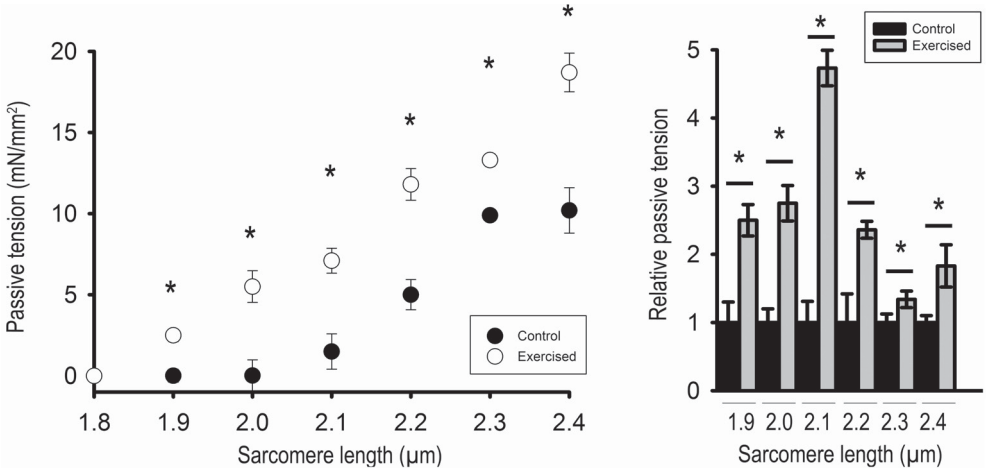

Figure 3.37.: Force extension curve showing PT (mN/mm^2) of chronic downhill exercised compared to control CM. Bar graphs highlight the statistically significant differences in PT at SL 1.9 to 2.4 μm. Statistical significance is marked by asterisks (p <0.05 in Student's t-test).

3.18. Exercise acutely modifies skeletal titin phosphorylation

Furthermore, the effects of a single exercise bout on skeletal titin phosphorylation was identified by analyzing the relative phosphorylation of Ser11878 and Ser12022 in the PEVK region of titin from the latissimus dorsi muscle (LAT). In order to determine putative differences in the response to concentric and eccentric exercise, LAT samples from animals after 15 minutes level running and from animals after 15 minutes downhill running were analyzed. Interestingly, unlike in the cardiac tissue, Western blot analysis of the level-exercised skeletal muscles showed that the relative titin phosphorylation at Ser11878 was significantly reduced by over 80% to 0.12 ± 0.02 compared to sedentary controls (Figure 3.38.). At the same time relative phosphorylation of Ser12022 was significantly increased nearly 200% to 1.84 ± 0.06 (Figure 3.38.). At least for one phosphosite, similar results were obtained from LAT muscles of downhill-exercised animals, in which relative titin phosphorylation at Ser11878 was also significantly reduced by 80% to 0.21 ± 0.09 but not altered for phosphorylation at Ser12022, compared to the control (Figure 3.39).

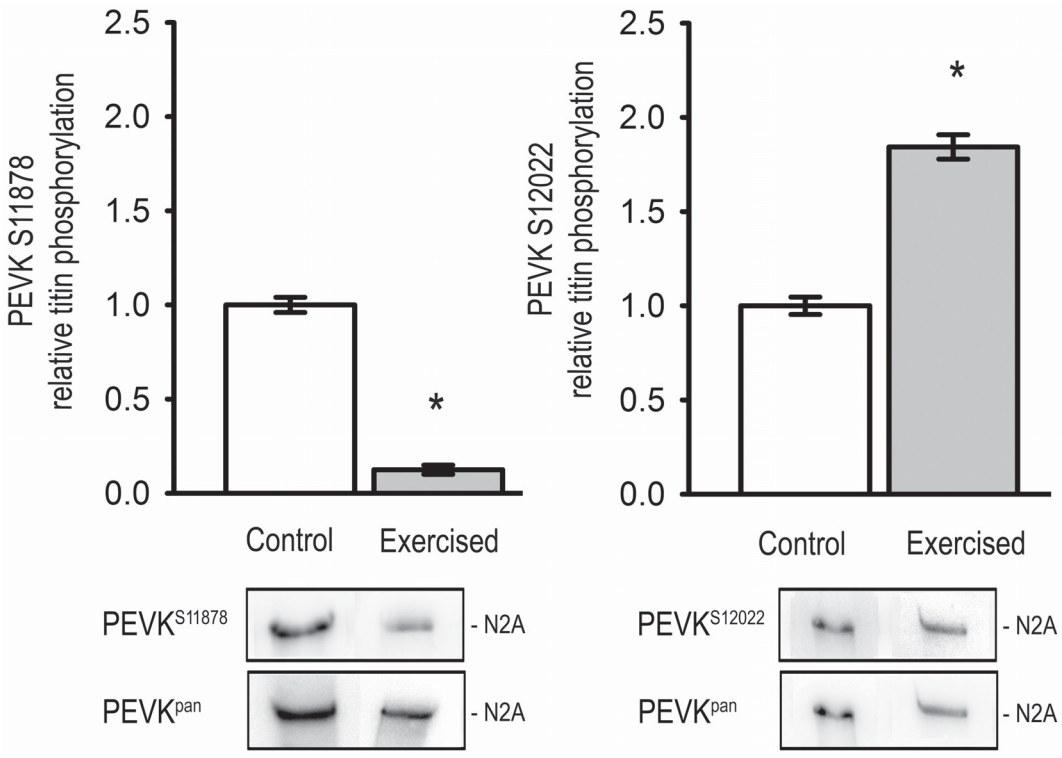

Figure 3.38.: Titin phosphorylation in skeletal (LAT) tissue from acutely level exercised (Exercised, n=7) and sedentary (Control, n=7) animals. Bar graphs show statistical data from Western blot analysis using antibodies recognizing pSer11878 (located on the left) and pSer12022 (located on the right). Statistical significance is marked by asterisks ($p < 0.05$ in Student's t-test).
Bottom: Representative Western blots show titin bands visualized by antibodies to total PEVK and the respective phosphosite (pPEVK).

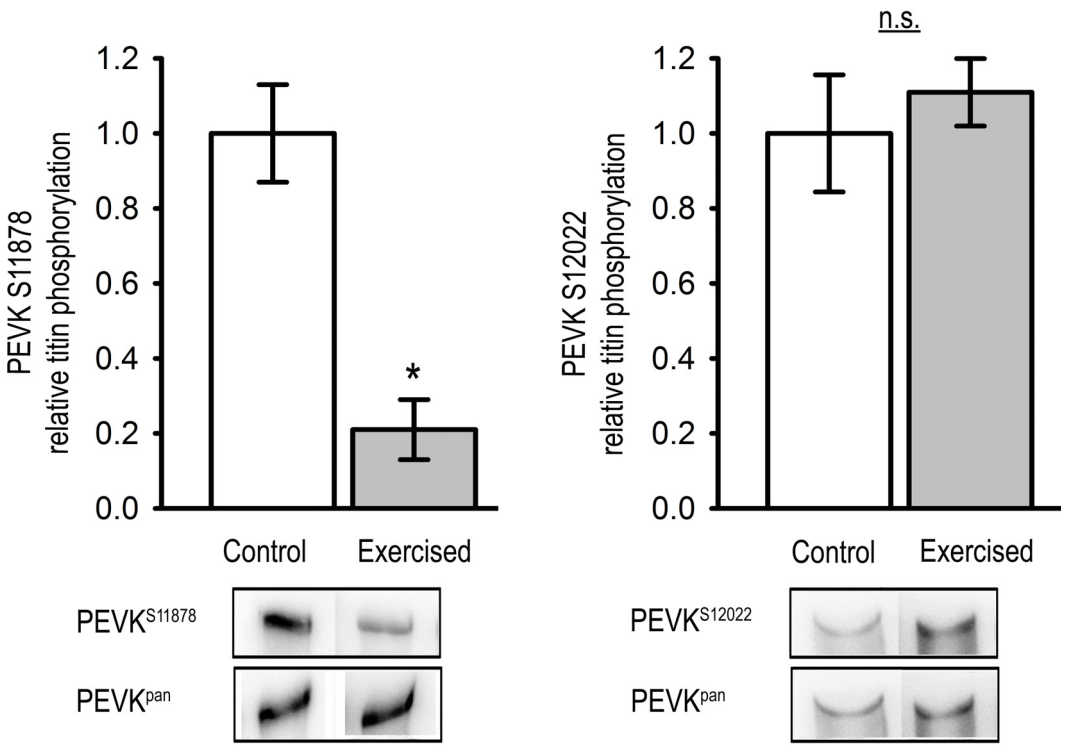

Figure 3.39.: Titin phosphorylation in skeletal (LAT) tissue from acutely downhill exercised (Exercised, n=7) and sedentary (Control, n=7) animals. Bar graphs show statistical data from Western blot analysis using antibodies recognizing pSer11878 (located on the left) and pSer12022 (located on the right). Statistical significance is marked by asterisks ($p < 0.05$ in Student's t-test).
Bottom: Representative Western blots show titin bands visualized by antibodies to total PEVK and the respective phosphosite (pPEVK).

3.19. Exercise increases PKCα and PLB phosphorylation at Thr497 in cardiac but does not significantly increase PKCα activity in skeletal muscle

It has previously been shown that the Threonine residue 497 is a critical site for permissive activation of protein kinase Cα [111]. In a first attempt to investigate the signaling cascades responsible for increased titin PEVK phosphorylation after acute exercise we tested for changes in PKCα activity by determining the relative phosphorylation of Thr497 in cardiac and skeletal samples from exercised and non-exercised animals. In cardiac tissue from level-exercised animals relative Thr497 phosphorylation significantly increased to 3.23 $\pm$ 0.43 compared to sedentary controls (Figure 3.40.). In skeletal muscle tissue relative phosphorylation of Thr497 was not significantly changed with a relative Thr497 phosphorylation of 1.08 $\pm$ 0.04 in LAT muscles after level running exercise, and 1.02 $\pm$ 0.06 in LAT muscles after downhill exercise compared to sedentary controls (Figure 3.41.). Phospholamban, known to regulate calcium pumps in membranes of skeletal and cardiac muscle myocytes is phosphorylated by PKA at Serine residue 16, it showed a 20% increase to 1.19 $\pm$ 0.03 in relative phosphorylation (pPLB S16), revealing elevated PKA activity in acutely downhill running rats compared to the control group with no exercise.

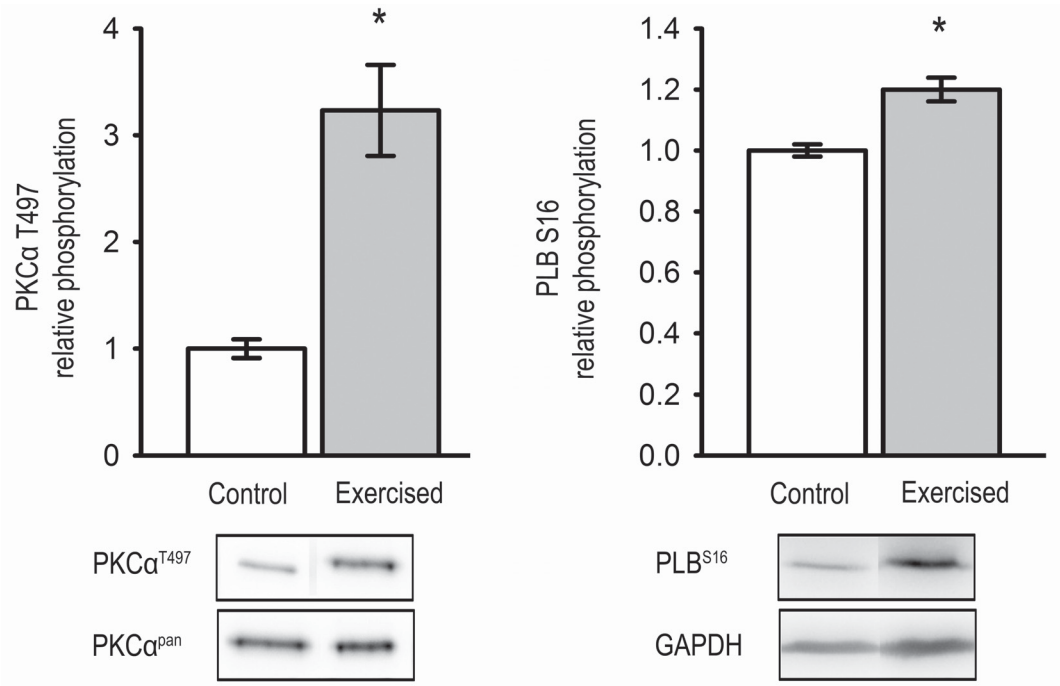

Figure 3.40.: Relative phosphorylation of PKCα at Thr497 (left), and of the PKA substrate phospholamban (pPLB S16) (right) in cardiac muscle tissue from sedentary (Control) and acutely level exercised (Exercised) animals. Statistical significance is marked by asterisks ($p < 0.05$ in Student's t-test).
Bottom: Representative Western blots show PKCα bands visualized by antibodies to total PKCα and the respective phosphosite (Thr497) as well as pPLB (S-16) and GAPDH.

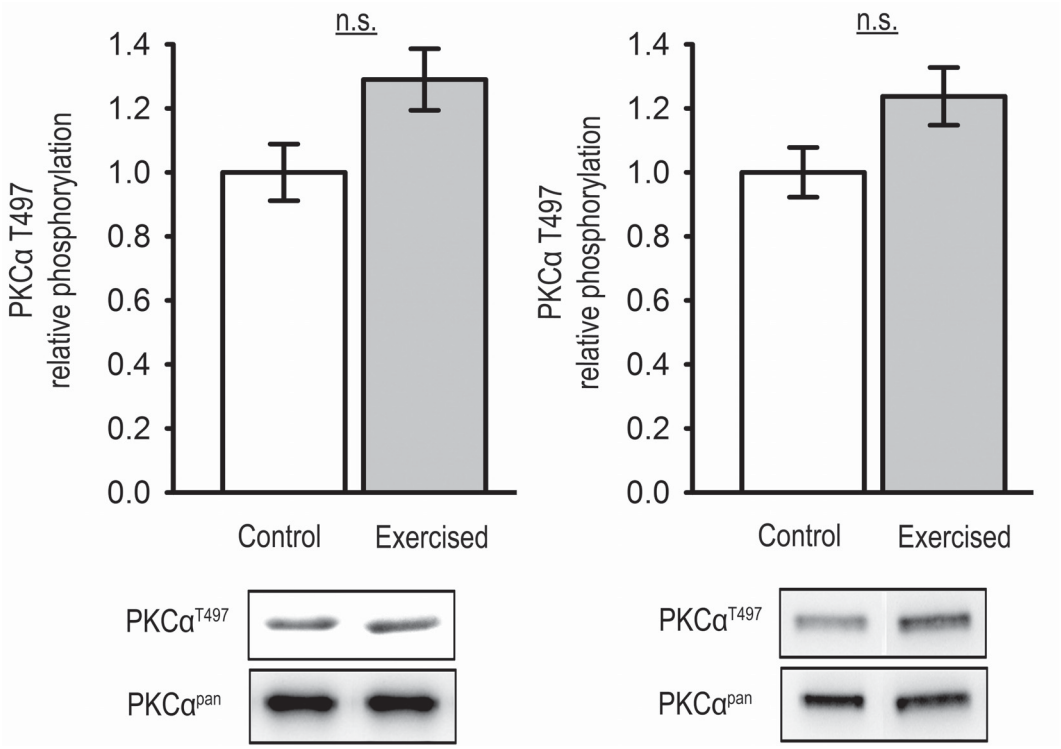

Figure 3.41.: Relative phosphorylation of PKCα at Thr497 in skeletal LAT muscle tissue from animals after (left) acute concentric exercise (Exercised) and (right) acute eccentric exercise (Exercised) compared to sedentary controls (Control).Statistical significance is marked by asterisks ($p < 0.05$ in Student's t-test).
Bottom: Representative Western blots show PKCα bands visualized by antibodies to total PKCα and the respective phosphosite (Thr497).

4. Discussion

4.1. Titin isoform composition is dependent on the HbA1c in type II diabetes mellitus patients

Diastolic dysfunction is known to be a prevalent comorbidity in type II diabetes mellitus, however physiological and pathological molecular settings remain unclear [26]. As an approach to deepen the insight in cellular processes leading to increased risks of prevalent heart conditions like diastolic dysfunction, the influences of both anti-diabetic drugs insulin and metformin on cardiac titin stiffness were investigated in aortic-stenosis patients with HbA1c levels ranging from 5% to over 9%, and in cell cultures of adult and embryonic rat cardiomyocytes. Many type II DM patients suffer from diverse heart conditions, where clinical and pharmacological treatments play a distinct role considering dose and side effects possibly interfering with the cell metabolism in cardiomyocytes. Thus far, only little is known about how insulin and particularly metformin affect cardiomyocytes. The effect of generally disturbed insulin signaling in type II DM patients on passive forces of cardiomyocytes has not been investigated until now. Regarding passive forces of the heart muscle, titin has been shown to be the only factor for myofibre passive stiffness in skinned myocytes, when evaluated in the physiological range of SLs from 1.9 μm to 2.2 μm [138]. In cell

culture models, it has been shown that titin isoform shift towards the stiffer N2-B isoform is influenced by T3 and insulin [75]. Consequently, decreased levels of insulin could therefore lead to isoform shifts towards the more compliant N2BA-isoform. This idea is supported by a small but significant isoform shift towards N2BA-titin found in insulin-deficient STZ- rats [75]. A study by Falcão-Pires et al. demonstrated that in biopsies from diabetic aortic-stenosis-patients undergoing surgical valve replacement, titin isoform composition is not changed in type II DM compared to controls. The study further reported that, titin phosphorylation leads to increased passive tension of cardiomyocytes of those patients investigated [50]. The results presented in the study at hand are in line with those observations when comparing biopsies from type II DM patients and non-diabetic patients. However, when additionally considering the long-term blood glucose level indicated by the HbA1c value, the present study shows that in patients with a HbA1c value higher than 7.5% the relative expression level of the compliant N2BA titin isoform was significantly increased. In contrast, in type II DM patients with a near to normal HbA1c value (below 6.5%), titin isoform composition was unchanged compared to non-diabetic patients. Conclusively, titin isoform composition in diabetic patients seems to be strongly dependent on long-term blood glucose levels. When generally comparing isoform ratios of the studied patient pool with those in other studies [22, 50], overall N2B contents are relatively low, suggesting an age, sex or heart condition-related shift backwards towards the more compliant N2BA from a ratio of $\sim$ 40:60 (N2BA:N2B) to $\sim$ 50:50. These profound differences in isoform composition affect diastolic functioning of the heart, where underlying mechansims are essential to be understood. In the human heart, increased amounts of N2BA represent higher compliance of the heart tissue and therefore may give rise to the passive stiffness changes. However, biopsies were obtained from the atria and not like in other studies from the ventricle, which may serve as a different possible explanation for this inconsistency.

4.2. Phosphorylation status of titin and titin based passive tension alterations in type II diabetes mellitus

Importantly, although the relative N2BA expression was significantly elevated, titin based myofilament stiffness was not decreased, but significantly increased in biopsies from diabetic patients. This increase is most probably caused by the significantly altered titin phosphorylation status in type II DM samples. Analysis of total titin phosphorylation using the phospho-protein stain ProQ Diamond has previously suggested a hypophosphorylation of titin and a subsequent increase in PT in cardiomyocytes from type II DM patients [50]. Here, titin domain phosphorylation was specifically analyzed by using phosphosite directed antibodies. Results demonstrate a significant hypophosphorylation of the elastic N2-B region of titin at position Ser4099 (PKG-targeted) and Ser4010 (PKA and ERK-targeted), but at the same time a significant increase in the phosphorylation of Ser11878 in the PEVK region. The observed changes in phosphorylation have previously been associated with an increase titin based myofilament stiffness [113, 76, 77, 78], which is in line with the increased passive tension measured in samples of patients with type II DM. The findings also support previous observations that the ProQ-diamond stain [24], frequently used to detect total titin phosphorylation, does not depict specific titin phosphorylations in the PEVK region [18].

This result further suggests elevated activity levels of the protein kinase responsible for PEVK phosphorylation. However, the kinase PKCα only shows a non-significant tendency for an increased activity in diabetics. Relative expression levels of the activated PKCα remain unchanged, but increases of total levels of active PKCα are the case, making activity and expression level of the PKCα a particular target of investigation. Potential phosphorylation of the various phosphosites of titin upon insulin stimulation may cause a substantital

effect on passive forces in the heart. The results further suggest a reduced activity of the kinases phosphorylating the N2-B region (PKA, PKG, ERK and possibly CaMKIIδ) in hearts from type II DM patients.

Western blot analysis showed increased PDE5A level and decreased sGC level in diabetic patients, indicating significantly reduced cellular cGMP level. Hence, it can be concluded that hypophosphorylation of Ser4099 in the titin N2-B region results at least partially from reduced activity of PKG in hearts from type II DM patients. It remains to be elucidated, whether the observed increase in PDE5A activity and the decrease in sGC activity, are due to the HF state or are a specific effect of altered insulin signaling. Altered activity of cGMP/PKG signaling has previously been reported in heart failure [95]. The NO pathway initiated upon oxidative stress targets titin, by activating the PKG via sGC and cGMP. Oxidative stress leads to an decrease in PT by phosphorylating the N2B. This nitric-oxide-signaling cascade that increases cardiac muscle elasticity, makes the modulation of PKG or cGMP levels a therapeutic approach through reduced stiffness in diastolic heart by blocking the PKG, normally decreased in heart disease [52]. It was additionally suggested that the hormone-induced control of titin-isoform expression requires activation of the PI3K/AKT/mammalian target of rapamycin (mTOR) signaling cascade [75]. Dysregulation of proteins that are insulin-influenced may contribute to altered cGMP concentrations and protein kinase G signaling, exacerbating diastolic dysfunction [82].

The actin-dynamics-regulating VASP phospho-protein was analyzed because VASP is a major substrate for cyclic nucleotide-dependent kinases and is known to be involved in cardiac pathology and activity in diabetics with underlying heart condition [61]. Phosphorylation of VASP at Serine residue 239 is specifically mediated by the cGMP-level-dependent PKG, making VASP phosphorylation an indicator for PKG activity. Tissue experiments showed a significant increase of active VASP (Ser239), thus indicating elevated PKG

activity. This finding matches previously observed elevated VASP phosphorylation and expression in hypertrophy, suggesting VASP characteristics as a marker for cardiac dysfunction [61].

Additionally, relative phosphorylation levels of the insulin receptor Y972 in diabetic patients were analyzed. A decrease in IR activity would have been expected [81], but instead the opposite was the case. Due to the fact that other studies [146, 46] also rule out correlations between activity and protein expression of the IR and diabetes or the IR activating tyrosine kinase activity [97], it can be assumed that other factors but the IR phosphorylation levels may cause insulin-uptaking cells to loose sensitivity or the ability for glucose channeling in type II diabetes.

The striking interferences with passive stiffness of cardiomyocytes upon stimulation could initiate the reevaluation of anti-diabetic drug doses, in particular when metformin and insulin are medically applied to type II DM patients with a heart condition. This could not only be the case in type II diabetics with a diastolic dysfunction-background, but also when diabetes patients are administered with insulin or metformin as a metabolic therapy to improve cardiac function [39]. However, similar results of increased PT in CMs from aortic stenosis patients with type II DM and isolated adult rat CMs treated with anti diabetic drugs were unexpected. The human biopsies represent tissue with disturbed insulin-signaling tissue, also due to the insulin resistance in type II DM. Nevertheless, all patients donating biopsies for this study were medicated with metformin, where the impact on cellular processes regarding protein expression and PT are still to be investigated. Notably, the profound differences in titin based passive tension of aortic stenosis patients diagnosed with DM and without DM are possibly also due to disturbed activity or expression levels of the kinases being responsible for titin phosphorylations, which in turn are able to regulate PT [18, 113].

4.3. Insulin modifies titin characteristics in cell culture models of adult and embryonic rat cardiomyocytes

To gain further insight in disturbed insulin signaling, particularly titin phosphorylation in adult rat cardiomyocytes (as a mammalian model) triggered by insulin or metformin, pathway activation *in vitro* upon stimulation was investigated. When treating the cells with insulin and metformin acutely for 15 minutes as well as long-term stimulation over 24 hours, significant increases in titin phosphorylation via PKG at Serine residue 4099 were detected. Since PKG mediated phosphorylation of titin is also known to decrease passive stiffness in myocytes [76, 79], force measurements of stimulated cells were additionally performed. Surprisingly, the latter revealed significant increases in PT after only 15 minutes treatment with insulin and metformin. Different phosphosites within the PEVK region, known to increase PT of cardiomyocytes when phosphorylated, possibly explain these findings [18].

Likewise, PEVK phosphorylation at Serine residue 12022 should be investigated in adult CMs in order to identify this phosphosite as a possible reason for the PT increases and PKCα involvement. Since the HbA1c value is linked to glucose levels and insulin and metformin trigger glucose uptake, glycans binding of titin was expected to be elevated after treatment [59]. Adult rat CMs were further treated with insulin and metformin and tested for titin glycosilation. Where and how titin is glycosilated, and whether titin glycosilation is altered in a disease stetting like diabetes mellitus, has not been investigated until now. However, it can be assumed that the binding of glycans to titin possibly leads to PT-alterations, since the amino acids proline (P) and lysine (K) are besides others predominantly glycosilated and both are particularly frequent within the PEVK region of titin. The significant increase in titin glycosilation observed, indicates an enhancement of insulin sensitivity. On

an organ level, myocardial insulin resistance may play an important role in the progression of diabetic cardiomyopathy and heart failure [28, 14, 124, 128]. Chronic hyperglycemia is a major characteristic of diabetes and also strongly correlated with higher incidence of myocardial infarction and markers of cardiac damage in humans [28, 37, 55]. Subsequently, disturbed insulin signaling may as well cause a decrease in relative titin glycosilation. Furthermore, effective glucose uptake and metabolism is of particular importance in ischemic hearts [28, 104], as well as to prevent cardiac dysfunction associated with heart failure [102, 28]. However, optimal glucose lowering interventions for the treatment of diabetic complications pose unique challenges within the clinical setting [100]. Thus, prevention of insulin resistance at an early stage is of utmost importance to prevent cardio-metabolic complications [28]. In order to confirm activation of insulin signaling via the PI3K pathway, AKT phosphorylation was investigated. In fact, insulin-dependent AKT phosphorylation in adult CMs on both Serine residues 473 and 308 were increased upon insulin stimulation. Interestingly, strong correlation between AKT (also known as PKB) activation and suppression of cell death with particular cardioprotection has been observed [127]. In other studies, AKT activation was already measurable after 5 minutes of insulin treatment on isolated mouse CMs, proposing an instant positive feedback mechanism via the PI3K/AKT/mTOR signaling cascade [127]. AKT also activates the endothelial nitric oxide synthase (eNOS), primarily present in endothelial cells and responsible for blood pressure regulation and an important member in cardiac signaling [140, 73]. Furthermore, eNOS induces the NO-survival pathway and therefore serves as a positive control for insulin dependent activation of the PKG pathway [75]. A role of eNOS in modulation of cardiovascular function in heart failure and insulin sensitivity is also assumed [107, 140]. In the present study, significantly increased eNOS concentrations in insulin and metformin stimulated cardiomyocytes, were detectable after only 15 minutes of stimulation. These findings indicate a very acute activation of cardio-protective signaling and support the previously found association of eNOS and type II DM to the increased incidence of cardiovascular disease and obesity-associated insulin resistance [145].

Primary embryonic CMs can be cultured longer and more stable than adult CMs. They serve as a suitable model for adult hearts, especiallly after day 9, where the isoform ratio is already 40:60 N2BA to N2B) and accordingly better comparable to patients treated with metformin. Therefore, they can easily be stimulated *in vitro* over longer periods of time. However, longer stimulation periods exceeding 96 hours in culture seemed to induce cell death. Notably, after 12 days in culture and metformin treatment for 96 hours, the relative content of titin's shorter and stiffer N2B isoform was significantly decreased. Reduced N2B content does implicate an increase of myofilament compliance, possibly altering systolic and diastolic performance.

These findings might identify a metformin-based potentially negative influence on cardiac function. Metformin is known to inhibit mTOR [110], which in turn has been identified to initiate titin isoform switch via the AKT-mTOR pathway by stimulating protein synthesis [6, 74], and may therefore explain altered isoform composition after metformin stimulation. Furthermore, metformin inhibits glucose regeneration in the liver and glucose resorption in the colon [110]. First studies indicate activation of AMPK signaling (known to improve insulin sensitivity), possibly interfering with proliferation, growth and cellular metabolism [110].

The same metformin administration led to significantly decreased levels of RBM20. The decrease in RBM20 levels may in fact explain the reduced N2B isoform expression. The splicing factor of titin is jointly responsible for the different titin isoforms co-expressed, due to incremental exon skipping between exons 50 and 219 of titin mRNA [130, 118]. RBM20 is a putative RNA-binding protein with one RNA recognition motif and one arginine-serine rich domain. Until today, there are no mechanistic studies on RBM20. However, titin splicing was found to be altered in a human cardiomyopathy with an a RBM20 mutation [118]. Post-transcriptional regulation is of particular importance in cardiac function and alternative splicing plays a major role in cardiac adaptive

responses [130]. The observed results indicate the role of metformin treatment in this process, given that altered expression level of titin's splicing factor RBM20 may be the cause for isoform alteration in patients medicated with metformin [130]. Furthermore, insulin treatment significantly increased relative titin phosphorylation at Ser4099 (PKG-targeted), Ser4010 (PKA, CaMKIIδ and ERK-targeted) and at Ser11878 (PKCα-targeted) in ERC. It was identified that, by inhibiting the PKG signaling cascade with LY, insulin induced titin phosphorylation, particularly at Ser4099, largely seems to depend on the activation of the NOS/sGC/PKG pathway.

In summary, disturbed insulin signaling in type II DM could explain the observed hypophosphorylation of the titin N2-B region. However, in cell culture experiments insulin treatment significantly activated PKCα and caused a substantial increase in PEVK-phosphorylation at Ser11878. This finding suggests that the increased Ser11878 phosphorylation in type II DM samples may not be a direct result of disturbed insulin signaling. Metformin however reacts similar to insulin on a cellular level, in particular the likewise activation of PKCα upon metformin treatment. There is a significant phosphorylation of titin's Ser11878 most likely via PKCα, Ser4010 probably via ERK and PKA and furthermore Ser4099 via possibly PKG after stimulation with metformin. Importantly, both insulin and metformin concomitantly increased passive forces in isolated CM significantly, suggesting interference with overall cardiac output. This provides grounds to reconsider prevalent and often even prophylactic administration of the anti-diabetic drugs.

Possible translocation of PKCα from the cytosol towards titin's Z-disc/I-band region upon stimulation was investigated additionally, since a sarcomeric location of PKCα would increase the probability of titin phosphorylation. The kinase seems to be present at the sarcomer in activated and inactivated forms and only in minor portions in the cytosol of myocytes treated with insulin and metformin as well as the control. Notably, other hormones such as T3

are known to trigger translocation from the cytosol to membrane fractions or unique subcellular sites of the cell [83, 84, 143]. Similar patterns in response of cellular reaction upon metformin and insulin stimulation can be shown here. Nevertheless, how the heart is directly affected remains unclear. The data obtained show, that metformin does lead to activation of titin phosphorylation cascades in adult and embryonic cardiomyocytes.

By taking HbA1c levels into consideration for type II DM patients and comparing metformin- and insulin-stimulated cardiomyocytes, insulin and metformin can be identified as potent modifiers of titin. Both significantly alter isoform composition, phosphorylation status and passive stiffnes (being regulated by wide-range signaling) in diabetic patients and in cell culture. Phosphorylation of titin strongly affects modifications in myocardial stiffness, thus overruling PT changes due to titin isoform composition. Further experiments including animal models are needed for a final understanding of oral antidiabetic drug-effects on the diastolic function of the myocardium.

4.4. Different modes of exercise cause cardiac and skeletal titin alterations

Exercise training is an effective method to improve physical fitness and physiological function in patients with type II diabetes [60]. How exercise beneficially affects the heart and skeletal muscle is commonly known, but the impact on titin in particular has been poorly investigated until now.

Therefore, effects of an acute exercise bout as well as chronic exercise (both concentric and eccentric) on titin based myofilament stiffness in cardiac and skeletal muscle tissue from adult rats were investigated. Eccentric muscle activation is the controlled lengthening of the muscle under tension, whereas contractions that permit the muscle to shorten, are referred to as concentric contractions [108]. Outstanding is the observation that in cardiac tissue training bouts of 15 minutes as well as long-term regular training bouts (period of six weeks) of level and downhill treadmill running induce a dramatic increase in passive cardiomyocyte tension. Analysis of Western blots from cardiac samples of exercised rats suggest that this increase is mainly due to altered titin modification. A significant decrease in the relative phosphorylation of the PKG-targeted Serine residue 4099 in the cardiac-specific N2-Bus, and a significantly increased phosphorylation of the PKCα-targeted Serine residue 11878 in the PEVK-region of titin was detectable in acutely level running and chronically downhill running rats. Both modifications have previously been identified to cause an increase in titin based myofilament stiffness [76, 18, 113]. The substantial activation of PKCα, indicated by an increased phosphorylation of Thr497 in the activation loop of the kinase [111], is most likely causing the increased phosphorylation of Serine residue 11878 in response to acute level and chronic downhill exercise. These findings are in line with previous studies demonstrating how acute exercise increases cardiac levels of PKCϵ (pSer729), PKCα (pSer657) and PKCδ (pThr507) [70]. The PKCα targets

the PEVK-region of titin not only at Ser11878 but also at Ser12022 [18]. In the cardiac samples from acutely level exercised animals, a significantly lower phosphorylation level of Ser12022 compared to sedentary controls was identified, which stands in contrast to the simultaneously measured increase in PKCα activation. Evidently, previous studies suggested that, based on differences in the amino acid composition around the PKC phosphorylation motifs within the PEVK region, PKCα has a lower affinity to Ser12022 than to Ser11878 [18]. Since the expression levels of PKCα were not changed within the 15 minutes exercise bout, the increased activity may be sufficient to increase the phosphorylation status of the high-affinity site Ser11878, but not that of the lower-affinity site Ser12022 [20]. Importantly, Ser12022 has also been shown to be targeted by CaMKIIδ, whereas CaMKIIδ-induced phosphorylation of Ser11878 is still in question [21, 95]. Hence, the adverse phosphorylation status of the two phosphorylation sites in the PEVK-region might be a result of differences in PKCα as well as CaMKIIδ expression levels and activity. Despite those differences, passive tension of isolated CMs was increased in exercised compared to control animals. The detected decrease in Ser12022 phosphorylation might possibly be overruled by the altered titin modification at Ser11878 and at Ser4099 in the N2-Bus region, which is targeted by PKG [113]. The reduced phosphorylation of Ser4099 suggests an exercise-induced decrease in ventricular PKG-activity. How cardiac PKG activity responses to acute and chronic exercise is not yet investigated.

The observations in acutely downhill running animals stand in contrast to the comparable results of acutely level and chronically downhill trained rats. No significant changes in the relative phosphorylation of the Serine residue 4099 in the cardiac-specific N2-Bus region were detectable here. Furthermore, significantly decreased phosphorylation of the Serine residue 11878 was measured. However, titin based myofilament stiffness was, as in all other exercised groups, significantly increased compared to the control group with no training. Certainly, a difference in cardiac tissue characteristics between downhill and

level running animals was not expected. The forces on the heart are basically identical, whereas they can be differentiated in skeletal muscle where they are physically stressed eccentric or concentric. CMs of chronic level running rats show a tendency towards an increase in titin based myofilament stiffness, but no significant changes were measurable (except for forces at a SL of $1.9\mu m$) and titin phosphorylation remains to be investigated with additional treadmill experiments necessary.

In humans, acute exercise is accompanied by activation of the β-adrenergic system, followed by activation of cAMP-dependent protein kinase A (PKA) [30]. Due to this fact, titin phosphorylation at position Ser4010 in the N2-Bus was analyzed in trained animals, which is targeted by ERK2 [8] and the PKA [113]. In fact, relative phosphorylation of this site varied substantially among the analyzed samples and therefore remained statistically unchanged for the acutely trained animals. To analyze for exercise-induced activation of PKA, the relative PKA-mediated phosphorylation of phospholamban at position Ser16 was determined, and a significantly increased activity of PKA in the exercised samples compared to the control group was confirmed. This increase does not influence phosphorylation of the PKA-sensitive site Ser4010 under the investigated conditions.

Titin-related PT is closely associated with ventricular function and increases in titin compliance are known to improve diastolic function [94]. Increased titin stiffness may therefore support the length-dependent activation involved in the Frank Starling Mechanism of cardiac muscle [82], and thus contribute to improved cardiac output in response to acute exercise. The exercise-induced effects on titin stiffness apparently seem to be different in chronically trained animals. Investigation of titin phosphorylation at Ser11878 and Ser12022 in a recent study involving animals trained for a period of 3 weeks shows a significant decrease in Ser12022 phosphorylation, whereas relative phosphorylation of Ser11878 remained unchanged [20]. The reduced Ser12022 phosphorylation of

the cardiac tissue from trained animals was linked to a simultaneous decline in PKCα expression. PKG-dependent titin phosphorylation was analyzed with a back-phosphorylation assay and no exercise-induced differences among both animal pools were discovered. From the study at hand, it can be concluded that chronic exercise lowers titin based stiffness through altered PEVK phosphorylation at Ser12022 and thereby improves diastolic function of the chronically trained heart [20]. These observations are interesting also from a clinical point of view as they imply adverse effects of acute and chronic exercise on ventricular function. Furthermore, acute exercise-induced titin modifications in skeletal muscle tissue from Latissimus dorsi were investigated. The Latissimus dorsi muscle was chosen for analysis, due to the fact that it is one of the key muscles for running in quadruped animals. Moreover, the effects of concentric (level running) and eccentric (downhill running) exercise were compared, too. Unlike concentric exercise, eccentric contractions have been shown to result in ultrastructural changes within the skeletal muscle fiber that involve severe myofibrillar disturbances such as Z-band disruption and streaming [54]. These disturbances usually result in muscle injury and soreness [53].

In LAT samples from rats exercised by level running, a significant decrease in titin phosphorylation at position Ser11878, but a significant increase in the relative phosphorylation of Ser12022 was detected. Interestingly, eccentric downhill running also caused a decreased phosphorylation of Ser11878 but no significant alteration at Serine residue 12022. PKCα phosphorylation at Thr497 was unchanged in exercised animals from both groups compared to sedentary controls. This finding stands in contrast to previous reports demonstrating that acute exercise bouts increase PKC activity in skeletal muscle within a few minutes after onset of exercise [10]. However, increased expression levels of PKCα may as well explain this discrepancy. Like in cardiac titin, Ser12022 from skeletal muscle can also be phosphorylated by CaMKIIδ, whose activity has previously been demonstrated to be increased in skeletal muscles upon exercise [12, 11]. Therefore, the substantial increase in skeletal muscle titin phosphory-

lation at Ser12022 after 15 minutes treadmill running could possibly arise from altered CaMKIIδ activity in the LAT samples. It can be assumed that, like in the cardiac tissue, the reduced relative phosphorylation of one serine residue (here Ser11878) is likely overruled by the substantial increase in the relative phosphorylation of another serine residue (here Ser12022), and will result in an overall increase in titin based myofilament stiffness of the exercised skeletal LAT muscle. Results are in line with a recent study reporting the effect of chronic exercise by investigating the diaphragm of mice after a 3 week training period with voluntary concentric treadmill exercise [20]. The study reports unchanged titin phosphorylation at Ser11878 and significantly increased phosphorylation of Ser12022 in exercised animals compared to sedentary controls. Importantly, in that study PKCα expression was unaltered by the chronic exercise regime [20]. Regardless of the duration and the type of running exercise the skeletal muscle seems to respond with rapidly increased titin based myofilament stiffening. Considering that stiffening of the titin spring will support A-band re-centering in the contracting sarcomere, the observed increase in phosphorylation-induced titin stiffness could be important to maintain the structural integrity, especially of the acutely exercised skeletal muscles [20]. In summary, data suggest that a single exercise bout induces rapid changes to titin based myofilament stiffness, which may help to improve cardiac output by supporting the Frank-Starling mechanism, and further augment the structural stability of exercised muscle, in order to prevent myofilament damage.

In a nutshell, the investigated effect of a single acute exercise unit on post-translational modification of titin in cardiac as well as skeletal muscle, was a first attempt to relate the observed changes to altered protein kinase activation. Titin phosphorylation is regulated by complex signaling mechanisms to fine-tune passive stiffness in myocytes. Results furhter indicate that exercise acutely increases titin based myofilament stiffness and may therefore support the positive inotropic response of the heart to the elevated physical activity.

Further investigations of cellular processes involving titin, that are induced by exercise and medication, are open for investigation. The influence of acute and chronic physical activity as well as that of medication with metformin and insulin on titin may be a key target in the future for improved medication and therapeutic measures in patients with diabetes suffering from a variety of comorbidities like heart conditions and obesity.

5. Conclusion

Conclusively, the presented data show that phosphorylation of the giant sarcomeric protein titin is regulated by complex signaling mechanisms to fine-tune passive myocardial stiffness and can acutely be influenced by different physiological and patho-physiological modulators:

- Insulin as well as metformin are powerful modulators of cardiac titin, and may therefore play an important role in modifying myocardial stiffness in human hearts. In type II diabetes mellitus patients titin isoform composition can be directly connected to their HbA1c levels.

- A single exercise bout affects titin domain phosphorylation and titin-based myocyte stiffness with obviously divergent effects in cardiac and skeletal muscle tissues. The observed changes in titin stiffness could play an important role in adapting the passive and active properties of the myocardium and the skeletal muscle to increased physical activity.

These findings deserve further efforts to elucidate the molecular mechanism of stimuli-regulated titin modifications. The current work provides the foundation for future studies.

6. Abbreviations

Name	Meaning
A	Ampere
A-Band	Anisotropoc Band
AMPK	Adenosinephosphate-activated Proteinkinase
APS	Ammoniumperoxodisulphate
Aq.dest.	Aqua destilated
bp	Base pairs
BSA	Bovine Serum Albumin
Ca^{2+}	Calcium
$CaCl_2$	Calcium chloride
CaMKIIδ	Ca^{2+}/calmodulin-dependent protein kinase II delta
cAMP	Cyclic adenosinmonophosphate
cGMP	Cyclic guanosine monophosphate
cDNA	Complementary desoxyribonuclease
°C	Celsius
CHD	Coronary heart disease
CM	Cardiomyocyte
ctrl	Control
Cy3	Cyanine
Da	Dalton

DMEM	Dulbecco Modified Eagle Medium
DMSO	Dimethylsulfide
DNA	Desoxyribonucleicacid
dNTP	Desoxyribonucleosidtriphosphate
DTT	Dithiothreitol
EDTA	Ethylendiamintetraacetate
et al.	Et alii (lat. and others)
EM	Electron Micrsocopy
eNOS	Endothelial nitric oxide synthase
ERK	Extracellular signal regulated kinase
FBS	Fetal Bovine Serum
FHL	Four-and-a-half LIM
Fig	Figure
g	Gramm
HEPES	4-(2-hydroxyethyl)-1-piperazineethanesulfonic acid
GLUT-4	Glucose-transporter type 4
h	Hour
HFpEF	Heart failure with preserved ejection fraction
HEK	Human ebryonic kidney
Ig	Immunoglobuline
IGF-1	Insulin-like growth factor
IMDM	Iscove's Modified Dulbecco's Medium
Ins	Insulin
IR	Insulin Receptor
IRS	Insulin Receptor Substrate
ITS	Insulin-Transferrin-Sodium Selenite
kg	Kilogramm
kDa	Kilo Dalton
KO	Knock Out
l	Litre

LAT	Latissimus Dorsi Muscle
LV	Left ventricle
LY	LY294001 (PI3-Kinase-Inhibitor)
μ	Mikro
m	Milli
M	Molar
M-Band	Middle Band
MAPK	Mitogen-activated protein kinase
MARPs	Muscle ankyrin repeat proteins
MDa	Mega Dalton
MHC	Myosin Heavy Chain
mRNA	Messenger Ribonucleic acid
mTOR	Mammalian target of Rapamycin
MuRF-1	Muscle RING-finger protein-1
MW	Molecular weight
n	Nano
NO	Nitric oxide
OD	Optical Density
Pa	Pascal
PAGE	Polyacrylamidegelelectrophoresis
PBS	Phosphate buffered system
PBST	Phosohate buffered system with Tween
PCR	Polymerase Chain Reaction
PDE5A	cGMP-specific phosphodiesterase type 5
PDK1	3-phosphosinositide-dependent protein kinase-1
PEVK	Proline glutamate valine lysin
PI3K	Phosphatidyl-Inositiol-3-Kinase
PKA	Protein Kinase A
PKB	Protein Kinase B
PKC	Protein Kinase C

PKG	Protein Kinase G
PL	Persistence lengths
PVDF	Polyvinyldifluoride
qRT-PCR	Quantitative real-time PCR
Raptor	Regulatory associated protein of mTOR
RBM20	RNA binding motif protein 20
RNA	Ribonucleic acid
rpm	Rounds per minute
SDS	Sodium Dodecyl Sulphate
Ser	Serine
sGC	Soluble guanylate cyclase
SL	Slack Length
T3	Thyroid hormone triiodo-l-thyronine
Tab	Table
TAE	Tris-Acetat-EDTA
TBS(T)	Tris buffered Saline (with 0.1% Tween)
TE Buffer	Tris EDTA Buffer
TEMED	Tetramethylethylendimine
Thr	Threonine
Tris	Tris (hydroxymethyl)-aminomethan
U	Unit
us	Unique sequence
VASP	Vasodilatator stimulating phospho protein
v/v	Volume/Volume
WB	Western Blot
WT	Wild type

Table 6.1.: List of abbreviations

7. Bibliography

[1] Borbély A., van der Velden J., Papp Z., Bronzwaer JG., Edes I., Stienen GJ., and Paulus WJ. Cardiomyocyte stiffness in diastolic heart failure. *Circulation*, 6(111):774–781, 2005.

[2] Ehsani A. A., Ogawa T., Miller T. R., Spina R. J., and Jilka S. M. Exercise training improves left ventricular systolic function in older men. *Circulation*, 9(83):96–103, 1991.

[3] Freiburg A., Trombitas K., Hell W., Cazorla O., Fougerousse F., Centner T., Kolmerer B., Witt C., Beckmann JS., Gregorio CC., Granzier H., and Labeit S. Series of exon-skipping events in the elastic spring region of titin as the structural basis for myofibrillar elastic diversity. *Circ. Res.*, 1(86):1114–1121, 2000.

[4] Fukuzawa A., Lange S., Holt M., Vihola A., Carmignac V., Ferreiro A., Udd B., and Gautel M. Interactions with titin and myomesin target obscurin and obscurin-like 1 to the M-band: implications for hereditary myopathies. *J. Cell Sci.*, 11(121):1841–1851, 2008.

[5] Kaminitz A., Stein J., Yaniv I., and Askenasy N. The vicious cycle of apoptotic beta-cell death in type 1 diabetes. *Immunol. Cell Biol.*, 8(85):582–589, 2007.

[6] Kenessey A. and Ojamaa K. Thyroid hormone stimulates protein synthesis

in the cardiomyocyte by activating the Akt-mTOR and p70S6K pathways. *J. Biol. Chem.*, 1(281):20666–20672, 2006.

[7] Kontrogianni-Konstantopoulos A., Ackermann MA., Bowman AL., Yap SV., and Bloch RJ. Muscle giants: molecular scaffolds in sarcomerogenesis. *Physiol. Rev.*, 3(89):1217–1267, 2009.

[8] Raskin A., Lange S., Banares K., Lyon RC., Zieseniss A., Lee LK., Yamazaki KG., Granzier HL., Gregorio CC., McCulloch AD., Omens JH., and Sheikh F. A novel mechanism involving four-and-a-half LIM domain protein-1 and extracellular signal-regulated kinase-2 regulates titin phosphorylation and mechanics. *J. Biol. Chem.*, 35(287):29273–29284, 2012.

[9] Vetere A., Choudhary A., Burns SM., and Wagner BK. Targeting the pancreatic β-cell to treat diabetes. *Nat. Re. Drug Discov.*, 4(13):278–289, 2014.

[10] Rose A.J., Michell B.J., Kemp B.E., and Hargreaves M. Effect of exercise on protein kinase C activity and localization in human skeletal muscle. *J. Physiol.*, 3(561):861–870, 2004.

[11] Rose A.J., Howlett K., King DS., and Hargreaves M. Effect of prior exercise on glucose metabolism in trained men. *Am. J. Physiol. Endocrinol. Metab.*, 4(281):766–771, 2001.

[12] Rose A.J. and Hargreaves M. Exercise increases Ca^2-calmodulin-dependent protein kinase II activity in human skeletal muscle. *J. Physiol.*, 1(553):303–309, 2003.

[13] Cheng AM., Rizzo-DeLeon N., Wilson CL., Lee WJ., Tateya S., Clowes AW., Schwartz MW., and Kim F. Vasodilator-stimulated phosphoprotein protects against vascular inflammation and insulin resistance. *Am. J. Physiol. Endocrinol. Metab.*, 7(307):571–579, 2014.

[14] Gustafsson B., Brendorp M., Seibaek H., Burchardt P., Hildebrandt L., and Kober L. Influence of diabetes and diabetes-gender interaction on the risk of death in patients hospitalized with congestive heart failure. *J. Am. Coll. Cardiol.*, 4(43):771–777, 2004.

[15] Lindman BR., Davila-Roman VG., Mann DL., McNulty S., Semigran MJ., Lewis GD., de las Fuentes L., Joseph SM., Vader J., Hernandez AF., and Redfield MM. Cardiovascular Phenotype in HFpEF Patients With or Without Diabetes. *J. Am. Coll. Cardiol.*, 6(64):541–549, 2014.

[16] Chauveau C., Rowell J., and Ferreiro A. A Rising Titan: TTN Review and Mutation Update. *Hum. Mutat.*, 10(1002):22611, 2014.

[17] Coen A. C., Ottenheijm, Hieronymus W. H. van Hees, Leo M. A. Heunks, and Granzier H. Titin-based mechanosensing and signaling: role in diaphragm atrophy during unloading? *Am. J. Physio.*, 300(10):161–166, 2011.

[18] Hidalgo C., Hudson B., Bogomolovas J., Zhu Y., Anderson B., Greaser M., Labeit S., and Granzier H. PKC phosphorylation of titin's PEVK element: A novel and conserved pathway for modulating myocardial stiffness. *Circ. Res.*, 617(105):631–638, 2009.

[19] Hidalgo C., Hudson B., Bogomolovas J., Zhu Y., Anderson B., Greaser M., Labeit S., and Granzier H. PKC phosphorylation of titin's PEVK element: a novel and conserved pathway for modulating myocardial stiffness. *Circ. Res.*, 7(105):631–638, 2009.

[20] Hidalgo C., Saripalli C., and Granzier H.L. Effect of exercise training on post-translational and post-transcriptional regulation of titin stiffness in striated muscle of wild type and IG KO mice. *Biochem. Biophys.*, 2(1016):10, 2014.

[21] Hidalgo C. and Granzier H. Tuning the molecular giant titin through

phosphorylation: Role in health and disease. *Trends in cardiovascular medicine*, 6(23):165–171, 2013.

[22] Neagoe C., Kulke M., del Monte F., Gwathmey JK., de Tombe PP., Hajjar RJ., and Linke WA. Titin isoform switch in ischemic human heart disease. *Circulation*, 7(9):280–283, 2002.

[23] Toyoshima C. and Mizutani T. Crystal structure of the calcium pump with a bound ATP analogue. *Nature*, 6999(430):529–535, 2004.

[24] Ottenheijm CA., Voermans NC., Hudson BD., Irving T., Stienen GJ., van Engelen BG., and Granzier H. Titin-based stiffening of muscle fibers in Ehlers-Danlos Syndrome. *J. Appl. Physiol*, 7(112):1157–1165, 2012.

[25] Bailey CJ. and Turner RC. Metformin. *N. Engl. J. Med.*, 57(334):4–9, 1996.

[26] Roos CJ., Auger D., Djaberi R., de Koning EJ., Rabelink TJ., Pereira AM., Bax JJ., Delgado V., Jukema JW., and Scholte AJ. Relationship between left ventricular diastolic function and arterial stiffness in asymptomatic patients with diabetes mellitus. *Int. J. Cardiovasc. Imaging*, 3(29):609–616, 2013.

[27] Chung CS., Bogomolovas J., Gasch A., Hidalgo CG., Labeit S., and Granzier HL. Titin-actin interaction: PEVK-actin-based viscosity in a large animal. *J. Biomed. Biotechnol.*, 10(310791):1155, 2011.

[28] Joseph D., Kimar C., Symington B., Milne R., and Essop MF. The detrimental effects of acute hyperglycemia on myocardial glucose uptake. *Life Sci.*, 2(105):31–42, 2014.

[29] Labeit D., Watanabe K., Witt C., Fujita H., Wu Y., Lahmers S., Funck T., Labeit S., and Granzier H. Calcium-dependent molecular spring elements in the giant protein titin. *Proc. Natl. Acad. Sci. U S A.*, 23(100):13716–13721, 2003.

[30] Leosco D., Parisi V., Femminella G.D., Formisano R., Petraglia L., Allocca E., and Bonaduce D. Effects of exercise training on cardiovascular adrenergic system. *Front. Physiol.*, 1(4):238, 2013.

[31] Linke WA.and Rudy DE., Centner T., Gautel M., Witt C., Labeit S., and Gregorio CC. I-band titin in cardiac muscle is a three-element molecular spring and is critical for maintaining thin filament structure. *J. Cell Biol.*, 3(146):631–644, 1999.

[32] Fuerst DO., Osborn M., Nave R., and Weber K. The organization of titin filaments in the half-sarcomere revealed by monoclonal antibodies in immunoelectron microscopy: a map of ten nonrepetitive epitopes starting at the Z line extends close to the M line. *J. Cell Biol.*, 5(106):1563–1572, 1988.

[33] Ehler E. and Gautel M. The sarcomere and sarcomerogenesis. *Adv. Exp. Med. Biol.*, 642(1):1–14, 2008.

[34] Rossi E., Faiella A., Zeviani M., Labeit S., Floridia G., Brunelli S., Cammarata M., Boncinelli E., and Zuffardi O. Order of six loci at 2q24-q31 and orientation of the HOXD locus. *Genomics*, 1(24):34–40, 1994.

[35] Takimoto E., Champion HC., Belardi D., Moslehi J., Mongillo M., Mergia E., Montrose DC., Isoda T., Aufiero K., Zaccolo M., Dostmann WR., Smith CJ., and Kass DA. cGMP catabolism by phosphodiesterase 5A regulates cardiac adrenergic stimulation by NOS3-dependent mechanism. *Circ. Res.*, 1(96):100–109, 2005.

[36] Richter EA. and Hargreaves M. Exercise, GLUT4, and skeletal muscle glucose uptake. *Physiol. Rev.*, 3(93):993–1017, 2013.

[37] Barr EL., Zimmet P., Welborn TA., Jolley D., Magliano DJ., Dunstan DW., Cameron AJ., Dwyer T., Taylor HR., Tonkin AM., McNeil J. Wong TY, and Shaw JE. Risk of cardiovascular and all-cause mortality in

individuals with diabetes mellitus, impaired fasting glucose, and impaired glucose tolerance: the Australian Diabetes, Obesity, and Lifestyle Study (AusDiab). *Circulation*, 2(116):151–157, 2007.

[38] Jeong EM. and Dudley SC. Jr. New diagnostic and therapeutic possibilities for diastolic heart failure. *R. I. Med. J.*, 2(97):35–37, 2014.

[39] Loiacono F., Alberti L., Lauretta L., Puccetti P., Silipigni C., Margonato A., and Fragasso G. Metabolic therapy for heart failure. *Recenti. Prog. Med.*, 7(105):288–294, 2014.

[40] Malik FS. and Taplin CE. Insulin therapy in children and adolescents with type 1 diabetes. *Pediatr. Drugs*, 2(16):141–150, 2014.

[41] Iribe G., Helmes M., and Koh P.l. Force-length relations in isolated intact cardiomyocytes subjected to dynamic changes in mechanical load. *Am. J. Physio.*, 292(10):1487–1497, 2007.

[42] Loeffler G. and Petrides P. Biochemie und Pathobiochemie. *Springer*, 14(1073):755–793, 2010.

[43] Szent-Györgyi A G. Calcium regulation of muscle contraction. *Biophys. J.*, 15(7):707–723, 1975.

[44] Nasri H. On the occasion of the world diabetes day 2013; diabetes education and prevention; a nephrology point of view. *J. Ren. Inj. Prev.*, 2(2):31–32, 2013.

[45] Nasri H., Baradaran A., Ardalan MR., Mardani S., Momeni A., and Rafieian-Kopaei M. Bright renoprotective properties of metformin: beyond blood glucose regulatory effects. *Iran J. Kidney Dis.*, 6(7):423–428, 2013.

[46] Qu H.M., Ye Y.H., Peng W., and Zhan Y. Relationship between tyrosine phosphorylation and protein expression of insulin receptor substrate-1

and insulin resistance in gestational diabetes mellitus. *Zhonghua Fu Chan Ke Za Zhi*, 4(42):249–252, 2007.

[47] Agarkova I., Ehler E., Lange S., Schoenauer R., and Perriard JC. M-band: a safeguard for sarcomere stability? *J. Muscle Res. Cell Motil.*, 2-3(24):191–203, 2003.

[48] Agarkova I. and Perriard JC. The M-band: an elastic web that crosslinks thick filaments in the center of the sarcomere. *Trends Cell Biol.*, 9(15):477–485, 2005.

[49] Agarkova I., Schoenauer R., Ehler E., Carlsson L., Carlsson E., Thornell LE., and Perriard JC. The molecular composition of the sarcomeric M-band correlates with muscle fiber type. *Eur. j. Cell Biol.*, 5(83):193–204, 2004.

[50] Falcao-Pires I., Hamdani N., Borbely A., Gavina C., Schalkwijk CG., van der Velden J., van Heerebeek L., Stienen GJ., Niessen HW., Leite-Moreira AF., and Paulus WJ. Diabetes mellitus worsens diastolic left ventricular dysfunction in aortic stenosis through altered myocardial structure and cardiomyocyte stiffness. *Circulation*, 2(124):1151–1159, 2011.

[51] Makarenko I., Opitz CA., Leake MC., Neagoe C., Kulke M., Gwathmey JK., del Monte F., Hajjar RJ., and Linke WA. Passive stiffness changes caused by upregulation of compliant titin isoforms in human dilated cardiomyopathy hearts. *Circ. Res.*, 7(95):708–716, 2004.

[52] Alegre-Cebollada J., Kosuri P., Giganti D., Eckels E., Rivas-Pardo JA., Hamdani N., Warren CM., Solaro RJ., Linke WA., and Fernandez JM. S-glutathionylation of cryptic cysteines enhances titin elasticity by blocking protein folding. *Cell*, 6(156):1235–1246, 2013.

[53] Fridén J. and Lieber R.L. The structural and mechanical basis of exercise-induced muscle injury. *Med. Sci. Sport Exerc.*, 6(24):521–530, 1992.

[54] Fridén J., Kjorell U., and Thornel L-E.l. An immunocytological study in man. *Int. J. Sports Med.*, 2(5):15–18, 1984.

[55] Rubin J., Matsushita K., Ballantyne CM., Hoogeveen R., Coresh J., and Selvin E. Chronic hyperglycemia and subclinical myocardial injury. *J. Am. Coll. Cardiol.*, 5(59):484–489, 2012.

[56] Sutherland F. J. and Hearse D. J. The Isolated Blood And Perfusion fluid Perfused Heart. *Cardiovasc. Res.*, 10(109):11–18, 2011.

[57] Kuzman JA., Gerdes AM., Kobayashi S., and Liang Q. Thyroid hormone activates Akt and prevents serum starvation-induced cell death in neonatal rat cardiomyocytes. *J. Mol. Cell Cardiol.*, 5(39):841–844, 2005.

[58] Waddle J.A., Cooper J.A., and Waterston RH. The alpha and beta subunits of nematode actin capping protein function in yeast. *Mo. Bio. Cell.*, 9(4):907–917, 1993.

[59] Moller J.B., Kristensen N.R., Klim S., Karlsson M.O., Ingwersen S.H., and Kjellsson M.C. Methods for Predicting Diabetes Phase III Efficacy Outcome From Early Data: Superior Performance Obtained Using Longitudinal Approaches. *CPT Pharmacometrics Syst. Pharmacol.*, 3(10):122, 2014.

[60] Taylor JD., Fletcher JP., Mathis RA., and Cade WT. Effect of Moderate Versus High Intensity Exercise Training on Physical Fitness and Physical Function in People With Type 2 Diabetes: A Randomized Clinical Trial. *Phys. Ther.*, page Epub ahead of print, 2014.

[61] Sartoretto JL., Jin BY., Bauer M., Gertler FB., Liao R., and Michel T. Regulation of VASP phosphorylation in cardiac myocytes: differential regulation by cyclic nucleotides and modulation of protein expression in diabetic and hypertrophic heart. *Am. J. Physiol. Heart Circ. Physiol.*, 5(297):1697–1710, 2009.

[62] Bishu K., Hamdani N., Mohammed SF., Krüger M., Ohtani T., Ogut O., Brozovich FV., Burnett JC. Jr., Linke WA., and Redfield MM. Sildenafil and b-type natriuretic peptide acutely phosphorylate titin and improve diastolic distensibility in vivo. *Circulation*, 1(124):2882–2891, 2011.

[63] Hoehn K. and Marieb E. Muscles and Muscle Tissue. *Human Anatomy and Physiology*, 7(9):280–283, 2014.

[64] Hoehn K. and Marieb E. Myofibrils. *Human Anatomy and Physiology*, 7(9):284–287, 2014.

[65] Ma K., Forbes JG., Gutierrez-Cruz G., and Wang K. Titin as a giant scaffold for integrating stress and Src homology domain 3-mediated signaling pathways: the clustering of novel overlap ligand motifs in the elastic PEVK segment. *J. Biol. Chem.*, 37(281):27539–275756, 2006.

[66] Trombitas K., Redkar A., Centner T., Wu Y., Labeit S., and Granzier H. Extensibility of isoforms of cardiac titin: variation in contour length of molecular subsegments provides a basis for cellular passive stiffness diversity. *Biophys. J.*, 6(79):3226–3234, 2000.

[67] Petersen KF. and Shulman GI. Etiology of insulin resistance. *Am. J. Med.*, 5(119):6–10, 2006.

[68] Capiotti KM., Antonioli R Jr., Kist LW., Bogo MR., Bonan CD., and Da Silva RS. Persistent impaired glucose metabolism in a zebrafish hyperglycemia model. *Comp. Biochem. Physiol. B. Biochem. Mol. Biol.*, 10(171):58–65, 2014.

[69] Tskhovrebova L. and Trinick J. Roles of titin in the structure and elasticity of the sarcomere. *J. Biomed. Biotechnol*, 4(8):612, 2010.

[70] Carson L.D. and Korzick D.H. Dose-dependent effects of acute exercise on PKC levels in rat heart: is PKC the heart's prophylactic? *Acta Physiol Scand.*, 2(178):97–106, 2003.

[71] Prado LG., Makarenko I., Andresen C., Krüger M., Opitz CA., and Linke WA. Isoform diversity of giant proteins in relation to passive and active contractile properties of rabbit skeletal muscles. *J. Genl. Physiol.*, 5(126):461–480, 2005.

[72] Somerville LL. and Wang K. In vivo phosphorylation of titin and nebulin in frog skeletal muscle. *Biochem. Biophys. Res. Commun.*, 3(147):986–992, 1987.

[73] Cocks M., Shaw CS., Shepherd SO., Fisher JP., Ranasinghe A., Barker TA., Tipton KD., and Wagenmakers AJ. Effect of resistance training on microvascular density and eNOS content in skeletal muscle of sedentary men. *Microcirculation.*, 5(10):11–15, 2014.

[74] Krüger M., Sachse C., Zimmermann WH., Eschenhagen T., Klede S., and Linke WA. Thyroid hormone regulates developmental titin isoform transitions via the phosphatidylinositol-3-kinase/ akt pathway. *Circ. Res.*, 1(102):439–447, 2008.

[75] Krüger M., Babicz K., von Frieling-Salewsky M., and Linke WA. Insulin signaling regulates cardiac titin properties in heart development and diabetic cardiomyopathy. *Journal of molecular and cellular cardiology*, 6(48):910–916, 2010.

[76] Krüger M., Kotter S., Grutzner A., Lang P., Andresen C., Redfield MM., Butt E., dos Remedios CG., and Linke WA. Protein kinase g modulates human myocardial passive stiffness by phosphorylation of the titin springs. *Circ. Res.*, 2(104):87–94, 2009.

[77] Krüger M. and Linke WA. Protein kinase-A phosphorylates titin in human heart muscle and reduces myofibrillar passive tension. *J. Muscle Res. Cell Motil.*, 5-7(27):435–444, 2006.

[78] Krüger M. and Linke WA. Titin-based mechanical signalling in normal and failing myocardium. *J. Mol. Cell Cardiol.*, 4(46):490–498, 2009.

[79] Krüger M. and Linke W.A. The giant protein titin: a regulatory node that integrates myocyte signalling pathways. *J. Biol. Chem.*, 12(286):9905–9912, 2011.

[80] Laakso M. and Kuusisto J. Insulin resistance and hyperglycaemia in cardiovascular disease development. *Nat. Rev. Endocrinol.*, 5(10):293–302, 2014.

[81] Massaro M., Scoditti E., Pellegrino M., Calabriso N., Carluccio M., Storelli C., and De Caterina R. P739Phosphodiesterase 5A expression is up-regulated in vascular endothelium under pro-inflammatory conditions: a newly disclosed anti-inflammatory activity by the omega-3 fatty acid docosahexaenoic acid. *Cardiovasc. Res.*, 10(103):135, 2014.

[82] Methawasin M., Hutchinson KR., Lee EJ., Smith JE. 3rd, Saripalli C., Hidalgo CG., Ottenheijm CA., and Granzier H. Experimentally increasing titin compliance in a novel mouse model attenuates the frank-starling mechanism but has a beneficial effect on diastole. *Circulation*, 129(19):1924–36, 2014.

[83] MackayK. and Mochly-Rosen D. Localization, Anchoring, and Functions of Protein Kinase C Isozymes in the Heart. *J. Mol. Cell Cardiol.*, 7(33):1301–1307, 2001.

[84] Disatnik MH., Buraggi G., and Mochly-Rosen D. Localization, Anchoring, and Functions of Protein Kinase C Isozymes in the Heart. *Exp. Cell Res.*, 2(210):287–297, 1994.

[85] Rhee MK., Slocum W., Ziemer DC., Culler SD., Cook CB., El-Kebbi IM., Gallina DL., Barnes C., and Phillips LS. Patient adherence improves glycemic control. *The Diabetes educator*, 6(31):240–250, 2005.

[86] Bang ML., Centner T., Fornoff F., Geach AJ., Gotthardt M., McNabb M., Witt CC., Labeit D., Gregorio CC., Granzier H., and Labeit S. The Complete Gene Sequence of Titin, Expression of an Unusual $\approx$ 700-kDa

Titin Isoform, and Its Interaction With Obscurin Identify a Novel Z-Line to I-Band Linking System. *Cardiovasc. Res.*, 89(11):1065–1072, 2001.

[87] LeWinter MM. and Granzier HL. Cardiac titin and heart disease. *J. Cardiovasc. Pharmacol.*, 3(63):207–212, 2014.

[88] Bristow M.R., Ginsberg R., Umans V., Fowler M., Minobe W., and Rasmussen R. β1- and β2-Adrenergic receptor subpopulations in nonfailing and failing human ventricular myocardium: coupling of both receptor subtypes to muscle contraction and selective b1 receptor down-regulation in heart failure. *Circ. Res.*, 1(59):297–309, 1986.

[89] Fukuda N., Terui T., Ishiwata S., and Kurihara S. Titin-based regulations of diastolic and systolic functions of mammalian cardiac muscle. *J. Mol. Cell Cardiol.*, 5(48):876–881, 2010.

[90] Hamann N., Zaucke F., Heilig J., Oberlaender K.D., Brüggemann G.P., and Niehoff A. Effect of different running modes on the morphological, biochemical, and mechanical properties of articular cartilage. *Scand. J. Med. Sci. Sports.*, 1(24):179–188, 2014.

[91] Hamann N., Zaucke F., Dayakli M., Brüggemann G.P., and Niehoff A. Growth-related structural, biochemical, and mechanical properties of the functional bone-cartilage unit. *J. Anat.*, 2(222):248–259, 2013.

[92] Hamdani N., Krysiak J., Kreusser M.M., Neef S., Dos Remedios C.G., Maier L.S., Krüger M., Back s J., and Linke W.A. Crucial role for Ca^2/calmodulindependent protein kinase- II in regulating diastolic stress of normal and failing hearts via titin phosphorylation. *Circ. Res.*, 1(112):664–674, 2013.

[93] Hamdani N., Bishu KG., von Frieling-Salewsky M., Redfield MM., and Linke WA. Deranged myofilament phosphorylation and function in experimental heart failure with preserved ejection fraction. *Cardiovasc. Res.*, 3(97):464–471, 2013.

[94] Hamdani N. and Linke WA. Myocardial Titin: An Important Modifier of Cardiac Stiffness. *Biophysical Journal*, 106(2, Supplement 1):346a – 355, 2014.

[95] Hamdani N. and Paulus WJ. Myocardial titin and collagen in cardiac diastolic dysfunction: Partners in crime. *Circulation*, 7(128):5–8, 2013.

[96] Gileadi O. Structures of soluble guanylate cyclase: implications for regulatory mechanisms and drug development. *Biochem. Soc. Trans.*, 1(42):108–113, 2014.

[97] Damm P. Gestational diabetes mellitus and subsequent development of overt diabetes mellitus. *Dan. Med. Bull.*, 5(45):495–509, 1998.

[98] Young P., Ehler E., and Gautel M. Obscurin, a giant sarcomeric Rho guanine nucleotide exchange factor protein involved in sarcomere assembly. *J. Cell Biol.*, 1(154):123–136, 2001.

[99] Davis PJ. and Davis FB. Nongenomic actions of thyroid hormone on the heart. *Thyroid.*, 6(12):459–466, 2002.

[100] Radke PW. and Schunkert H. Glucose-lowering therapy after myocardial infarction: more questions than answers. *Eur. Heart J.*, 2(29):141–143, 2008.

[101] Buresh R. Exercise and glucose control. *J. Sports Med. Phys. Fitness*, 4(54):373–382, 2014.

[102] Liao R., Jain M., Cui L., D'Agostino J., Aiello F., Luptak I., Ngoy S., Mortensen RM., and Tian R. Cardiac-specific overexpression of GLUT1 prevents the development of heart failure attributable to pressure overload in mice. *Circulation*, 16(106):2125–2131, 2002.

[103] Schmidt R. and Lang F. Herz und Kreislauf. *Physiologie des Menschen*, 30(4):565–609, 2014.

[104] Tian R. and Abel ED. Responses of GLUT4-deficient hearts to ischemia underscore the importance of glycolysis. *Circulation*, 24(103):2961–2966, 2001.

[105] Yamasaki R., Berri M., Wu Y., Trombitas K., McNabb M., Kellermayer MS., Witt C., Labeit D., Labeit S., Greaser M., and Granzier H. Titin-actin interaction in mouse myocardium: passive tension modulation and its regulation by calcium/S100A1. *Biophys. J.*, 4(81):2297–2313, 2001.

[106] Yamasaki R., Wu Y., McNabb M., Greaser M., Labeit S., and Granzier H. Protein kinase A phosphorylates titin's cardiac-specific N2B domain and reduces passive tension in rat cardiac myocytes. *Circ. Res.*, 11(90):1181–1188, 2002.

[107] Sheldon RD., Laughlin MH., and Rector RS. Reduced hepatic eNOS phosphorylation is associated with NAFLD and type 2 diabetes progression and is prevented by daily exercise in hyperphagic OLETF rats. *J. Appl. Physiol. (1985).*, 9(116):1156–1164, 2014.

[108] Eston R.G., Mickleborough J., and Baltzopoulos V. Eccentric activation and muscle damage: biomechanical and physiological considerations during downhill running. *Br. J. Sports Med.*, 2(29):89–94, 1995.

[109] Spina R.J., Turner M.J., and Ehsani A.A. Beta-adrenergic-mediated improvement in left ventricular function by exercise training in older men. *Am. J. Physiol.*, 1(274):397–404, 1998.

[110] Mackenzie RW. and Elliott BT. Akt/pkb activation and insulin signaling: A novel insulin signaling pathway in the treatment of type 2 diabetes. *Diabetes, metabolic syndrome and obesity: targets and therapy*, 1(7):55–64, 2014.

[111] Cazaubon S., Bornancin F., and Parker P.J. Threonine-497 is a critical site for permissive activation of protein kinase C alpha. *Biochem. J.*, 2(301):443–448, 1994.

[112] Danzi S. and Klein I. Thyroid disease and the cardiovascular system. *Endocrinol. Metab. Clin. North. Am.*, 2(43):517–528, 2014.

[113] Koetter S., Gout L., von Frieling-Salewsky M., Mueller A.E., Helling S., Marcus K., dos Remedios C., Linke W.A., and Krueger M. Differential changes in titin domain phosphorylation increase myofilament stiffness in failing human hearts. *Cardiovasc. Res.*, 99(4):648–656, 2013.

[114] Labeit S. and Kolmerer B. Titins: giant proteins in charge of muscle ultrastructure and elasticity. *Science*, 270(5234):293–296, 1995.

[115] Labeit S., Kolmerer B., and Linke WA. The giant protein titin. Emerging roles in physiology and pathophysiology. *Circ. Res.*, 2(80):290–294, 1997.

[116] Lange S., Xiang F., Yakovenko A., Vihola A., Hackman P., and Rostkova E. The kinase domain of titin controls muscle gene expression and protein turnover. *Science*, 1(308):1599–1603, 2005.

[117] Li S., Guo W., Schmitt BM., and Greaser ML. Comprehensive analysis of titin protein isoform and alternative splicing in normal and mutant rats. *Journal of cellular biochemistry*, 7(113):1265–1273, 2012.

[118] Li S., Guo W., Dewey CN., and Greaser ML. Rbm20 regulates titin alternative splicing as a splicing repressor. *Nucleic Acids Res.*, 4(41):2659–2672, 2013.

[119] Mueller S., Lange S., Gautel M., and Wilmanns M. Rigid conformation of an immunoglobulin domain tandem repeat in the A-band of the elastic muscle protein titin. *J. Mol. Biol.*, 2(371):469–480, 2007.

[120] Pernigo S., Fukuzawa A., Bertz M., Holt M., Rief M., Steiner RA., and Gautel M. Structural insight into M-band assembly and mechanics from the titin-obscurin-like-1 complex. *Proc. Natl. Acad. Sci. USA*, 7(107):2908–2913, 2010.

[121] Rain S., Bos Dda S., Handoko ML., Westerhof N., Stienen G., Ottenheijm C., Goebel M., Dorfmueller P, Guignabert C., Humbert M, Bogaard HJ., Remedios CD., Saripalli C., Hidalgo CG., Granzier HL., Vonk-Noordegraaf A., van der Velden J., and de Man FS. Titin-based mechanosensing and signaling: role in diaphragm atrophy during unloading? *Am. Heart Assoc.*, 3(3):113, 2014.

[122] Scotland S., Saland E., Skuli N., de Toni F., Boutzen H., Micklow E., Senegas I., Peyraud R., Peyriga L., Theodoro F., Dumon E., Martineau Y., Danet-Desnoyers G., Bono F., Rocher C., Levade T., Manenti S., Junot C., Portais JC., Alet N., Recher C., Selak MA., Carroll M., and Sarry JE. Mitochondrial energetic and AKT status mediate metabolic effects and apoptosis of metformin in human leukemic cells. *Leukemia*, 11(27):2129–2138, 2013.

[123] Srikanth S. and Deedwania P. Management of coronary artery disease in patients with type 2 diabetes mellitus. *Current cardiology reports*, 1(9):264–271, 2007.

[124] Chmura SJ., Dolan ME., Cha A., Mauceri HJ., Kufe DW., and Weichselbaum RR. In vitro and in vivo activity of protein kinase C inhibitor chelerythrine chloride induces tumor cell toxicity and growth delay in vivo. *Clin. Cancer Res.*, 2(6):737–742, 2000.

[125] Cuny T., Guerci B., and Cariou B. New avenues for the pharmacological management of type 2 diabetes: An update. . *Ann. Endocrinol.*, 1(73):459–468, 2012.

[126] Heller T., Blum M., Spraul M., Wolf G., and Mueller UA. Diabetic co-morbidities: prevalences in Germany. *D. Med. W.*, 15(139):786–791, 2014.

[127] Yano T., Ferlito M., Aponte A., Kuno A., Miura T., Murphy E., and Steenbergen C. Pivotal role of mTORC2 and involvement of ribosomal

protein S6 in cardioprotective signaling. *Circ. Res.*, 8(114):1268–1280, 2014.

[128] Chavali V., Tyagi SC., and Mishra PK. Predictors and prevention of diabetic cardiomyopathy. *Clin. Cancer Res.*, 6(11):151–160, 2013.

[129] von Bibra H. and St. John Sutton M. Impact of diabetes on postinfarction heart failure and left ventricular remodeling. *Current heart failure reports*, 1(8):242–251, 2011.

[130] Guo W., Schafer S., Greaser ML., Radke MH., Liss M., Govindarajan T., Maatz H., Schulz H., Li S., Parrish AM., Dauksaite V., Vakeel P., Klaassen S., Gerull B., Thierfelder L., Regitz-Zagrosek V., Hacker TA., Saupe KW., Dec GW., Ellinor PT., MacRae CA., Spallek B., Fischer R., Perrot A., Ozcelik C., Saar K., Hubner N., and Gotthardt M. RBM20, a gene for hereditary cardiomyopathy, regulates titin splicing. *Nat. Med.*, 5(18):766–773, 2012.

[131] Guo W., Bharmal SJ., Esbona K., and Greaser ML. Titin diversity–alternative splicing gone wild. *J. Biomed. Biotechnol.*, 3(10):675, 2010.

[132] Linke WA. Sense and stretchability: The role of titin and titin-associated proteins in myocardial stress-sensing and mechanical dysfunction. *Cardiovasc. Res.*, 1(77):637–648, 2008.

[133] Linke WA. and Gruetzner A. Pulling single molecules of titin by AFM–recent advances and physiological implications. *Pflugers Arch*, 1(456):101–115, 2008.

[134] Linke WA., Ivemeyer M., Olivieri N., Kolmerer B., Ruegg JC., and Labeit S. Towards a molecular understanding of the elasticity of titin. *J. Mol. Bio.*, 1(261):62–71, 1996.

[135] Linke WA., Ivemeyer M., Mundel P., Stockmeier MR., and Kolmerer B. Nature of PEVK-titin elasticity in skeletal muscle. *Proc. Natl. Acad. Sci. U S A.*, 14(95):8052–8057, 1998.

[136] Linke WA., Ivemeyer M., Labeit S., Hinssen H., Rueegg JC., and Gautel M. Actin-titin interaction in cardiac myofibrils: probing a physiological role. *Biophys. J.*, 2(73):905–919, 1997.

[137] Linke WA. and Bruecker S. King of hearts: a splicing factor rules cardiac proteins. *Nat. Med.*, 5(18):660–661, 2012.

[138] Linke WA., Popov VI., and Pollack GH. Passive and active tension in single cardiac myofibrils. *Biophys. J.*, 2(67):782–792, 1994.

[139] Paulus WJ. and Tschope C. A novel paradigm for heart failure with preserved ejection fraction: Comorbidities drive myocardial dysfunction and remodeling through coronary microvascular endothelial inflammation. *Journal of the American College of Cardiology*, 1(62):263–271, 2013.

[140] Niu X., Zhao L., Li X., Xue Y., Wang B., Lv Z., Chen J., Sun D., and Zheng Q. β3-adrenoreceptor stimulation protects against myocardial infarction injury via eNOS and nNOS activation. *PLoS One*, 6(9):271–279, 2014.

[141] Fumisawa Y., Funase Y., Yamashita K., Yamauchi K., Miyamoto T., Tsunemoto H., Sakurai S., and Aizawa T. Systematic analysis of risk factors for coronary heart disease in japanese patients with type 2 diabetes: A matched case-control study. *Giornale italiano di cardiologia*, 5(19):918–923, 2012.

[142] Liu Y., Dillon AR., Tillson M., Makarewich C., Nguyen V., Dell Italia L., Sabri AK., Rizzo V., and Tsai EJ. Volume overload induces differential spatiotemporal regulation of myocardial soluble guanylyl cyclase in eccentric hypertrophy and heart failure. *J. Mol. Cell Cardiol.*, 1(60):72–83, 2013.

[143] Nishizuka Y. Intracellular signaling by hydrolysis of phospholipids and activation of protein kinase C. *Science*, 5082(258):607–614, 1992.

[144] Wu Y., Tobias AH., Bell K., Barry W., Helmes M., Trombitas K., Tucker R., Campbell KB., and Granzier HL. Cellular and molecular mechanisms of systolic and diastolic dysfunction in an avian model of dilated cardiomyopathy. *Journal of molecular and cellular cardiology*, 5(37):111–119, 2004.

[145] Yu Y., Rajapakse AG., Montani JP., Yang Z., and Ming XF. p38 mitogen-activated protein kinase is involved in arginase-II-mediated eNOS-Uncoupling in Obesity. *Cardiovasc. Diabetol.*, 1(13):113, 2014.

[146] Chu YL., Gong YD., Su ZH., Yu HN., Cui Q., Jiang HY., and Qu HM. Relationship between tyrosine phosphorylation and protein expression of insulin receptor and insulin resistance in gestational diabetes mellitus. *CJ Huazhong Univ. Sci. Technolog. Med. Sci.*, 3(34):393–397, 2014.

Eidesstattliche Erklärung

Hiermit bestätige ich, dass ich die vorliegende Arbeit selbständig angefertigt habe. Ich versichere, dass ich ausschließlich die angegebenen Quellen und Hilfen in Anspruch genommen habe.

Düsseldorf, den

Unterschrift